



**Calhoun: The NPS Institutional Archive**  
**DSpace Repository**

---

Theses and Dissertations

Thesis and Dissertation Collection

---

1986-12

## Remote sensing of ocean sediment volume reverberation

Chang, Chin-wen

---

<http://hdl.handle.net/10945/22072>

*Downloaded from NPS Archive: Calhoun*



Calhoun is a project of the Dudley Knox Library at NPS, furthering the precepts and goals of open government and government transparency. All information contained herein has been approved for release by the NPS Public Affairs Officer.

Dudley Knox Library / Naval Postgraduate School  
411 Dyer Road / 1 University Circle  
Monterey, California USA 93943

<http://www.nps.edu/library>



DUDLEY KNOX LIBRARY  
NAVAL POSTGRADUATE SCHOOL  
MONTEREY, CALIFORNIA 93943-5002









# NAVAL POSTGRADUATE SCHOOL

## Monterey, California



# THESIS

REMOTE SENSING OF OCEAN SEDIMENT  
VOLUME REVERBERATION

by

Chang, Chin-Wen

December 1986

Co-Advisor  
Co-Advisor

James V. Sanders  
Alan B. Coppens

Approved for public release; distribution is unlimited.

T230165



## REPORT DOCUMENTATION PAGE

1a REPORT SECURITY CLASSIFICATION		1b RESTRICTIVE MARKINGS			
2a SECURITY CLASSIFICATION AUTHORITY UNCLASSIFIED		3 DISTRIBUTION/AVAILABILITY OF REPORT Approved for public release; distribution unlimited			
2b DECLASSIFICATION/DOWNGRADING SCHEDULE					
4 PERFORMING ORGANIZATION REPORT NUMBER(S)		5 MONITORING ORGANIZATION REPORT NUMBER(S)			
6a NAME OF PERFORMING ORGANIZATION Naval Postgraduate School	6b OFFICE SYMBOL (If applicable) 35	7a NAME OF MONITORING ORGANIZATION Naval Postgraduate School			
6c ADDRESS (City State and ZIP Code)  Monterey, California 93943-5000		7b ADDRESS (City State and ZIP Code)  Monterey, California 93943-5000			
8a NAME OF FUNDING/SPONSORING ORGANIZATION	8b OFFICE SYMBOL (If applicable)	9 PROCUREMENT INSTRUMENT IDENTIFICATION NUMBER			
8c ADDRESS (City State and ZIP Code)		10 SOURCE OF FUNDING NUMBERS			
		PROGRAM ELEMENT NO	PROJECT NO	TASK NO	WORK UNIT ACCESSION NO
11 TITLE (Include Security Classification)  REMOTE SENSING OF OCEAN SEDIMENT VOLUME REVERBERATION					
12 PERSONAL AUTHOR(S) Chang, Chin-Wen					
13a TYPE OF REPORT Master's Thesis	13b TIME COVERED FROM	TO	14 DATE OF REPORT (Year Month Day) 1986 December	15 PAGE COUNT 118	
16 SUPPLEMENTARY NOTATION					
17 COSATI CODES		18 SUBJECT TERMS (Continue on reverse if necessary and identify by block number)  volume reverberation, waveform envelope, transducer, receiver, sound speed, slope, decay constant, scattering coefficient			
19 ABSTRACT (Continue on reverse if necessary and identify by block number)  An experimental study was performed to establish a technique for measuring the volume reverberation from ocean sediments. Two types of sediments (aggregate and fine sand) were used in this study. The inhomogeneity within the sediment caused considerable sample-to sample fluctuation in the scattered waveform. This fluctuation was removed by spatial averaging to obtain a mean value over the sampling area. A approximate model for volume reverberation from sediments was developed for an acoustic pulse with an exponential decay. The results are promising. Combining the model and experimental results, the volume scattering coefficient obtained for the aggregate is $0.0624 \pm 0.007$ m and for fine sand is $0.0413 \pm 0.007$ m . The latter result is					
20 DISTRIBUTION/AVAILABILITY OF ABSTRACT <input checked="" type="checkbox"/> CLASSIFIED/UNLIMITED <input type="checkbox"/> SAME AS RPT <input type="checkbox"/> DTIC USERS			21 ABSTRACT SECURITY CLASSIFICATION Unclassified		
22a NAME OF RESPONSIBLE INDIVIDUAL James V. Sanders/Alan B. Cottens			22b TELEPHONE (Include Area Code) (408) 646-2117	22c OFFICE SYMBOL 61sd	

19. ABSTRACT (continued)

close to the coefficient obtained from a cloud-of-small-spheres model for wavelengths much greater than the particle size.

Approved for public release; distribution is unlimited.

Remote Sensing of Ocean Sediment  
Volume Reverberation

by

Chang, Chin-Wen  
Lieutenant, Republic of China Navy  
B.S., Chung Cheng Institute of Technology, 1979

Submitted in partial fulfillment of the  
requirements for the degree of

MASTER OF SCIENCE IN HYDROGRAPHIC SCIENCE

from the

NAVAL POSTGRADUATE SCHOOL  
December 1986

## ABSTRACT

An experimental study was performed to establish a technique for measuring the volume reverberation from ocean sediments. Two types of sediments (aggregate and fine sand) were used in this study. The inhomogeneity within the sediment caused considerable sample-to-sample fluctuation in the scattered waveform. This fluctuation was removed by spatial averaging to obtain a mean value over the sampling area. A approximate model for volume reverberation from sediments was developed for an acoustic pulse with an exponential decay. The results are promising. Combining the model and the experimental results, the volume scattering coefficient obtained for the aggregate is  $0.0624 \pm 0.007 \text{ m}^{-3}$  and for fine sand is  $0.0413 \pm 0.007 \text{ m}^{-3}$ . The latter result is close to the coefficient obtained from a cloud-of-small-spheres model for wavelengths much greater than the particle size.

## THESIS DISCLAIMER

The reader is cautioned that computer programs developed in this research may not have been exercised for all cases of interest. While every effort has been made, within the time available, to ensure that the programs are free of computational and logic errors, they cannot be considered validated. Any application of these programs without additional verification is at the risk of the user.

## TABLE OF CONTENTS

I.	INTRODUCTION .....	13
II.	BACKGROUND .....	15
III.	DESCRIPTION OF VOLUME REVERBERATION .....	17
IV.	EXPERIMENT DESIGN .....	23
A.	MATERIAL AND TANK SELECTED .....	23
B.	ELECTRONIC EQUIPMENT .....	23
C.	VERIFICATION OF MEASUREMENTS .....	25
D.	MEASUREMENT CONSIDERATION .....	28
1.	Effects of Sampling Rate .....	29
2.	Effects of Bottom Reflection Interference .....	35
3.	Effects of Near Field Interference .....	41
4.	Effects of Water/Air Interface Interference .....	41
5.	Effects of Side Lobe .....	42
6.	Effects of Sediment Inhomogeneity .....	42
E.	PROGRAMMING .....	45
1.	Program "THESIS3" .....	45
2.	Program "MAXIMUM" .....	46
3.	Program "PLOT3" .....	46
4.	Program "AVERAGE" .....	47
V.	RESULTS .....	49
VI.	CONCLUSION AND RECOMMENDATION .....	53
	LIST OF REFERENCES .....	55
	APPENDIX A: DERIVATION OF SCATTERING FROM THE SEDIMENT .....	57

APPENDIX B: COMPUTER PROGRAM .....	66
APPENDIX C: DECAY ENVELOPE GRAPHS FOR AGGREGATE .....	76
APPENDIX D: DECAY ENVELOPE GRAPHS FOR FINE SAND .....	95
BIBLIOGRAPHY .....	115
INITIAL DISTRIBUTION LIST .....	116

## LIST OF TABLES

1. WATER AIR REFLECTION .....	28
2. SEDIMENT/WATER REFLECTION AND SCATTERING .....	35
3. ORIGINAL AGGREGATE REFLECTION .....	49
4. AVERAGED AGGREGATE REFLECTION .....	50
5. ORIGINAL FINE SAND REFLECTION .....	51
6. AVERAGED FINE SAND REFLECTION .....	52

## LIST OF FIGURES

3.1	Portion of ocean scattering .....	18
3.2	Theoretical echo waveform for water and sediment .....	20
3.3	Real echo waveform displayed on CRT .....	22
4.1	Schematic of equipment .....	24
4.2	Decay envelope for reflection from water/air interface, transducer 70 cm below the surface (data set 20) .....	26
4.3	Decay envelope for reflection from water/air interface, transducer 55 cm below the surface (data set 21) .....	27
4.4	Decay envelope for reflection from water air interface, transducer was 30 cm below surface (data set 23) .....	29
4.5	Decay envelope for reflection from water/air interface, trnsduceer was 30 cm below surface (data set 24) .....	30
4.6	Decay envelope for reflection from water/air interface, transducer was 80 ciñ below surface (data set 25) .....	31
4.7	Decay envelope for reflection from water/air interface, transducer was 70 cm below surface (data set 26) .....	32
4.8	Decay envelope for reflection from water/air interface, transducer was 50 cm below surface (data set 27) .....	33
4.9	Decay envelope for reflection from water/air interface, transducer was 30 cni below surface (data set 28) .....	34
4.10	Decay envelope for reflection from aggregate/water interface. transducer was 30 cm above surface (data set 31) .....	36
4.11	Decay envelope for reflection from aggregate, water interface, transducer was 30 cm above surface (data set 32) .....	37
4.12	Decay envelope for reflection from aggregate/water interface, transducer was 30 cm above surface (data set 33) .....	38
4.13	Decay envelope for reflection from aggregate/water interface, transducer was 50 cm above surface (data set 34) .....	39
4.14	Decay envelope for reflection from aggregate/water interface, transducer was 70 cm above surface (data set 35) .....	40
4.15	Decay envelope for reflection from aggregate/water interface in the glass tank (data det 51) .....	43
4.16	Decay envelope for reflection from aggregate/water interface in the glass tank (data set 52) .....	44
A.1	For the aggregate, the decay envelope obtained from the model vs. the decay enveloppe obtained from the experiment .....	62

A.2	For the fine sand, the decay envelope obtained from the model vs. the decay envelope obtained from the experiment .....	63
A.3	For the fine sand, the decay envelope obtained from the model vs. the decay envelope obtained from the experiment .....	64
A.4	For the fine sand, the decay envelope obtained from the model vs. the decay envelope obtained from the experiment .....	65
C.1	Decay envelope for reflection from aggregate water interface, transducer was 30 cm above surface (data set 42) .....	77
C.2	Decay envelope for reflection from aggregate water interface, transducer was 30 cm above surface (data set 43) .....	78
C.3	Decay envelope for reflection from aggregate water interface, transducer was 30 cm above surface (data set 44) .....	79
C.4	Decay envelope for reflection from aggregate water interface, transducer was 30 cm above surface (data set 45) .....	80
C.5	Decay envelope for reflection from aggregate/water interface, transducer was 30 cm above surface (data set 46) .....	81
C.6	Decay envelope for reflection from aggregate water interface, transducer was 30 cm above surface (data set 47) .....	82
C.7	Decay envelope for reflection from aggregate water interface, transducer was 30 cm above surface (data set 48) .....	83
C.8	Decay envelope for reflection from aggregate water interface, transducer was 30 cm above surface (data set 49) .....	84
C.9	Decay envelope for reflection from aggregate water interface, transducer was 30 cm above surface (data set 50) .....	85
C.10	Decay envelope resulted from the average of data set 42 and 43 for the aggregate/water surface (data set DAT2) .....	86
C.11	Decay envelope resulted from the average from data set 42 to 44 for the aggregate/water surface (data set DAT3) .....	87
C.12	Decay envelope resulted from the average from data set 42 to 45 for the aggregate/water surface (data set DAT4) .....	88
C.13	Decay envelope resulted from the average from data set 42 to 46 for the aggregate/water surface (data set DAT5) .....	89
C.14	Decay envelope resulted from the average from data set 42 to 47 for the aggregate/water surface (data set DAT6) .....	90
C.15	Decay envelope resulted from the average from data set 42 to 48 for the aggregate/water surface (data set DAT7) .....	91
C.16	Decay envelope resulted from the average from data set 42 to 49 for the aggregate/water surface (data set DAT8) .....	92
C.17	Decay envelope resulted from the average from data set 42 to 50 for the aggregate/water surface (data set DAT9) .....	93
C.18	Decay envelope resulted from the average from data set 42 to 51 for the aggregate/water surface (data set DAT10) .....	94
D.1	Decay envelope for reflection from fine-sand/water interface, transducer was 30 cm above surface (data set 55) .....	96

D.2	Decay envelope for reflection from fine-sand water interface, transducer was 30 cm above surface (data set 56) . . . . .	97
D.3	Decay envelope for reflection from fine-sand water interface. transducer was 30 cm above surface (data set 57) . . . . .	98
D.4	Decay envelope for reflection from fine-sand water interface, transducer was 30 cm above surface (data set 58) . . . . .	99
D.5	Decay envelope for reflection from fine-sand water interface, transducer was 30 cm above surface (data set 59) . . . . .	100
D.6	Decay envelope for reflection from fine-sand water interface, transducer was 30 cm above surface (data set 60) . . . . .	101
D.7	Decay envelope for reflection from fine-sand water interface, transducer was 30 cm above surface (data set 61) . . . . .	102
D.8	Decay envelope for reflection from fine-sand water interface, transducer was 30 cm above surface (data set 62) . . . . .	103
D.9	Decay envelope for reflection from fine-sand water interface, transducer was 30 cm above surface (data set 63) . . . . .	104
D.10	Decay envelope for reflection from fine-sand water interface, transducer was 30 cm above surface (data set 64) . . . . .	105
D.11	Decay envelope resulted from the average of data set 55 and 56 for the fine-sand water surface (data set DAT12) . . . . .	106
D.12	Decay envelope resulted from the average from data set 55 to 57 for the fine-sand water surface (data set DAT13) . . . . .	107
D.13	Decay envelope resulted from the average from data set 55 to 58 for the fine-sand water surface (data set DAT14) . . . . .	108
D.14	Decay envelope resulted from the average from data set 55 to 59 for the fine-sand water surface (data set DAT15) . . . . .	109
D.15	Decay envelope resulted from the average from data set 55 to 60 for the fine-sand water surface (data set DAT16) . . . . .	110
D.16	Decay envelope resulted from the average from data set 55 to 61 for the fine-sand water surface (data set DAT17) . . . . .	111
D.17	Decay envelope resulted from the average from data set 55 to 62 for the fine-sand water surface (data set DAT18) . . . . .	112
D.18	Decay envelope resulted from the average from data set 55 to 63 for the fine-sand water surface (data set DAT19) . . . . .	113
D.19	Decay envelope resulted from the average from data set 55 to 64 for the aggregate water surface (data set DAT20) . . . . .	114

## ACKNOWLEDGEMENTS

The author expresses his appreciation to Professors James V. Sanders and Alan B. Coppens, Lieutenant Commender David Gardner, Lieutenant Federico R. Diaz, Mr. Grag Pless, and Mr. Dale Garlowitz for their support, advice and direction in this project. Also, I would like to thank my parents for their many years encouragement.

## I. INTRODUCTION

In hydrography, the character of the bottom should be determined for nautical charting, particularly in harbors, anchorage areas or other areas where the bottom characteristic is a significant factor to be considered for navigation safety. Conventional sampling methods, using clamshell snappers (Umbach, 1976), are used to define the characteristics of the bottom surface layer. It is tedious and time consuming, especially in off-shore geologic investigations. If some kind of theory or model existed to remotely classify the sediments, the task could be carried out easier and faster. Moreover, this ability would permit nautical charts to contain much more information.

In the ocean bottom, the magnitude and nature of the sound scattering are functions of both the particle size of the bottom and surface (bottom) relief (McKinney and Anderson, 1964). The sound echo from sediments is subject to three types of reflecting or scattering (Clark, Proni, Seem, Tsai, 1985) :

- 1) coherent reflection from the water-sediment interface; the signal amplitude will be approximately that given by spherical spreading of the wave front from the image source modified by the plane wave reflection coefficient (Clay, 1966),
- 2) incoherent or statistically variable scattering from the surface irregularities of the sediment, and
- 3) incoherent scattering from within the volume of the sediment caused by the acoustically irregular matrix of the sediment.

Items 1 and 2 arise from the surface of the sediments and item 3 from the sound pulse penetrating into the sediment volume and then being scattered back to the transducer by the granular matrix of the sediment. Since different sediments have different acoustic matrices, they have different volume reverberation characteristics and there should exist a mathematical relationship between sediment properties and the volume reverberation.

The major goal of this experiment was to establish a fundamental laboratory procedure for the remote sensing of ocean sediment volume reverberation. This was to be accomplished by accurately measuring the properties of a pulse reflected from the

sediment. In application, since the reflected sound pulse is received by the same transducer, i.e., "monostatic sonar", our discussion is restricted to "back-reflection" and "backscattering".

## II. BACKGROUND

Bradshaw (1981) used Monterey #31 fine sand, the same material used in this experiment, to study the sound propagation into a fast bottom medium. In his study, air bubbles were removed from within the sediment based on heating the water sand system. Bleach was added at a ratio of one-half gallon bleach to 70 gallons of water plus sand in order to control biologic growth. The physical properties, such as density, porosity, speed of sound, reflecton coefficient etc., were measured. Kosnik (1984) used a high pressure water jet to remove the air bubbles from the water sand mixture. However, no volume scattering measurements were made by either investigator.

Morse and Ingard (1968) give a theoretical derivation on incoherent scattering. Under the assumptions that : 1) the scattering objects are quite small compared with wave length  $\lambda$ , 2) the dimensions of scattering region are much larger than  $\lambda$ , 3) the scatterers are all spheres, and 4) the scatterers are populated sparsely and no mutiple scattering existed, the incoherently scattered intensity  $I_{is}$ , per unit incident intensity  $I_i$ , at angle  $\theta$  to the incident wave, for frequency  $\omega/2\pi$ , is

$$\frac{I_{is}}{I_i} = N V \frac{(2\pi)^{1/2}}{9} K^4 a^6 |\gamma_K + \gamma_p \cos\theta|^2 \left( \frac{1}{8} K^2 a^2 \sin^2(1/2)\theta \exp(-2K^2 a^2 \sin^2(1/2)\theta) \right) \quad (2.1)$$

where  $N$  is the total number of scatterers within unit volume,  $K$  is the wave number for the mixture,  $a$  is the radius of scatterers. Furthermore, for monostatic sonar, the volume scattering coefficient for unit volume can be reduced as

$$s_v = N (2\pi)^{1/2} K^6 a^8 |\gamma_K - \gamma_p|^2 \quad (2.2)$$

where

$$\gamma_K = \frac{\kappa_n - \kappa_o}{\kappa_o}$$

$$\gamma_p = \frac{3 \rho_n - 3 \rho_o}{2 \rho_n - \rho_o}$$

and  $\kappa_n$  is the compressibility of the scatterer,  $\kappa_o$  is the compressibility of the fluid,  $\rho_n$  is the density of the scatterer and  $\rho_o$  is the density of fluid.

For a small ( $ka \ll 1$ ) rigid sphere, the backscattering cross section is given (Urick, 1983) as

$$\sigma = 2.8 (\pi a^2)(K a)^4$$

Note that, as a single sphere, it must be a single scattering. The scattering coefficient for unit volume can be obtained as

$$s_v = N \sigma \quad (2.3)$$

Both theories are not very appropriate for the real ocean sediment volume reverberation. However, these are the only two theories available. The backscattering of sound from the ocean bottom has been studied for many years, but unfortunately no papers were found to discuss the volume reverberation of ocean sediments.

### III. DESCRIPTION OF VOLUME REVERBERATION

As sound propagates in a fluid, part of the sound is intercepted and reradiated by inhomogeneities in the fluid. The reradiation of sound is called scattering. The total of the scattering contributions from all the scatterers is called reverberation (Urick, 1983).

Volume reverberation is defined as sound scattered back to the transducer by scattering centers in the volume of the sea (National Defense Research Committee, 1969). Volume reverberation may be considered as a blending of large number of echoes. It has been studied mostly in the Deep Scattering layer, a region of high biological activity. Reverberation level, in decibels, is used to measure volume reverberation. Consider a directional projector in an ocean containing a large number of volume scatterers (Figure 3.1). Let the axial intensity at unit distance be  $I_o$ . At a distance  $r$  where there is a volume element  $dV$  of volume scatterers, the incident intensity is

$$I_i = I_o / r^2$$

The scattered intensity 1 m from the volume  $dV$  is

$$dI_s(1) = I_i s_v dV$$

where  $s_v$  is the volume scattering coefficient. The scattered intensity back at the receiver is

$$\begin{aligned} dI_s(r) &= I_i s_v dV / r^2 \\ &= (I_o / r^4) s_v dV \end{aligned}$$

and the scattered intensity from all scatterers contributing to the scattered intensity at time  $t$  is

$$I_s(r) = (I_o / r^4) s_v V$$

where  $V$  is the total volume contributing for the geometry of Figure 3.1 calculated by (Urick, 1983)

$$V = \Omega r^2 c \tau / 2$$

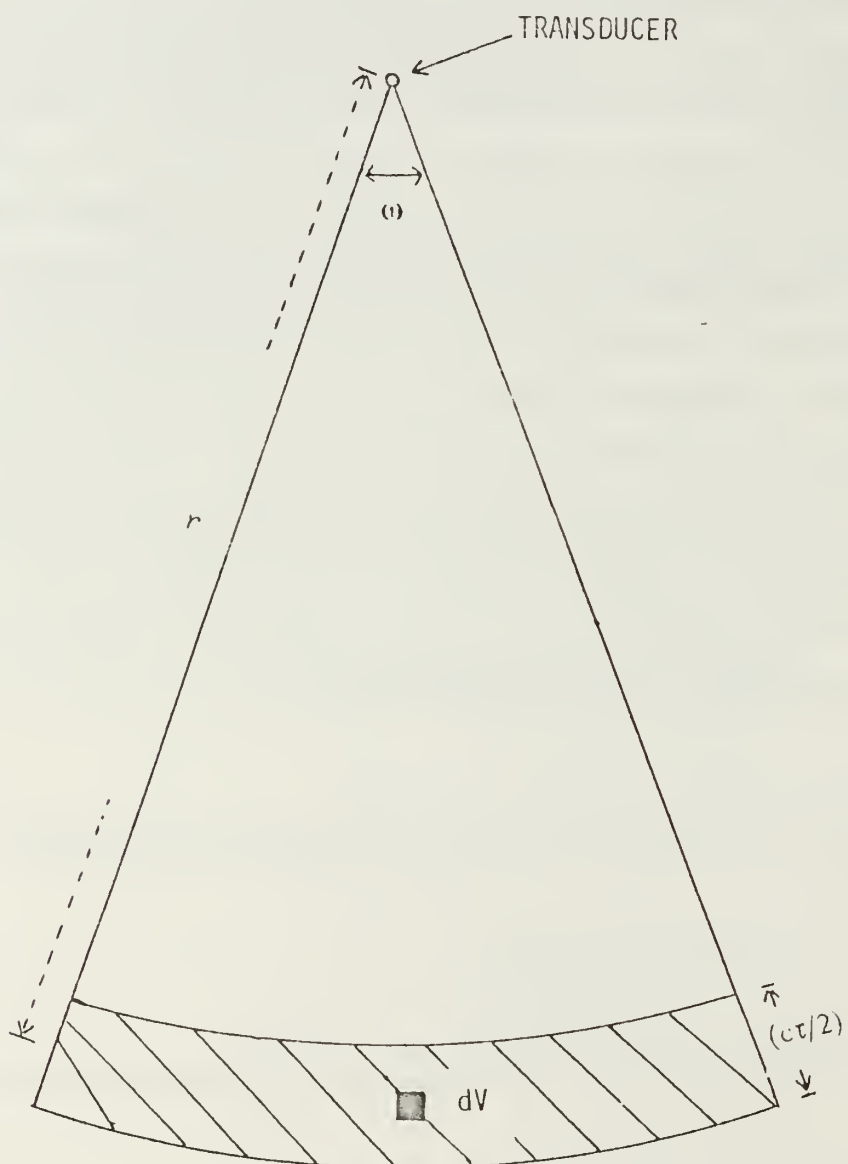


Figure 3.1 Portion of ocean scattering.

where  $\Omega$  is the solid angle of the sound beam,  $\tau$  is the pulse length and  $c$  is the sound speed, so

$$I_s(r) = (I_0 r^2) s_v \Omega c \tau / 2$$

The reverberation level is

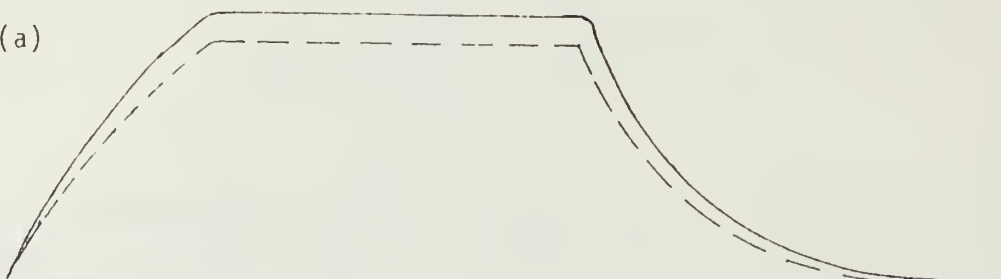
$$\begin{aligned} RL &= 10 \log I_s(r) / I_{ref} \\ &= SL - TL + S_v + 10 \log (\Omega c \tau / 2) \end{aligned}$$

where  $TL$  is the transmission loss for spherical spreading  $20\log(r)$  and  $S_v$  is the scattering strength for unit volume  $10\log(s_v)$ . In Deep Scattering Layer studies, this reverberation level equation is sufficient, because the received pulse is regarded as totally coming from volume reverberation, i.e. negligible reflection and surface scattering. Furthermore, the derivation of  $V$  is based on a square acoustic pulse. But for a real transducer, the square pulse is transformed into a pulse with an exponential rise, a flattened top and an exponential decay. The sound pulse reflected from the sediment and received by the transducer combines coherent reflected, incoherent scattering from the surface and volume reverberation.

Let a transducer located in the water send out a sound pulse to a smooth water air interface. The received echo waveform is purely reflection. If the water interface is rough, then the received echo waveform includes both reflection and surface scattering. Since sound energy is scattered by the rough surface, the received waveform amplitude is reduced. Consider first-order scattering and suppose that the surface roughness is the same for every position. The amplitude of the combined sound wave (reflected and scattered) is reduced proportional to the purely reflected wave amplitude. In Figure 3.2(a), the solid line represents an ensemble of reflected waveform, and the dashed line represents an ensemble of reflected and scattered waveform.

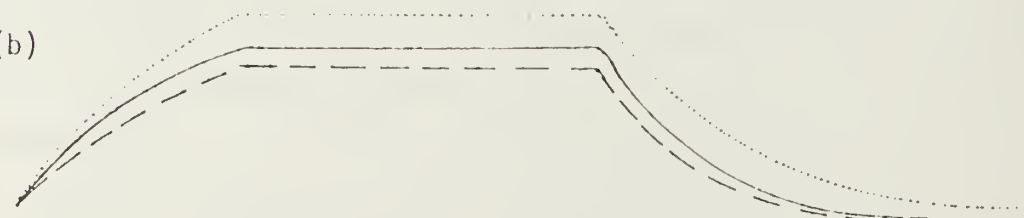
The contributions to a pulse reflected from a sediment surface is shown on Figure 3.2(b). The dashed line is the contribution by reflection and surface scattering; again, only first order scattering is considered. The dotted line includes volume reverberation. The level of the signal is raised above that of a dashed line because of energy returned from within the sediment. In particular, the tail decays more slowly than for reflection from the water/air interface. This is the significant feature of sediment volume reverberation that we are after in this paper.

(a)



WAVEFORM ENVELOP FOR WATER/AIR SURFACE

(b)



WAVEFORM ENVELOP FOR SEDIMENT SURFACE

Figure 3.2 Theoretical echo waveform for water and sediment.

Two alternative assumptions have to be made for reflection from the sediment surface : either 1) the surface scattering is negligible compared with volume reverberation, or 2) if it is not negligible, it must have the same amplitude factor as discussed in Figure 3.2(b).

According to these assumptions, if a sediment echo is subtracted from the water echo it will give a measure of the volume reverberation in the sediment (Figure 3.3). The decaying tail of the echo reflected from the smooth water-air interface is an exponential decay.

$$V_W(t) = V_0 e^{-\delta t}$$

where  $V_W(t)$  is the received voltage at time  $t$ ,  $\delta$  is the decay constant,  $V_0$  is a constant voltage, and  $t$  is the time starting from the beginning of decay. If we assume the sediment echo also decays exponentially, then we will obtain a similar function

$$V_S(t) = V'_0 e^{-\eta t}$$

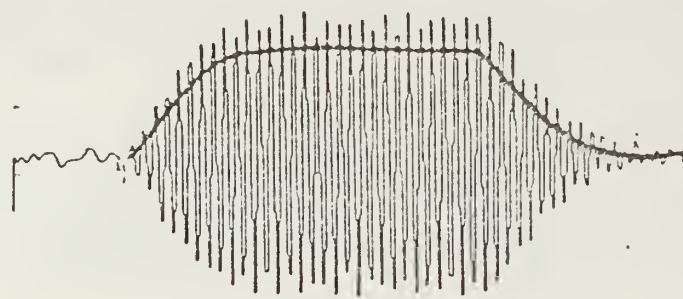
where  $V_S(t)$  is the received voltage from sediment at time  $t$  and  $\eta$  is a decay constant. If  $V_W$  and  $V_S$  are both normalized to the same initial value  $K$ , the difference becomes

$$V_V(t) = K (e^{-\eta t} - e^{-\delta t}) \quad (3.1)$$

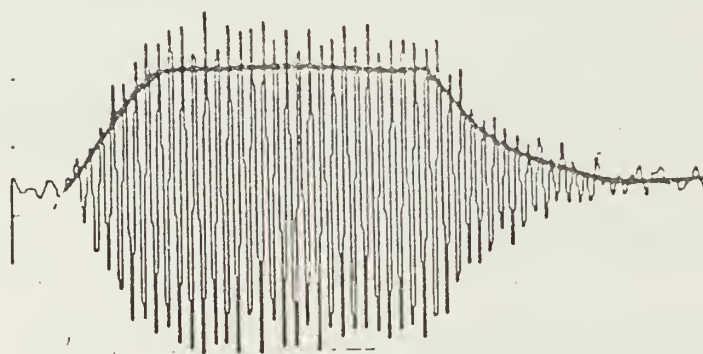
If both  $\eta t$  and  $\delta t$  are much less than unity,

$$V_V(t) = K (\eta - \delta)t \quad t \ll 1/\eta \text{ and } 1/\delta$$

This initial decay is linear and depends on the difference  $\delta-\eta$ .



ECHO FROM WATER SURFACE



ECHO FROM SEDIMENT SURFACE

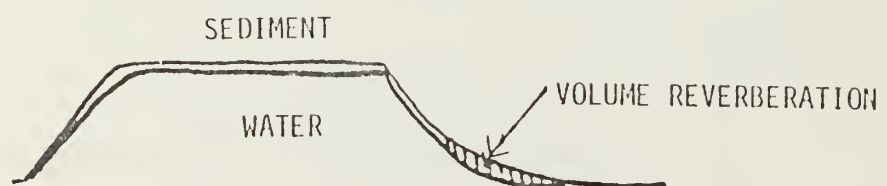


Figure 3.3 Real echo waveform displayed on CRT.

## IV. EXPERIMENT DESIGN

### A. MATERIAL AND TANK SELECTED

Fresh (tap) water, #30 Monterey fine sand and Monterey Aquarium #2 for a rough gravel sediment were the media used in the experiment. The grain size of #30 fine sand varies from 0.15 mm to 0.7 mm (Bradshaw, 1981) with an average size 0.3 mm. The Aquarium #2 has a mean size 5.3 mm (Diaz, 1986). The sand-water mixture was repeatedly stirred to remove air bubble trapped while transferring the sand to different tanks.

Initial experiments were conducted in the NPS anechoic tank to measure the reflection from the water/air surface, with the transducer located at different depth. The second tank, a wooden tank measuring 80 cm x 80 cm x 60 cm, was constructed to hold about 30 cm of aggregate. This tank was lowered and suspended 85 cm below the water/air surface of the anechoic tank. A third tank, a steel glass tank, measuring 70 cm x 70 cm x 60 cm was filled with 24 cm of fine sand or aggregate with 36 cm of water above.

### B. ELECTRONIC EQUIPMENT

A schematic drawing of the equipment is shown in Figure 4.1. Except a high pass filter, all components were off-the-shelf. General Radio model 1310 oscillator with a frequency of 182.0 kHz was fed simultaneously into a Hewlett-Packard 5233L frequency counter, and a General Radio Type 396-A tone burst generator was used to generate a 16 cycle pulse. Signal output from Hewlett-Packard 467-A amplifier was fed through a Datasonic Transmit Receive (T/R) switch and a small 21 to 28 kHz high pass filter, then into the F-41 transducer. The F-41 transducer was discussed in detail by both Borchardt (1985) and Diaz (1986). Signals returned from the sediment were amplified 20 dB by a Hewlett-Packard 465-A pre-amplifier, then passed through a Spencer-Kennedy Laboratories, Inc. model 302 variable electronic filter (set at 135 kHz high pass) to eliminate low frequency noise before being passed to the digital and analog oscilloscopes.

The waveform displayed on 3091 Nicolet Digital Oscilloscope was sampled and sent as a stream of characters to the computer. To reduce manual operations on the Nicolet 3091 during the experiment, a HIP-3421A Data Acquisition and Control Unit

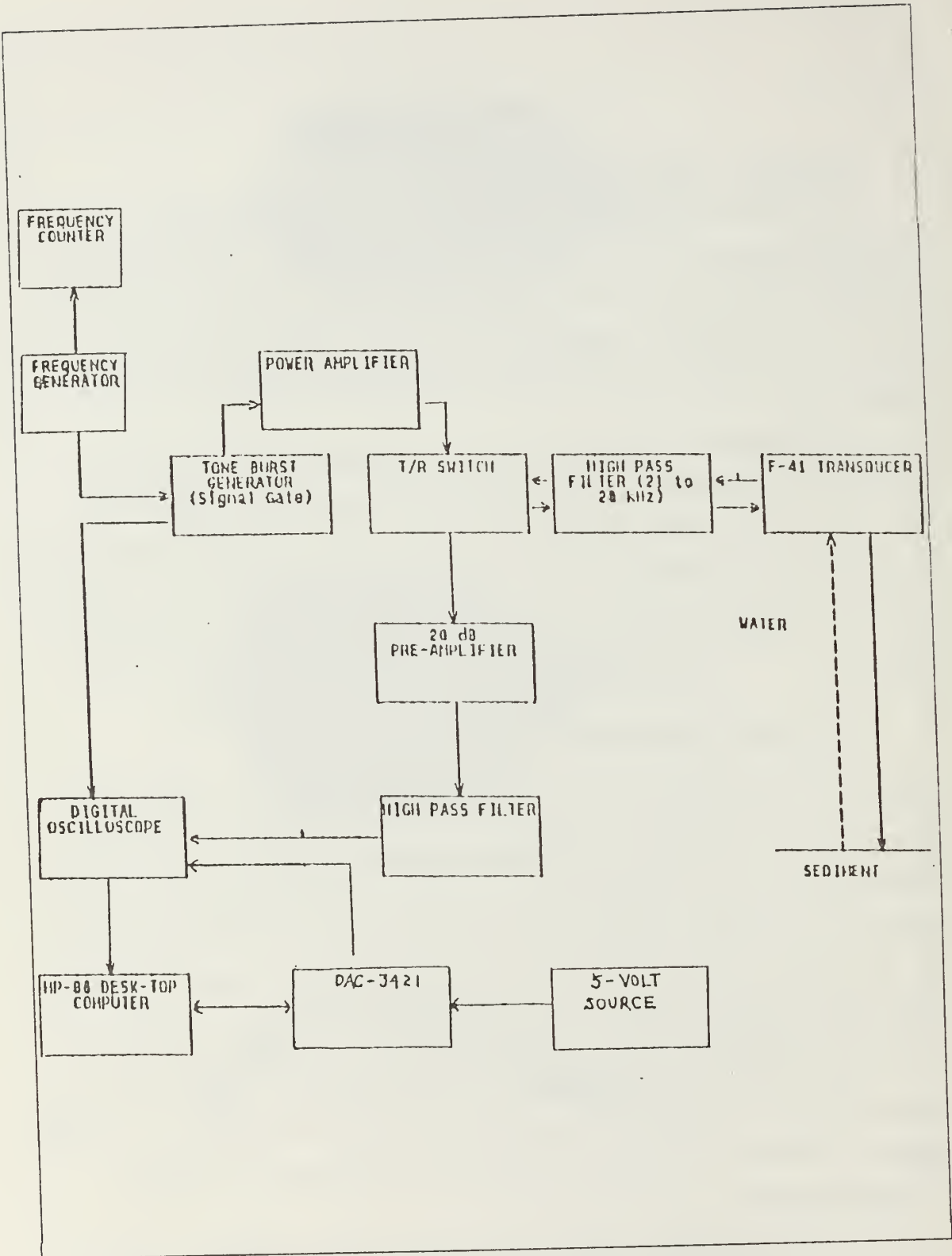


Figure 4.1 Schematic of equipment.

was adopted to receive commands from a HP-86 computer and then automatically operate the Nicolet 3091. However, it was noticed that if the Nicolet 3091 was not "warmed up" enough, the DC-offset jumped up and down, and continual manual adjustment was needed. After 2 or 3 hours of running, it became stable and no further adjustment was required.

### C. VERIFICATION OF MEASUREMENTS

No matter how deep the transducer is located below the water air surface, as long as the transducer is level, the exponential decay of the tail should be the same. In Diaz's thesis, the measurements were inconclusive because the transducer was fixed at one position throughout the experiment. This was not adequate to prove the system functioned properly. To prove that the previous experiments were run properly and results were obtained correctly, a verification was attempted by measuring the reflection from the water air interface with the same procedure, but with the transducer at various depths. Data set 20 (Figure 4.2) for the transducer 70 cm below the surface, gives a slope of  $-3.75 \times 10^{-2} \text{ Np } \mu\text{s}$ . Data set 21 (Figure 4.3) was obtained by raising the transducer 15 cm and the slope is  $-3.77 \times 10^{-2} \text{ Np } \mu\text{s}$ . Both results were close to the previous results obtained by Diaz (1986). After these two data sets were collected, a new transducer mounting was built and adopted to improve the experimental precision and operation ability. The transducer was leveled by a counter-weight on the new carriage. To ensure the system and operation worked properly, more locations were tried to obtain the decay constant of the water/air surface.

Data sets 23 and 24 were obtained at the same transducer depth, but separated 40 cm horizontally. Data sets 24 and 25 were obtained at the same horizontal position but with 50 cm difference in depth. Data set 26 was acquired by changing 10 cm in both the depth and position from data set 25. Data sets 26 to 28 resulted from changing the depth from 70 cm to 30 cm below the water air interface. The results of these experiments are listed in Table 1 and show consistencies between each other. Waveform ensembles of the tail for each data set are plotted on Figure 4.4 to Figure 4.9.

The average slope  $-3.77 \pm 0.077 \times 10^{-2} \text{ Np } \mu\text{s}$  is smaller than  $-3.84 \pm 0.14 \times 10^{-2} \text{ Np } \mu\text{s}$  which was measured in Diaz's thesis. Statistically, these two slopes are the same. The smaller standard deviation might suggest that the new carriage has achieved a better precision.

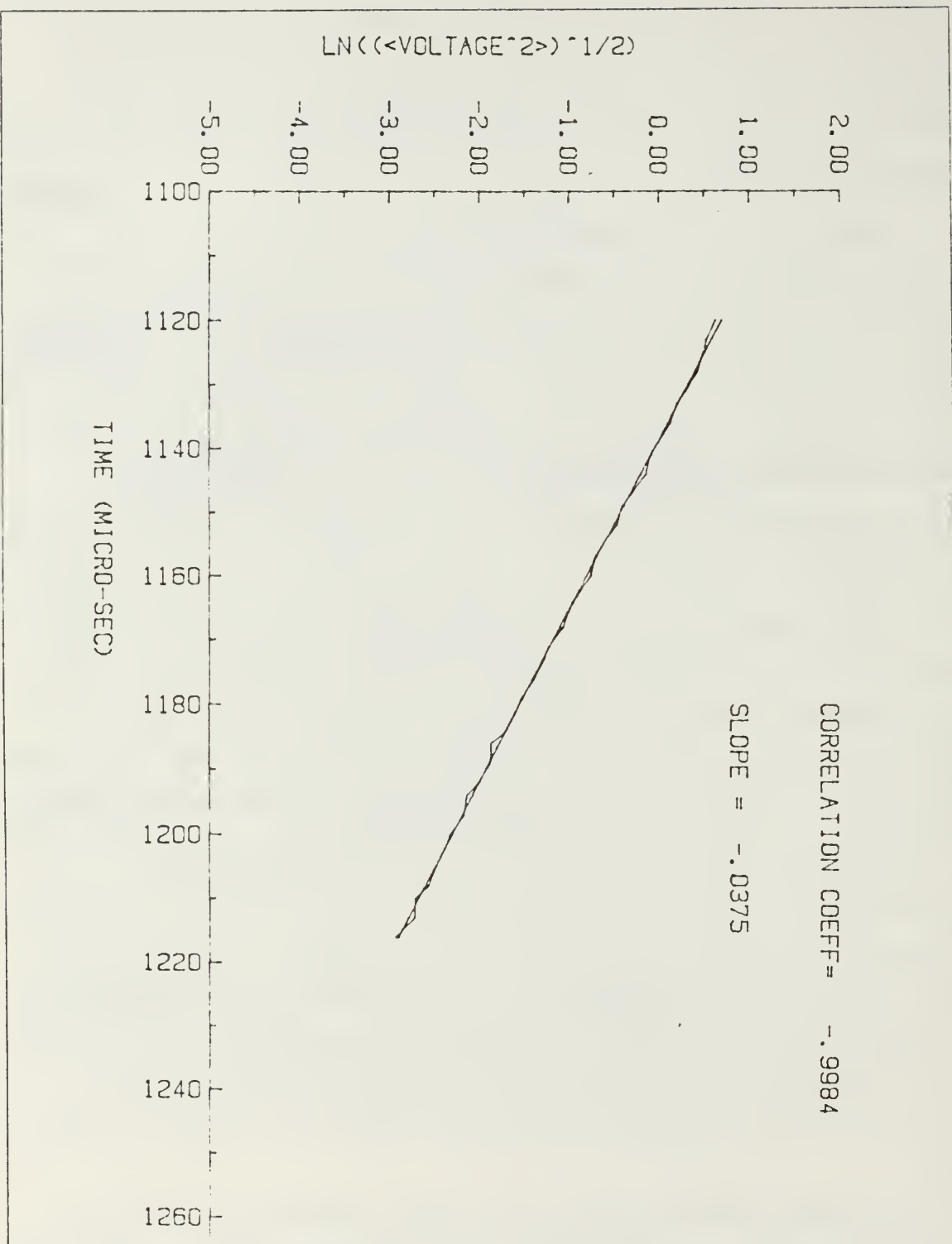


Figure 4.2 Decay envelope for reflection from water/air interface, transducer 70 cm below the surface (data set 20).

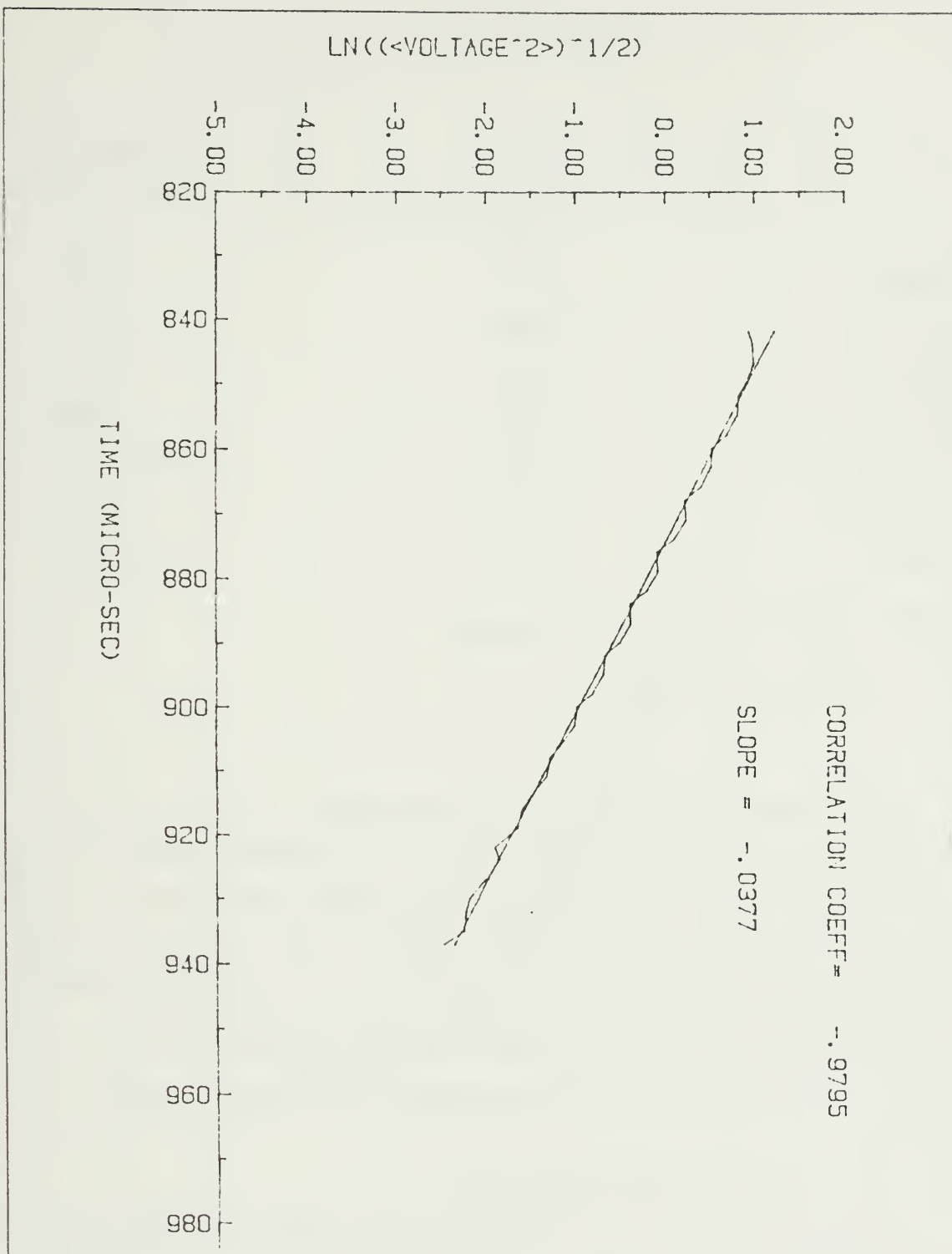


Figure 4.3 Decay envelope for reflection from water/air interface, transducer 55 cm below the surface (data set 21).

TABLE 1  
WATER/AIR REFLECTION

DATA SET	SLOPE ( $\times 10^{-2}$ )	CORRELATION COEFFICIENT
DATA20	-3.75	-0.9984
DATA21	-3.77	-0.9795
DATA22	-3.86	-0.9979
DATA23	-3.62	-0.9724
DATA24	-3.68	-0.9895
DATA25	-3.86	-0.9956
DATA26	-3.80	-0.9679
DATA27	-3.84	-0.9888
DATA28	-3.79	-0.9810

$$\text{MEAN SLOPE} = -3.77 \times 10^{-2} \text{ Np}/\mu\text{s}$$

$$\sigma = 0.07 \times 10^{-2} \text{ Np}/\mu\text{s}$$

After dealing with the water/air surface, the transducer was turned over and pointed downward toward the sediment which was contained within the 80 cm x 80 cm x 60 cm wooden tray. Different transducer positions were chosen. Data sets 31 to 33 were at the same depth, but horizontally 3 cm away from each other. The results show the waveform were totally inconsistent. Data sets 33 to 35 were at the same horizontal position but different depths; results were also inconsistent. Above results are presented on Table 2 and plotted on Figure 4.10 through Figure 4.14. So far, experiments reveal the lack of isotropic homogeneity of the volume contributes reverberation.

#### D. MEASUREMENT CONSIDERATION

During the course of these experiments some other effects were considered and studied to ensure that the experiment was working properly.



Figure 4.4 Decay envelope for reflection from water/air interface,  
transducer was 30 cm below surface (data set 23).



Figure 4.5 Decay envelope for reflection from water/air interface,  
transducer was 30 cm below surface (data set 24).

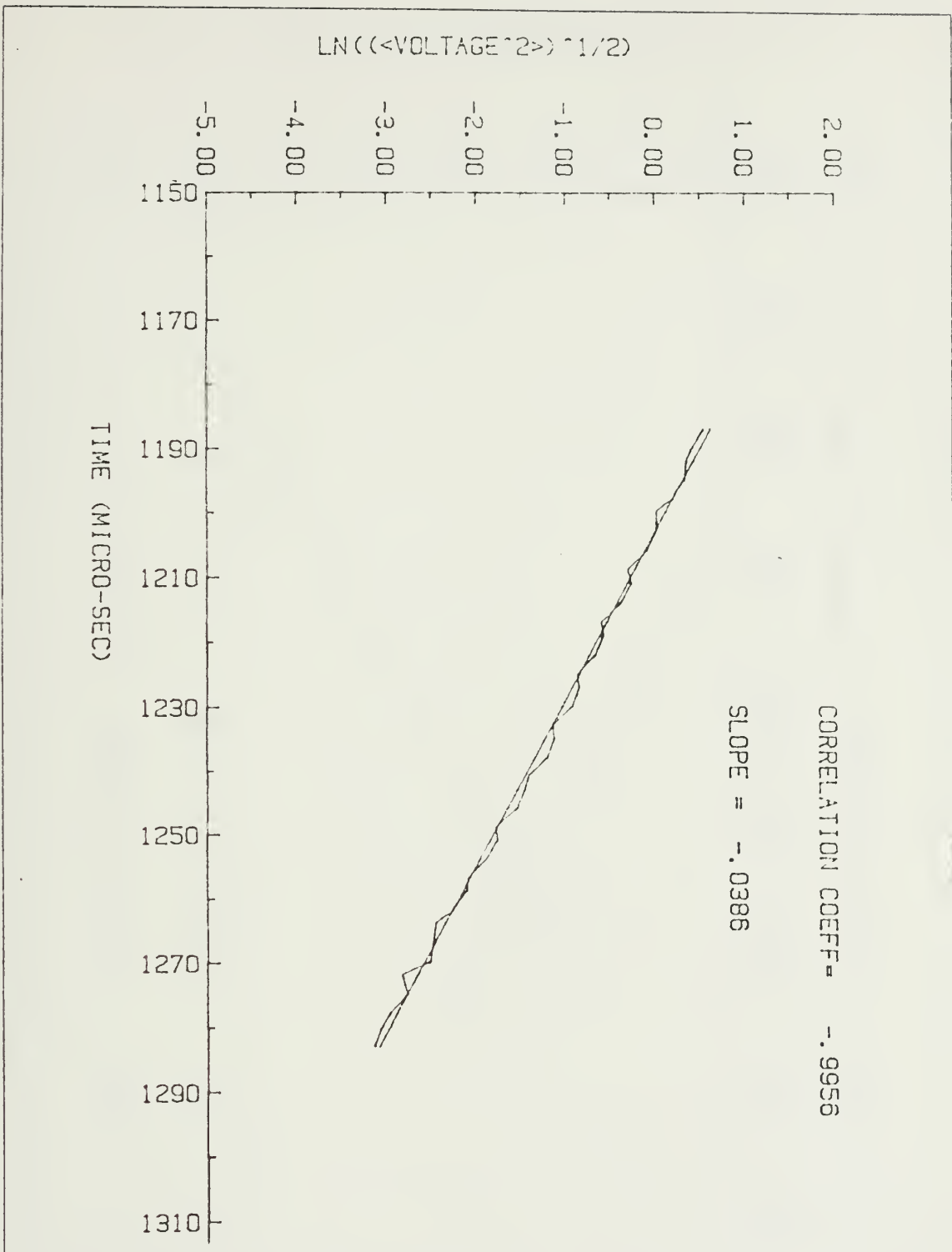


Figure 4.6 Decay envelope for reflection from water/air interface,  
transducer was 80 cm below surface (data set 25).

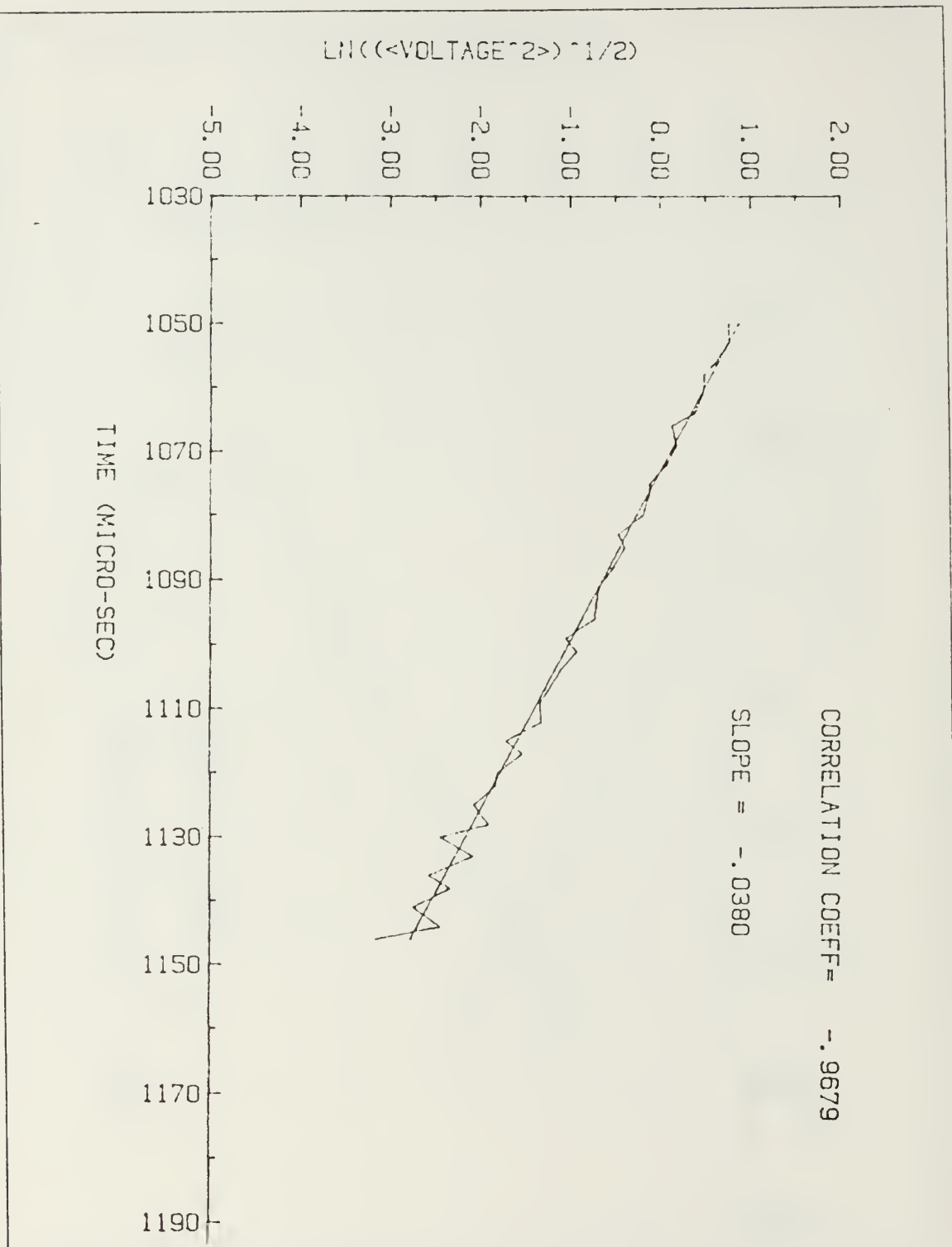


Figure 4.7 Decay envelope for reflection from water/air interface, transducer was 70 cm below surface (data set 26).

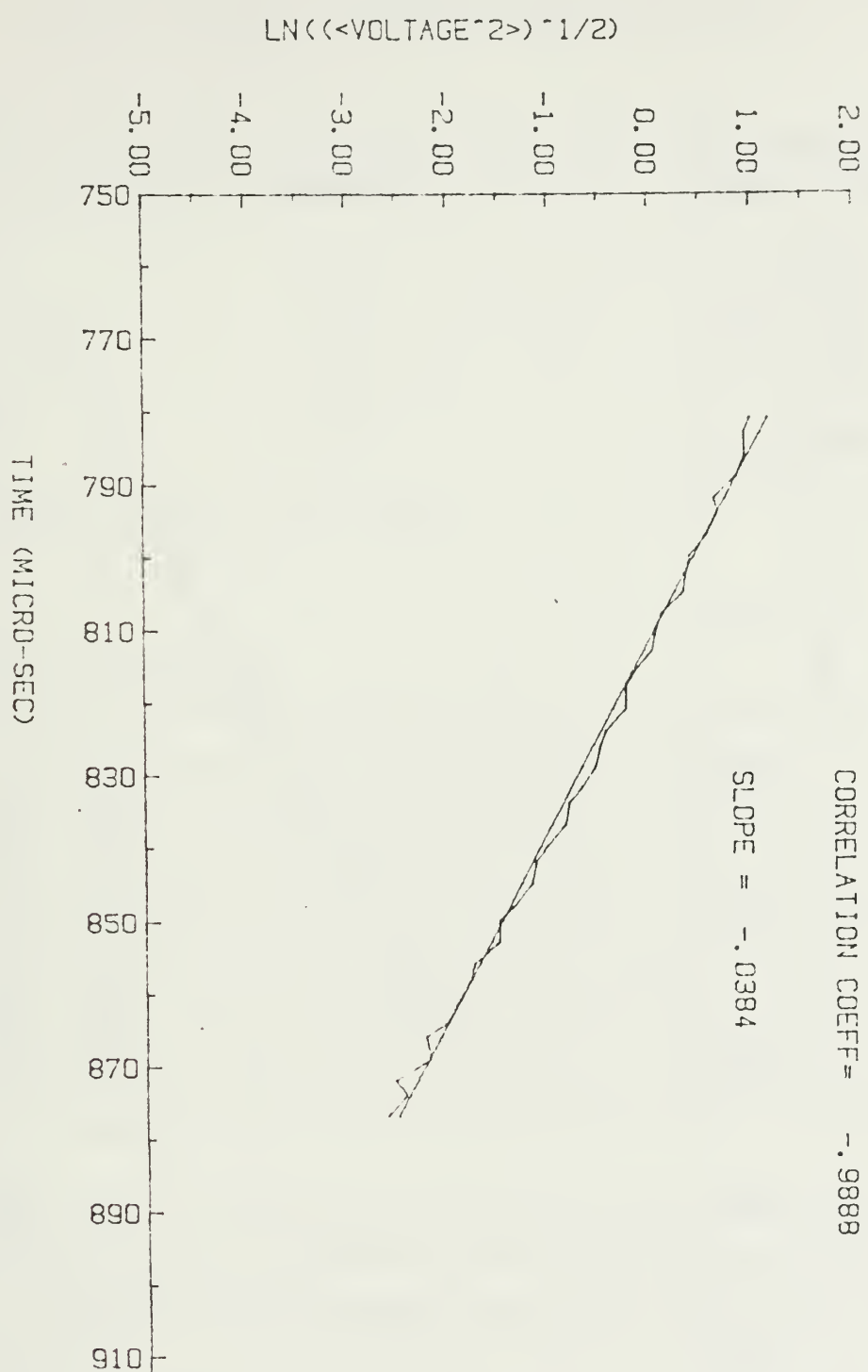


Figure 4.8 Decay envelope for reflection from water/air interface, transducer was 50 cm below surface (data set 27).

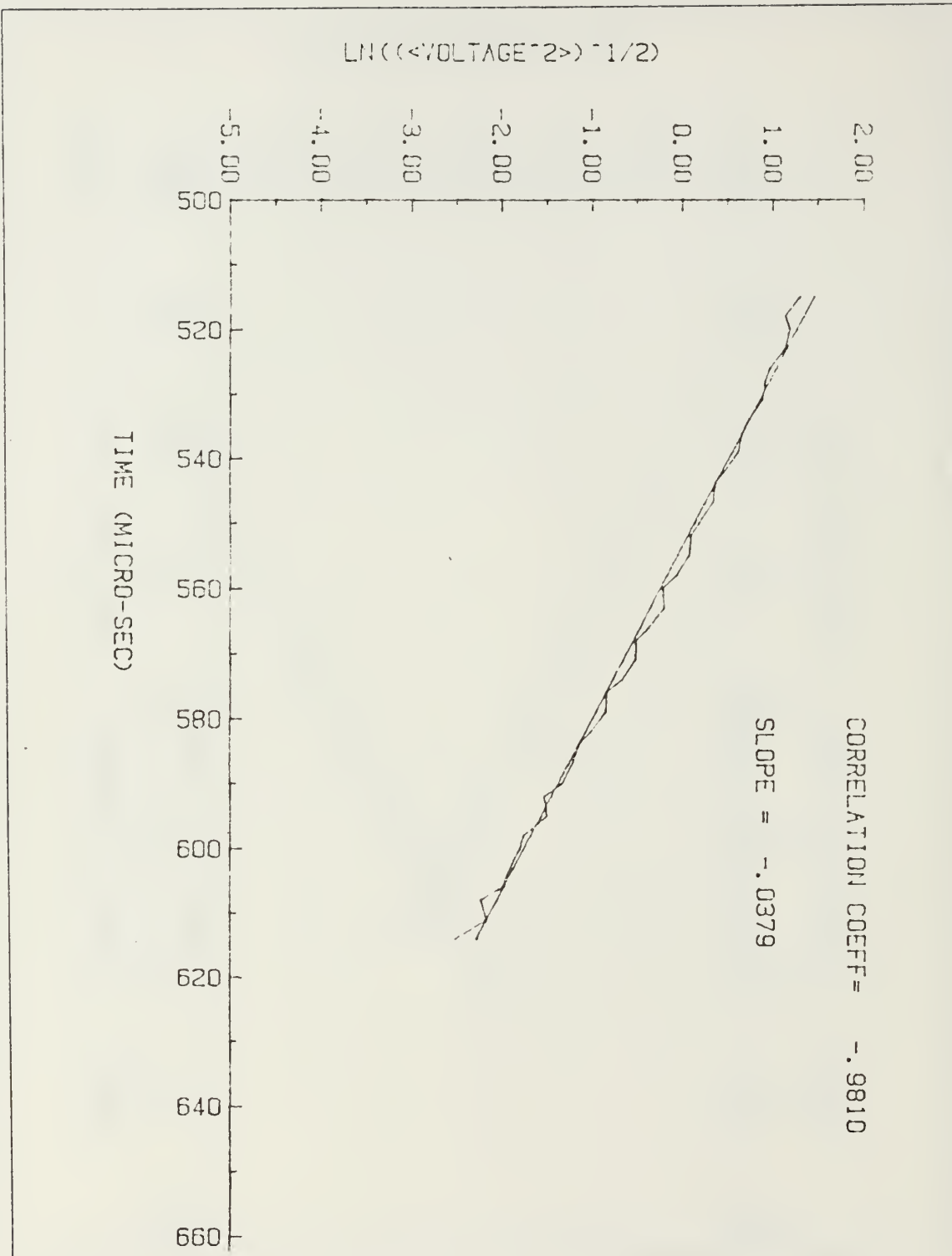


Figure 4.9 Decay envelope for reflection from water/air interface,  
transducer was 30 cm below surface (data set 28).

TABLE 2  
SEDIMENT/WATER REFLECTION AND SCATTERING

DATA SET	SLOPE ( $\times 10^{-2}$ )	CORRELATION COEFFICIENT
DATA31	-2.20	-0.9138
DATA32	-2.98	-0.8908
DATA33	-1.94	-0.7838
DATA34	-3.06	-0.8174
DATA35	-2.90	-0.9844

$$\text{MEAN SLOPE} = -2.62 \times 10^{-2} \text{ Np}/\mu\text{s}$$

$$\sigma = 0.86 \times 10^{-2} \text{ Np}/\mu\text{s}$$

### 1. Effects of Sampling Rate

The sound signal being used was fixed at 182 kHz (5.5  $\mu$ s period). The Nicolet 3091 digital oscilloscope has as its fastest sampling rate 1  $\mu$ s which is inadequate to give a precise reproduction of the numeric waveform. However, observations have shown "jitter" in the triggering of the scope, so for consecutive pulses the scope would sample different parts of the waveform. To obtain an accurate waveform, a large number of waveform were sampled and averaged. If sufficient "jitter" is present, the voltage measured in a given bin should vary between the maximum and minimum voltage in the waveform in the vicinity of the corresponding time. Since the sine wave varies between minus and plus, the voltage values were squared before averaging in order to give an accurate representation of the waveform envelope.

To determine the maximum number of samples required for each data set (average waveform), the water/air interface was measured with different number of samples. The results showed that 50 samples for each data set were enough to give a true waveform.

### 2. Effects of Bottom Reflection Interference

For a 16 cycle signal with a frequency 182 kHz, the pulse length is 88  $\mu$ s. Since the sound pulse emitted had a decay time of approximately 100  $\mu$ s, the echo from

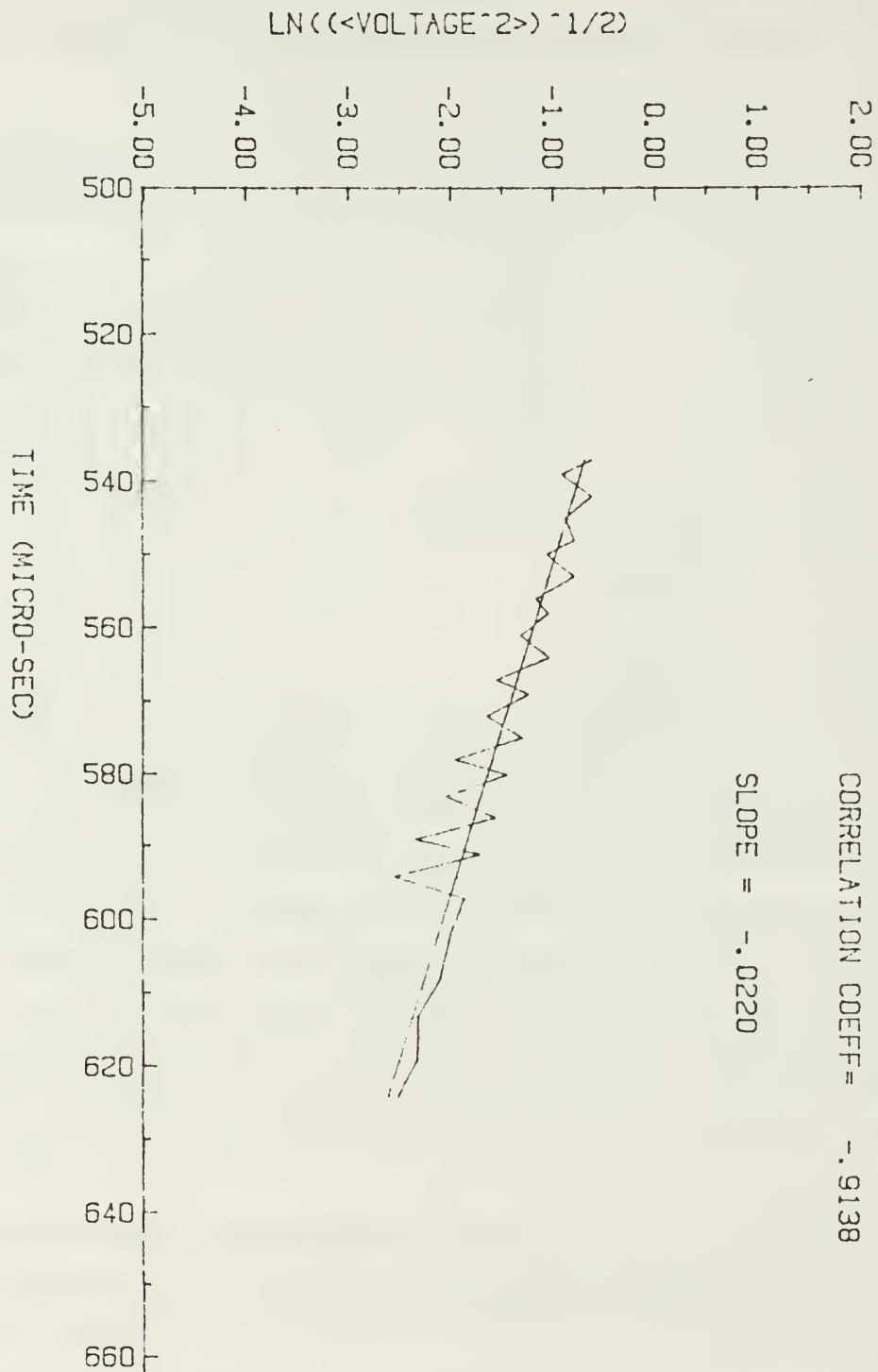


Figure 4.10 Decay envelope for reflection from aggregate/water interface, transducer was 30 cm above surface (data set 31).

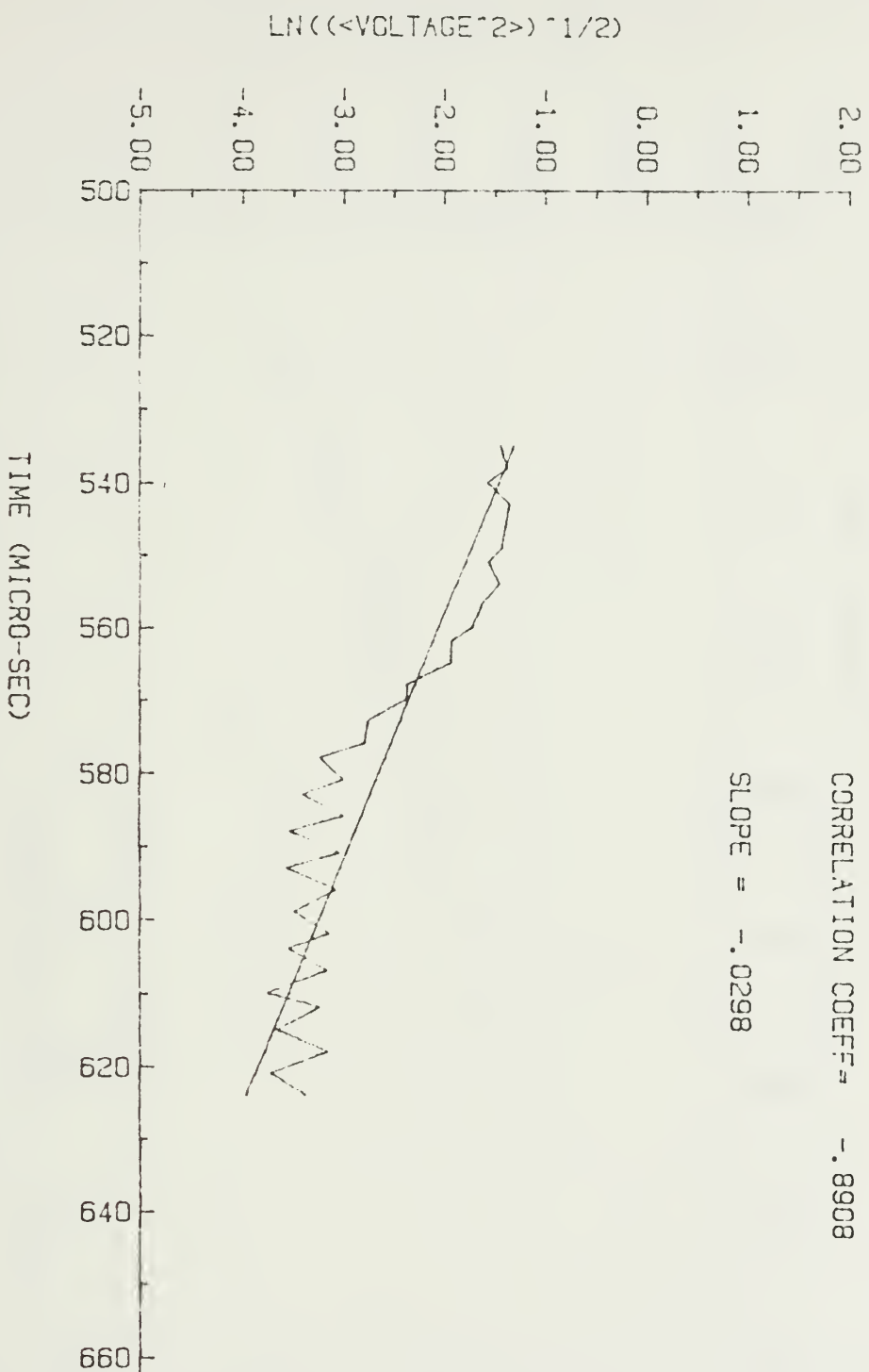


Figure 4.11 Decay envelope for reflection from aggregate/water interface, transducer was 30 cm above surface (data set 32).

$\text{LN}((\langle \text{VOLTAGE}^2 \rangle)^{1/2})$

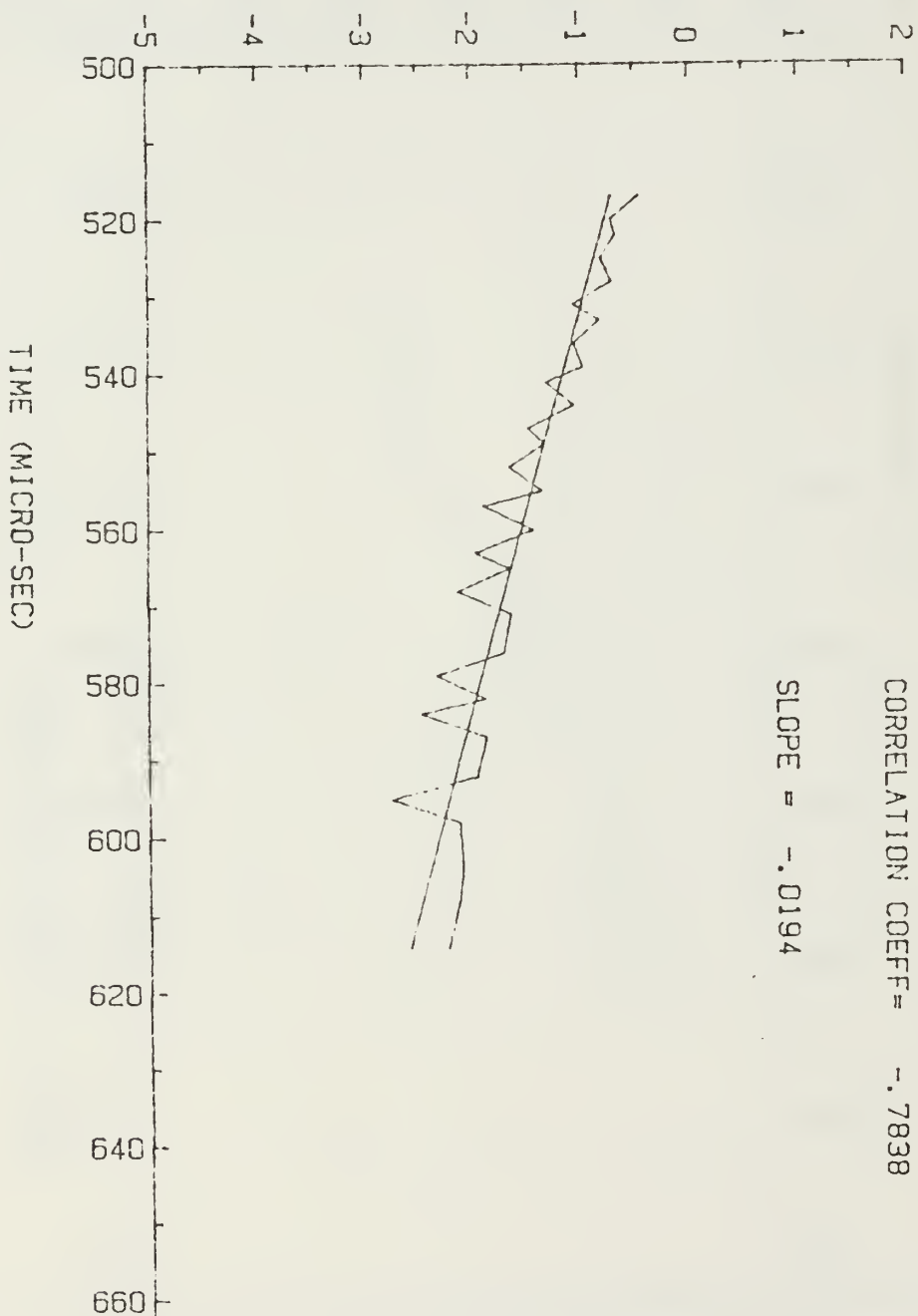


Figure 4.12 Decay envelope for reflection from aggregate/water interface, transducer was 30 cm above surface (data set 33).

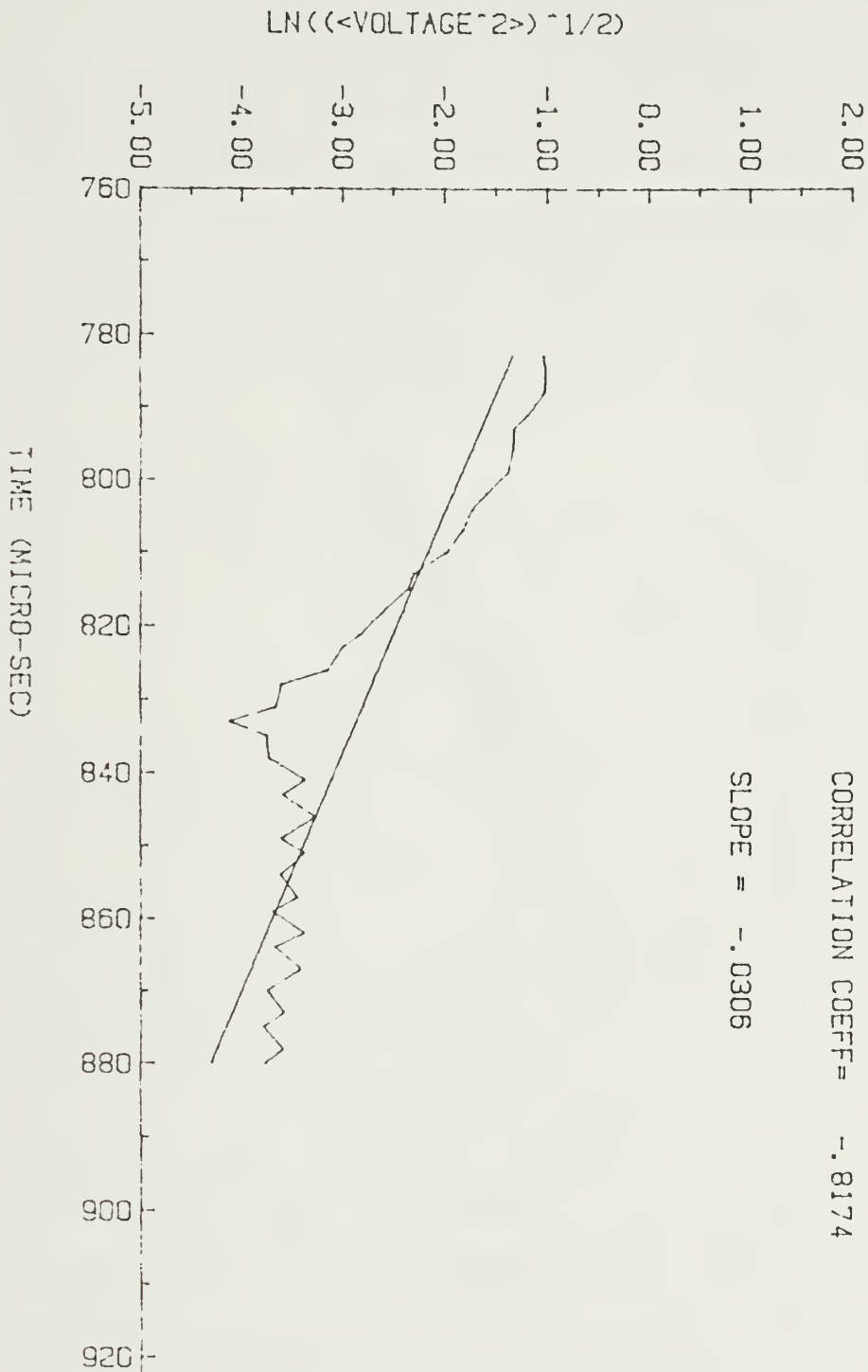


Figure 4.13 Decay envelope for reflection from aggregate/water interface, transducer was 50 cm above surface (data set 34).

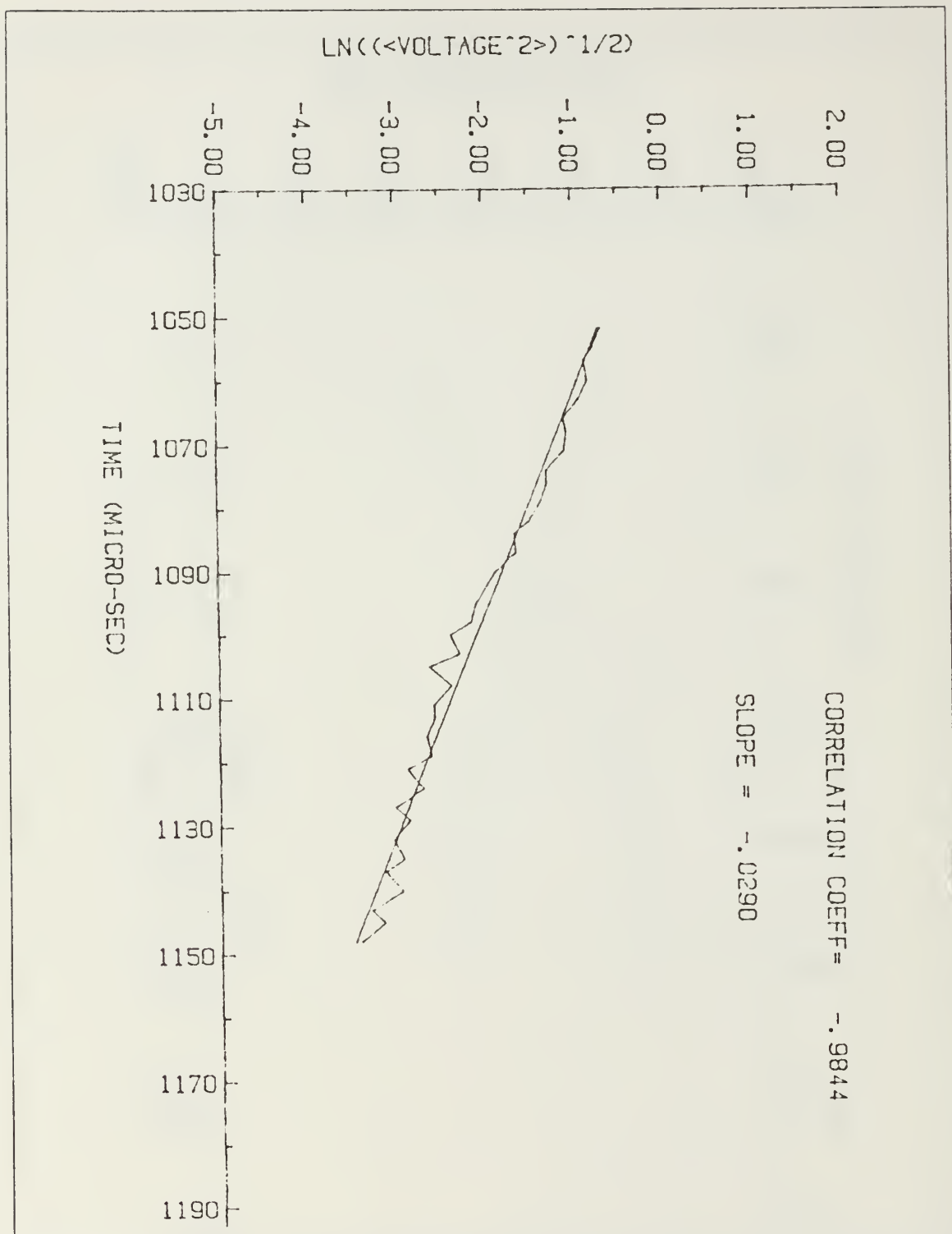


Figure 4.14 Decay envelope for reflection from aggregate/water interface, transducer was 70 cm above surface (data set 35).

the smooth water air interface should also have the same decay time. Since the purpose of this project was to compare the decay portion of echos reflected from water and sediments, the waveform was sampled for a 100  $\mu$ s interval from the begining of decay. The sound speed in the aggregate was measured to be 1555 m/s. For the fine sand, Bradshaw (1981) obtained the speed of sound to be 1610 m/s. Combining these sound speeds and the time interval 188  $\mu$ s, the depth of sediment that contributes to the main echo is 14.6 cm for aggregate and 15.1 cm for fine sand. Interference caused by reflection from the bottom of the tank will not affect the experiment as long as the sand is thicker than 15.1 cm and the aggregate is thicker than 14.6 cm. Throughout our experiments, we kept both sediments more than 24 cm deep in the glass tank to avoid interference.

### 3. Effects of Near Field Interference

In the near field of a transmitter, the axial pressure exhibits strong interference effects (Kinsler, Frey, Coppens, Sanders, 1982). Thus, the sound field is irregular and does not fall off smoothly with distance as it does in the far field. To avoid measurements in the near field, an experiment was run to find the transition distance which separates the near field and far field. This distance is 20 cm from the transducer center. No problems should occur as long as the target is more than 20 cm from the transducer. In the glass tank, we placed the transducer 30 cm above sediment. The water/air interface measurement also gave a check that 30 cm distance is satisfied. Since a pulse moving in water at 1480 m/s, takes 405  $\mu$ s to travel the 30 cm to the sediment interface and back, the 30 cm distance is long enough so that the transducer, which is on about 188  $\mu$ s, stops ringing before the first echo from the sediment arrives.

### 4. Effects of Water/Air Interface Interference

Ideally, the transducer should be far enough away from all unwanted surfaces to avoid interference. As the transducer faces down and projects a major part of its energy to the sediment surface, some energy is transmitted to the water surface and reflected back toward the sediment. If the transducer is close to the water/air surface, the reflected energy will interfere with the transmitted energy. Restricted by the size of the glass tank, we had to locate the transducer close to the water surface. To test how important this interference could be, the water surface was agitated by fingers. The waveform displayed on both analog and digital oscilloscope was unchanged during the ruffling. It was concluded that this source of interference is negligible for this experiment.

## 5. Effects of Side Lobe

The half beamwidth (to the first null) for the F-41 transducer was measured to be  $10.0^\circ$ . For a 30 cm distance from sediment to the transducer, the sediment surface ensonified by the major lobe is a circle area with radius 5.3 cm. If the distance is 80 cm, the radius will be 14.1 cm. For both the glass tank and wood tank, if the transducer is located above the center of the tank, the major lobe will not produce interference caused by the sides of the tank.

The glass tank was too small to avoid the interference, if any, caused by the side lobe. To test how much the interference was, sediments outside the center 30 cm x 30 cm square area were disturbed and left in a very irregular surface. Waveforms returned from sediment were measured before and after the disturbance. Data set 51 (Figure 4.15) shows the waveform measured before the sediment was disturbed and data set 52 (Figure 4.16) shows the waveform after disturbance. By comparing the two waveforms, it is found that the F-41 transducer gave negligible side lobe interference in this experiment.

## 6. Effects of Sediment Inhomogeneity

Before the test findings on side lobe effects, we were bothered by the drastic changes on the waveform whenever the transducer was moved parallel to the smoothed aggregate surface. It was assumed that the waveform fluctuation was caused by the inhomogeneities of the aggregate. To prove this, we placed the transducer at a fixed position in the glass tank and repeatedly ensonified the aggregate. After each data set was acquired, the aggregate was disturbed and smoothed again. Ten sets of waveform data were obtained and each of them differed from the others.

It was thought the fine sand would be more homogeneous than aggregate and it might produce more consistant waveforms as the transducer was moved horizontally. Measurements made with the fine sand, however, showed that the waveform still fluctuated. After each data set was obtained from the smoothed fine sand, the transducer was moved horizontally to different position. All the transducer positions were at least 15 cm from the wall to avoid interference caused by reflection from the sides of tank. Also, the positions were at least a length of transducer diameter from each other to avoid a waveform replication. A metal plate was set on top of the sand and the transducer was moved horizontally. As expected, the waveform on the oscilloscope was unchanged but totally different from sand.

LN(( $\langle \text{VOLTAGE}^2 \rangle$ )  $^{1/2}$ )

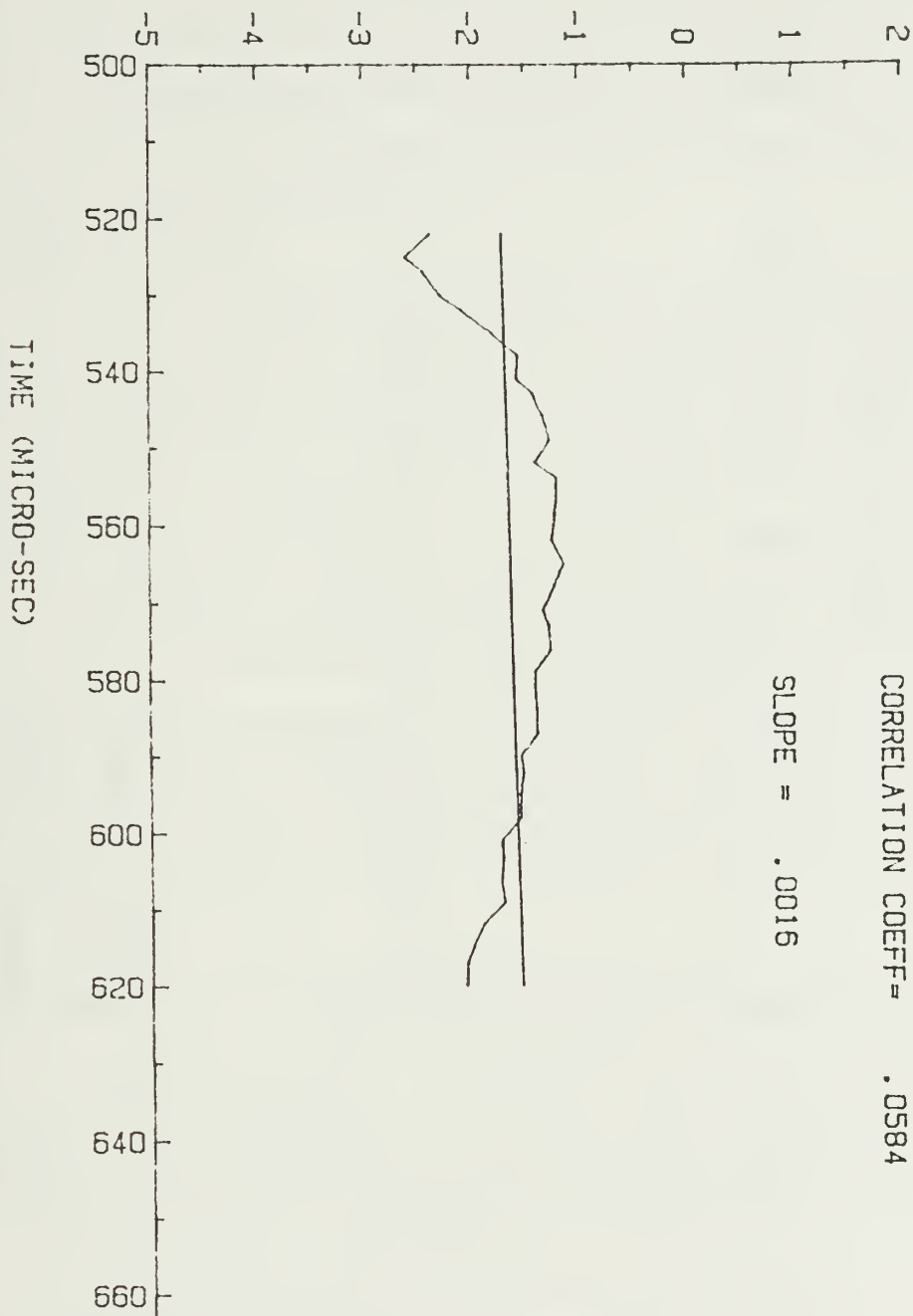


Figure 4.15 Decay envelope for reflection from aggregate/water interface in the glass tank (data det 5f).

$\text{LN}((\langle \text{VOLTAGE}^2 \rangle)^{1/2})$

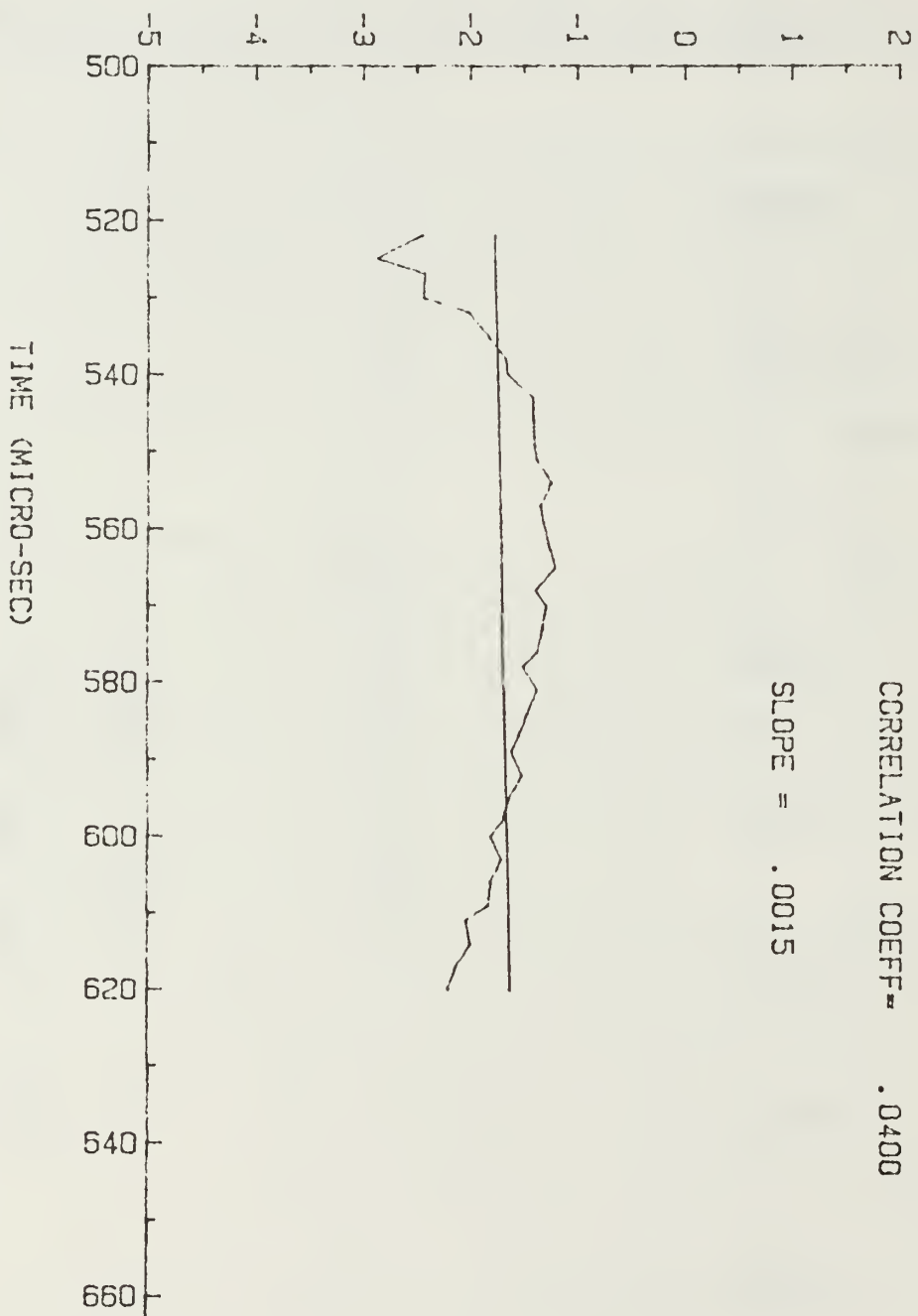


Figure 4.16 Decay envelope for reflection from aggregate/water interface in the glass tank (data set 52).

## E. PROGRAMMING

An HP-86 desktop computer was adopted to collect and analyze the waveform data. The computer program was written to be interactive. This enables 1) the collection of data sets with different delay time intervals and 2) the collecting and processing of numerous data sets. The interactive programs allowed essential information to be entered via the key board, eliminating the need to modify the program whenever data sets were changed. The interactive prompts were useful for people unfamiliar with Basic programming.

### 1. Program "THESIS3"

This program was designed as the initial step in the data collection processing. Before the selected waveform data displayed on the 3091 Nicolet Digital Oscilloscope were output to the computer, it was switched into "freeze" or "store" mode from "live" mode. Through the interface RS-232, the computer received the stored waveform data and then processed them. After processing the waveform data and before receiving the next sampling data, the Nicolet 3091 had to be switched into "live" mode again. An HP-3421A Data acquisition and Control Unit was interfaced between the Nicolet 3091 and HP-86. The HP-3421A reduced the amount of manual operations in the data collection process. A five volts source were input to the HP-3421A. Commands form the HP-86 and 5 volts signal were used to control, by closing and opening the channel in the HP-3421A, the "mode switching" of the oscilloscope. To avoid errors, the oscilloscope should be warmed up enough while entering the initial information. Once this initial information was entered and the oscilloscope was warmed up enough; the whole system runs automatically.

Waveform data output from the oscilloscope were a stream of characters. To obtain the voltage and time value, all these characters needed to be normalized and converted by the computer. A program, listed in the Nicolet 3091 operation manual, was used for data value normalization. A data set, the waveform of the decay portion, was obtained by squaring and averaging 50 samples of waveform data for each transducer position. The running average formula used in the program was

$$\langle V^2 \rangle_n = ((n-1)\langle V^2 \rangle_{n-1} + V_n^2)/n$$

where  $\langle V^2 \rangle_n$  is n samples averaged squared-voltage,  $\langle V^2 \rangle_{n-1}$  is n-1 samples averaged squared-voltage and  $V_n^2$  is squared voltage for the nth sample. Note that the average window for the waveform is 100  $\mu s$  from the beginning of the decay. The above formula was processed for each corresponding time bin.

During each data set processing, some error messages, such as STRING OVF (which stands for the string variable overflow), were displayed on the HP-86 screen. This error message could be fatal to the data set if the data has not been stored on the disk. To avoid this problem, the program was designed so that after every 10 samples processed the updated data were stored on the disk over the previous updated data. The program eliminated the problem of the disk being full before the final data set was stored on the disk. This prevention could increase the processing time, but compared to the time wasted from the above problems, it is worthwhile. The final result for this program was 3 data files : one stored the squared voltage, one for time data and one for the number count of the samples.

### 2. Program "MAXIMUM"

In order to obtain the envelope of the waveform, this program was designed to pick up the local maximum of the voltage data. The voltages, stored in the data file from "THESIS3", were read and compared with the neighboring voltage data to decide the local maximum. The determined local maximums and corresponding time bins were stored in separate files and printed out. The data files were differentiated by number according to the order they were acquired.

### 3. Program "PLOT3"

After the local maximums were determined, the decay portion of the waveform can be plotted by program "PLOT3". The experiments, for this project, took place mainly in the glass tank. A decay envelope measured in the glass tank has an interval between 520 and 619  $\mu$ s starting from transmitting time. Some exceptions existed and gave different time frames.

To determine the decay constant, the voltage data were converted logarithmically and plotted vs. the time

$$V = V_0 e^{-at}$$

$$\ln(V) = -at + \ln(V_0)$$

If the cursor on the oscilloscope was not centered, the resulting envelope showed a "zig-zag" instead of a straight line for a perfect exponential decay.

The least-square method was adopted to calculate the best fit of straight line

$$y = ax + b$$

where  $a$ , which is similar to the decay constant, is the slope and  $b$  is the intercept on the y-axis. According to Beers (1953),

$$a = \frac{k \sum (x_n y_n) - \sum x_n \sum y_n}{k \sum x_n^2 - (\sum x_n)^2}$$

$$b = \frac{\sum x_n^2 \sum y_n - \sum x_n \sum (x_n y_n)}{k \sum x_n^2 - (\sum x_n)^2}$$

where  $k$  is the total number of pairs of  $(x,y)$  values,  $n$  is the number between 1 and  $k$ ,  $\sum x_n$  is the sum of the total  $x$  value,  $\sum y_n$  is the sum of the total  $y$  value,  $\sum x_n^2$  is the sum of the squared  $x$  value,  $\sum y_n^2$  is the sum of the squared  $y$  value and  $\sum (x_n y_n)$  is the sum of the multiples of  $x_n$  and  $y_n$ .

Note that  $\sum x_n^2$  and  $\sum (x_n)^2$  are not the same.  $\sum x_n^2$  implies that each value of  $x$  is squared and then a sum is made of these squares, while  $\sum (x_n)^2$  implies that all of the values of  $x$  added together and then this sum is squared. There is an analogous distinction between  $\sum (x_n y_n)$  and  $\sum x_n \sum y_n$ . In our case, the  $x$ -coordinate is the time value and the  $y$ -coordinate is the natural-log of the voltage. To check how close the observed and least-square estimated  $y$ -value, compare, a correlation coefficient was calculated (Chatfield, 1984)

$$r = \frac{(x_n - \bar{x})(y_n - \bar{y})}{(\sum (x_n - \bar{x})^2 \sum (y_n - \bar{y})^2)^{1/2}}$$

where  $r$  is the correlation coefficient,  $\bar{x}$  is the mean value of  $x$  and  $\bar{y}$  is the mean value of  $y$ . Slope and correlation coefficient were both printed with the graph.

#### 4. Program "AVERAGE"

The received echo waveform varies from position to position because of the inhomogeneous sediment. To find the decay constant, we have to average out the

inhomogeneities to obtain a mean value of the waveform. This program performs a running average on the original data sets, producing the final averaged waveform of the sediment.

The above four programs are given in Appendix A.

## V. RESULTS

The data sets for reflection from aggregate water interface are data 42 to 51, Figure C.1 to Figure C.9, and Figure 4.15. Table 3 shows the slope obtained for each data set varied between data sets. To get a mean value for the slope, the running average method was used to process the data sets. The running average method also shows how fast the average processing became stable. Data sets DAT2 to DAT10, Figure C.10 to Figure C.18, are the results for each average process. The slopes are listed on Table 4. It is evident that the slope becomes stable after 8 sets of data are averaged. The final averaged slope is  $2.13 \times 10^{-2}$  Np  $\mu$ s and is quite different from the value reflected from the water air interface. The difference between the two slopes resulted from the effects of volume reverberation in the aggregate, and the scattering is significant.

TABLE 3  
ORIGINAL AGGREGATE REFLECTION

DATA SET	SLOPE ( $\times 10^{-2}$ )	CORRELATION COEFFICIENT
DATA42	-0.94	-0.5278
DATA43	-1.35	-0.5874
DATA44	-2.68	-0.7848
DATA45	-2.64	-0.8509
DATA46	-0.12	-0.1162
DATA47	-1.81	-0.3971
DATA48	-0.95	-0.3990
DATA49	-3.77	-0.8654
DATA50	-2.47	-0.9756
DATA51	-0.16	-0.0584

The data sets for reflection from fine-sand water interface are data 55 to 64, Figure D.1 to Figure D.10. The slope of each data set is listed on Table 5. Evidently,

TABLE 4  
AVERAGED AGGREGATE REFLECTION

DATA SET	SLOPE ( $\times 10^{-2}$ )	CORRELATION COEFFICIENT
DAT2	-1.19	-0.6051
DAT3	-1.97	-0.9720
DAT4	-2.32	-0.9175
DAT5	-2.18	-0.9343
DAT6	-2.10	-0.9914
DAT7	-1.98	-0.9952
DAT8	-2.16	-0.9932
DAT9	-2.20	-0.9943
DAT10	-2.13	-0.9958

the waveform changes very much for different data sets. The same running average method was used to remove the inhomogenities. Data sets DAT12 to DAT20 were produced from the average process. They are listed on Table 6 and plotted from Figure D.11 to Figure D.19. The slope became stable after 6 data sets were averaged. This might suggest that the fine sand has a greater homogeneity. The averaged slope for the fine sand is  $2.37 \times 10^{-2} \text{ Np } \mu\text{s}$  and is greater than the aggregate. However, the slope difference between them is not as distinguished when compared to the slope difference between the sediment and the water/air surface.

According to Equation 3.1, the decay portion volume scattering, represented in voltage, for the aggregate is

$$V_a = K ( e^{-21300t} - e^{-37700t} )$$

and for the fine sand is

$$V_s = K ( e^{-23700t} - e^{-37700t} )$$

The above relations only existed without surface scattering or the surface scattering was negligible.

TABLE 5  
ORIGINAL FINE SAND REFLECTION

DATA SET	SLOPE ( $\times 10^{-2}$ )	CORRELATION COEFFICIENT
DATA55	-1.51	-0.8178
DATA56	-3.03	-0.9581
DATA57	-2.50	-0.8112
DATA58	-0.75	-0.7290
DATA59	-1.00	-0.6776
DATA60	-3.41	-0.9957
DATA61	-3.33	-0.9050
DATA62	-1.42	-0.4922
DATA63	-2.41	-0.9389
DATA64	-1.03	-0.5784

A simplistic model for sediment volume reverberation was developed and is described in Appendix A. Combining the experimental results and the newly developed model, the volume scattering coefficient obtained was  $0.0413 \pm 0.007 \text{ m}^{-3}$  for fine sand and  $0.0624 \pm 0.007 \text{ m}^{-3}$  for aggregate. These values are reasonable compared to the difference between the decay constant obtained from the experiment. They are produced as a best fit using the least square method. The correlation coefficients, approximately 0.88, indicate they are quite a good fit. As a first model, the result is promising. However, the discrepancy between the experiment and model might suggest the model is still very crude. Also mentioned in the Appendix A is that this is only a first step to try to obtain a theory to describe the volume scattering effect of the sediment; it needs to be improved by further effort.

The  $k_a$  value for fine sand is 0.12, which is quite small compared to 1. From Equation 2.2, cloud-of-small-spheres model, the volume scattering coefficient for the fine sand is  $0.0082 \text{ m}^{-3}$  and is not too far from  $0.0413 \text{ m}^{-3}$ . As mentioned in Chapter 2, Equation 2.2 was derived under various assumptions and does not apply to real sediment. From Equation 2.3, single-small-sphere model, the volume scattering

TABLE 6  
AVERAGED FINE SAND REFLECTION

DATA SET	SLOPE ( $\times 10^{-2}$ )	CORRELATION COEFFICIENT
DAT12	-1.84	-0.9265
DAT13	-2.09	-0.9051
DAT14	-1.46	-0.9309
DAT15	-1.47	-0.9223
DAT16	-2.36	-0.9912
DAT17	-2.39	-0.9904
DAT18	-2.39	-0.9902
DAT19	-2.38	-0.9903
DAT20	-2.37	-0.9916

coefficient is  $0.34 \text{ m}^{-3}$  which is an order of magnitude different from the measured value  $0.0413 \text{ m}^{-3}$ . These values suggest that the cloud-of-small-spheres model is closer to the newly developed model than the single-small-sphere model.

The scattering coefficient obtained from Equation 2.2 is  $9456 \text{ m}^{-3}$  and from Equation 2.3 is  $1134 \text{ m}^{-3}$ . Obviously the two values deviate considerably from the true value. The  $ka$  value is equal to 2.1, which is outside the Rayleigh scattering limit. Thus Equations 2.2 and 2.3 can not be applied to the aggregate.

## VI. CONCLUSION AND RECOMMENDATION

The following conclusions are possible:

1. The inhomogeneities within the sediment caused the reflected waveform to change considerably for various transducer positions. The changes can be removed by averaging over the inhomogeneities and the averaging yields a mean decay constant.
2. The glass tank works very well, and therefore a bigger tank to contain the sediment is not necessary.
3. The laboratory procedure to measure the volume reverberation, using off-the-shelf equipment and a high pass filter in a water-over-sediment system, is workable.
4. The basic program, written for a HP-86 desktop computer, is sufficient for this experiment.
5. Although Equations 2.2 and 2.3 can not be applied to aggregate since it has a  $ka$  greater than 1, the aggregate does have a higher volume reverberation than fine sand. The aggregate has a larger size than the fine sand; this might suggest that the larger size sediment causes more volume reverberation.
6. From the scattering coefficient  $0.0413 \pm 0.007 \text{ m}^{-3}$  for the fine sand and  $0.0624 \pm 0.007 \text{ m}^{-3}$  for the aggregate, the scattered energy received by transducer is quite small compared to the incident energy.
7. For fine sand sediment, the cloud-of-small-spheres model works better than the single-small-sphere model.
8. The simplistic model, derived from the true acoustical pulse and described in Appendix A, gives a crude formulated volume scattering relationship. Combining with the experiment result, the sediment's volume scattering coefficient can be estimated.

Further study of the volume reverberation from ocean sediment is recommended. Future experimentation should include further variation of the sediment size and of the acoustic frequency to find a relationship combining the  $ka$  value and volume reverberation. The developed model should be improved to obtain a better result

coincident with the experimental result. The absorption coefficient of different sediment with the frequency used should be measured to compare the value obtained from Urick's formula described in appendix A. Equations 2.2 and 2.3 should be improved to obtain the scattering coefficient, which can be used to check the above model. Continued use of the experimental procedure, equipment and computer programs, written for this project on the HP-86, is highly recommended.

## LIST OF REFERENCES

Beers, Y., *Introduction to The Theory of Error*, First Edition, Addison-Wesley Publishing Company Inc., 1953.

Borchardt, J. A., *Measurement of the Acoustic Pressure Everywhere Over a Modeled Continental Shelf*, M.S. Thesis, Naval Postgraduate School, Monterey, CA, December 1985.

Bradshaw, J. A., *Laboratory Study of Sound Propagation Into a Fast Bottom Medium*, M.S. Thesis, Naval Postgraduate School, Monterey, CA, June 1981.

Chatfield, C., *The Analysis of Time Series an Introduction*, Third Edition, Chapman and Hall Ltd., 1984.

Clarke, T. L., Proni, J. R., Seem, D. A., and Tsai, J. J., *Joint CGS-AOML Acoustical Bottom Echo-Formation Research I: Literature Search and Initial Modeling Results*, NOAA Technical Memorandum ERL-AOML, Miami, FL, 1984.

Clay, C. S., *Coherent Reflection of Sound from the Ocean Bottom*. *Journal of Geophysical Research*, Volume 71, No. 8, April 1966.

Diaz, Federico R., *Preliminary Study of a Technique for Measuring the Volume Backscattering from Sediments*, M.S. Thesis, Naval Postgraduate School, Monterey, CA, September 1986.

Kinser, L. E., Frey, A. R., Coppens, A. B. and Sanders, J. V., *Fundamentals of Acoustics*, Third Edition, Wiley & Sons, Inc., 1982.

Kosnik, M. E., *The Implicit Finite-Difference (I.F.D.) Acoustic Model in a Shallow water Environment*, M.S. Thesis, Naval Postgraduate School, Monterey, CA, June 1984.

McKinney, C. M. and Anderson, C. D., *Measurements of Backscattering of Sound from the Ocean Bottom*. *The Journal of The Acoustical Society of America*, Volume 36, No. 7, January 1964.

Morse P. M. and Ingard, K. U., *Theoretical Acoustics*, First Edition, McGraw-Hill, Inc., 1968.

National Defense Research Committee, *Physics of Sound in the Ocean*, Headquarters Naval Material Command, Department of Navy, 1969.

*Nicholet 3091 Operating Manual*, Nicholet Instrument Corporation, 1985.

Sanders, J. V. and Coppens, A. B., Personal Interview with Author, Naval Postgraduate School, Monterey, CA, 1986.

Umbach, M. J., *Hydrographic Manual*, Fourth Edition, U.S. Department of Commerce, U.S. Govt. Printing Office, 1981.

Urick, R. J., *Principle of Underwater Sound*, Third Edition, McGraw-Hill, 1983.

Urick, R. J., *Sound Propagation in The Sea*, Defense Advanced Research Projects Agency (DARPA), 1979.

## APPENDIX A

### DERIVATION OF SCATTERING FROM THE SEDIMENT

The generated electrical pulse can be described by the step unit function, H, as follows:

$$I(t) = I_0 ( H(t) - H(t-\tau) ) \quad (A.1)$$

where  $I(t)$  is the intensity at time  $t$ ,  $I_0$  is the intensity amplitude,  $\tau$  is the pulse length.

$$H(t) = \begin{cases} 0 & t < 0 \\ 1 & t \geq 0 \end{cases}$$

and

$$H(t-\tau) = \begin{cases} 0 & t-\tau < 0 \\ 1 & t-\tau \geq 0 \end{cases}$$

Since the transducer is a resonant system with damping, the square electrical pulse was transformed into an acoustic pulse with an exponential rise, an approximately flattened top and exponential decay. The shape of the acoustic waveform can be described, (Sanders and Coppens, 1986), as

$$f(t) = (1 - e^{-\alpha t}) H(t) + (1 - e^{-\alpha \tau}) H(t-\tau) \quad (A.2)$$

where  $t$  is the delay time and  $\alpha$  is the decay constant.

Let a transducer, located in the water, send out a sound pulse to a smoothed sediment surface. To assure the surface scattering is negligible and the volume scattering is only single scattering, reflected pulse received, by the same transducer, should have an intensity (Sanders and Coppens, 1986)

$$I = (\int T_i^2 s_v e^{-\beta \xi} I_0 f(t-2\xi/c) d\xi / (r+\xi)^2 + R_i I(t)/r^2) / r^2 \quad (A.3)$$

Where  $T_i$  is the intensity transmission coefficient,  $s_v$  is the volume scattering coefficient,  $\beta$  is the absorption coefficient in the sediment,  $\xi$  is the affected sediment depth.  $R_i$  is the intensity reflection coefficient and  $r$  is the distance between the transducer and sediment. From above equation, the intensity contributed by scattering is

$$I_s = \int T_i^2 s_v e^{-\beta \xi} I_0 f(t-2\xi/c) d\xi (r+\xi)^2 r^2 \quad (A.4)$$

and the intensity contributed by the reflection is

$$I_r = R_i I_0 f(t) r^4 \quad (A.5)$$

If  $r > > \xi$ , then

$$I_s = (T_i^2 s_v I_0 r^4) \int e^{-\beta \xi} f(t-2\xi/c) d\xi \quad (A.6)$$

where

$$f(t-2\xi/c) = (1 - e^{-a(t-2\xi/c)}) H(t-2\xi/c) - (1 - e^{-a(t-\tau-2\xi/c)}) H(t-\tau-2\xi/c) \quad (A.7)$$

During the integration, the lower boundary of  $\xi$  is zero; the upper boundary is  $ct/2$  for  $H(t-2\xi/c)$  and  $c(t-\tau)/2$  for  $H(t-\tau-2\xi/c)$ . Note that only the decay portion,  $t > \tau$ , was interested. After the integration,

$$\begin{aligned} I_s = A & (-(e^{-c\beta t/2} - 1)\beta - (e^{-c\beta t/2} - e^{-at})/(-\beta + 2a/c)) \\ & + (e^{-c\beta(t-\tau)} - 1)\beta + (e^{-c\beta(t-\tau)/2} - e^{-a(t-\tau)})/(-\beta + 2a/c)) \end{aligned} \quad (A.8)$$

where

$$A = T_i^2 s_v I_0 / r^4 \quad (A.9)$$

From the experimental formula  $\beta = 0.25f$  (Urick, 1979) and  $f$  is 182 kHz, the absorption coefficient

$$\beta = 45.5 \text{ dB/m} = 5.2 \text{ Np/m},$$

$c\beta/2$  is 4030 Np/s for aggregate and is 4186 Np/s for the fine sand. The intensity decay constant  $\alpha$  is twice the pressure decay constant  $\delta$ . From the experiment,  $\delta$  is 37700 Np/s and it gives an  $\alpha$  equal to 75400 Np/s;  $2\alpha c$  is 97.2 Np/m for the aggregate and is 93.6 Np/m for the fine sand. After plugging in the above values for the aggregate, Equation A.8 becomes

$$I_s = A(e^{-4030t}/11.6) - A(8.3 e^{-75400t}) \quad (\text{A.10})$$

For the fine sand, Equation A.7 becomes

$$I_s = A(e^{-4186t}/11.0) - A(8.6 e^{-75400t}) \quad (\text{A.11})$$

$$R_i = R^2$$

$$R_i + T_i = 1$$

The pressure reflection coefficient  $R$  is 0.356 for the aggregate (Diaz, 1986) and 0.36 for the fine sand (Bradshaw, 1981). For the aggregate,

$$R_i = 0.1270$$

$$T_i = 0.8730$$

For the fine sand,

$$R_i = 0.1296$$

$$T_i = 0.8704$$

The pulse length is 88  $\mu\text{s}$  and from equation A.5,

$$I_r = I_o R_i (e^{-\alpha\tau} - 1) e^{-75400t/r^4} \quad (\text{A.12})$$

Using the above values, the reflected intensity for the aggregate becomes

$$I_r = 96.6 e^{-75400t} I_o / r^4 \quad (\text{A.13})$$

and for the fine sand

$$I_r = 98.5 e^{-75400t} I_o / r^4 \quad (\text{A.14})$$

The intensity contributed by the scattering for the aggregate is

$$I_s = (s_v I_o / r^4) (e^{-4030t} / 15.2 - 6.3 e^{-75400t}) \quad (A.15)$$

and for the fine sand,

$$I_s = (s_v I_o / r^4) (e^{-4186t} / 14.5 - 6.5 e^{-75400t}) \quad (A.16)$$

Combining the above equations, the reflected intensity from the aggregate received by the transducer is:

$$I = (I_o / r^4) B \quad (A.17)$$

where

$$B = (s_v e^{-4030t} / 15.2 - 6.3 s_v e^{-75400t} + 96.6 e^{-75400t}) \quad (A.18)$$

For the fine sand,

$$I = (I_o / r^4) D \quad (A.19)$$

where

$$D = (s_v e^{-4186t} / 14.5 - 6.5 s_v e^{-75400t} + 98.5 e^{-75400t}) \quad (A.20)$$

By inputting a series of scattering coefficients and computing the  $\text{Log}(B)^{1/2}$  and  $\text{Log}(D)^{1/2}$ , the theoretical envelope was determined. A least-square-fit slope was obtained for each envelope. The scattering coefficient for each sediment can be estimated by the value of  $s_v$ , for which the slope of the theoretical envelope is equal to the slope of experiment data. For the fine sand, measured the decay constant 23700 Np/s gave a scattering coefficient of  $0.0413 \text{ m}^{-3}$ . For the aggregate, the scattering coefficient  $0.0624 \text{ m}^{-3}$  was obtained from the measured decay constant 21300 Np/s.

Figure A.1 and Figure A.2 show the envelopes determined theoretically from the above values of  $s_v$  for the aggregate and fine sand respectively. The theoretical

envelope is plotted by normalizing the left end of the best fit slope line to the same value obtained from the experiment and then applying this normalization to the whole theoretical envelope.

Results from the fine sand were selected to find the uncertainty of scattering coefficient obtained from the above method. By comparing a series of envelope plots for different scattering coefficient, the uncertainty  $\pm 0.007$  was determined. Figure A.3 and A.4 show the envelopes for scattering coefficients  $\pm 0.007$  different from  $0.0413 \text{ m}^{-3}$ . The slope changes as the scattering coefficient changes. In the beginning of decay, the dominant term in equation A.20 is the reflection term which is independent on  $s_v$ , and the scattering term which depends on  $s_v$  is negligible. The theoretical value will not change much in the beginning of decay as the scattering coefficient changes. The normalization, described previously, still gave a good approximation to the plot of the theoretical envelope vs. the experimental envelope for different scattering coefficients.

Note that the model derived and described in this appendix is crude. A later improvement on this model is suggested.

$\ln(\langle \text{VOLTAGE}^2 \rangle^{1/2})$

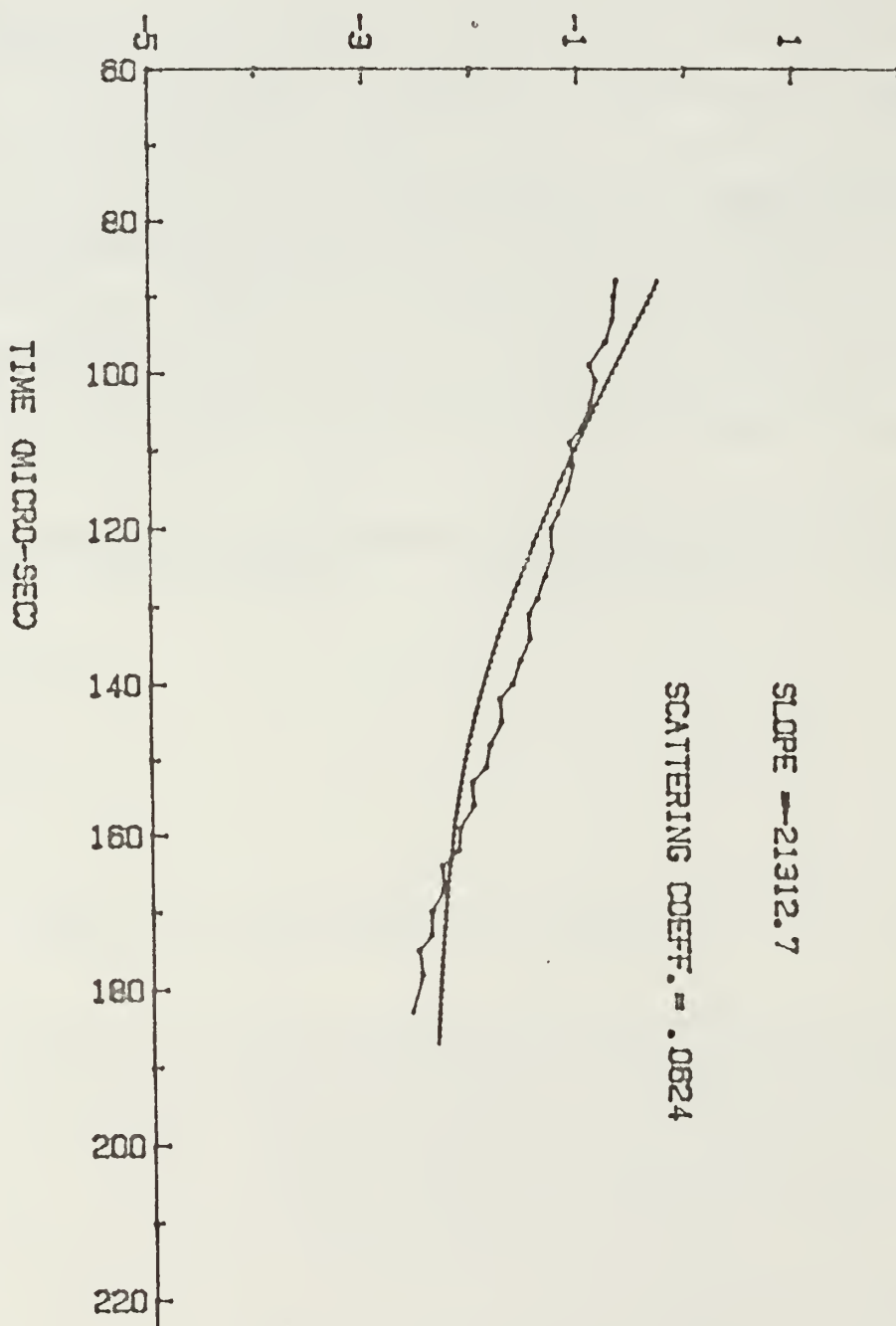


Figure A.1 For the aggregate, the decay envelope obtained from the model vs. the decay envelope obtained from the experiment.

$\ln(\langle \text{VOLTAGE}^2 \rangle^{1/2})$

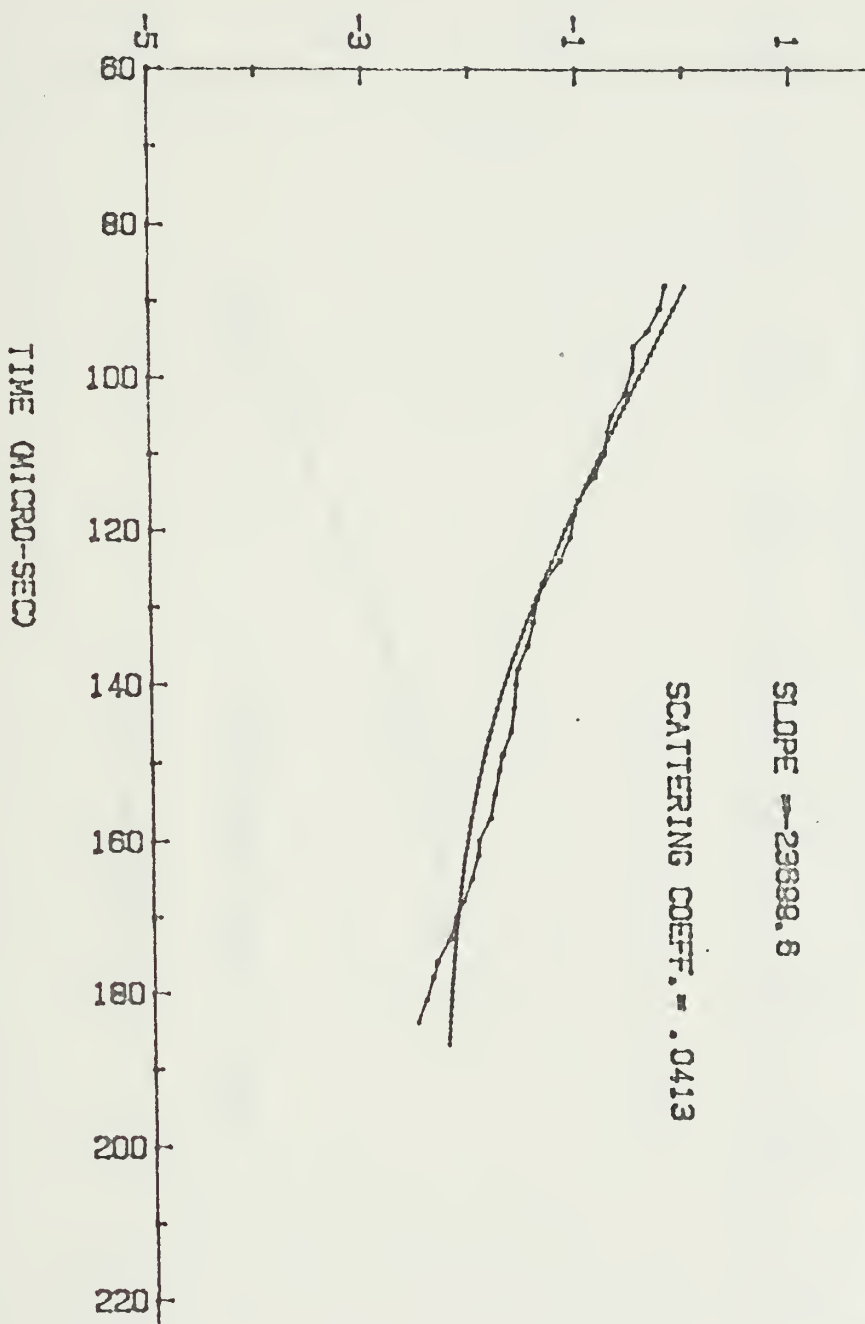


Figure A.2 For the fine sand, the decay envelope obtained from the model vs. the decay envelope obtained from the experiment.

$\text{LN}(\langle \text{VOLTAGE}^2 \rangle^{1/2})$

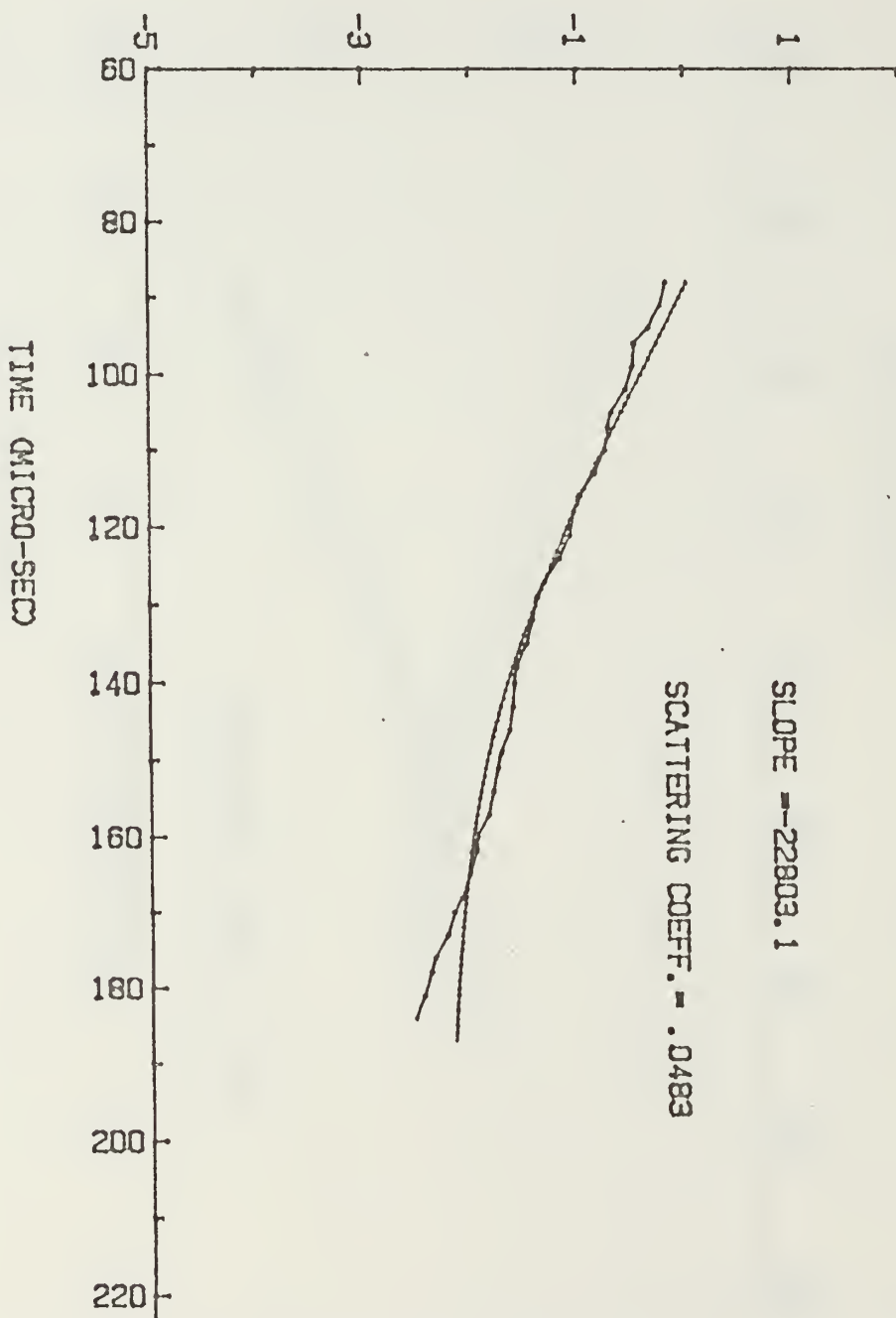


Figure A.3 For the fine sand, the decay envelope obtained from the model vs. the decay envelope obtained from the experiment.

$\ln(\langle \text{VOLTAGE}^2 \rangle^{-1/2})$

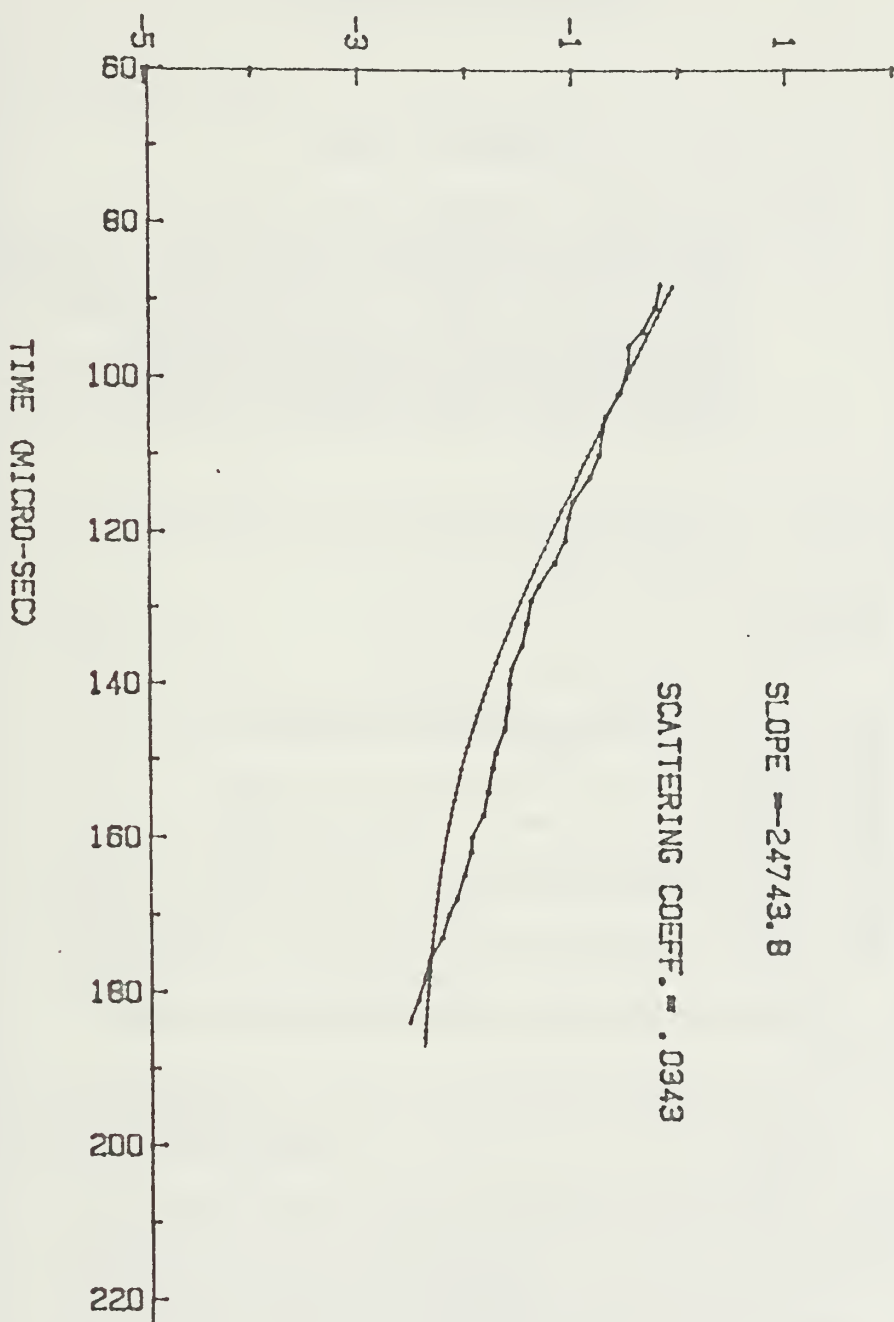


Figure A.4 For the fine sand, the decay envelope obtained from the model vs. the decay envelope obtained from the experiment.

## APPENDIX B

### COMPUTER PROGRAM

```

2292 !
2300 !
2301 OUTPUT 709 ;"OFN4"
2302 !
2303 ! ABOVE STATEMENT IS LET THE CRT TO "LIVE" CONDITION
2304 !
2305 !
2306 ! FOLLOWING ONE IS TO LET THE CRT IN "STORE" CONDITION
2307 !
2308 !
2310 OUTPUT 709 ;"CLS5"
2311     WAIT 1000
2312 !
2313 ! FRESS BOTTOM ONLY USED WITHOUT THE HF-3421 UNIT
2314 ! DISP "FRESS 3091 BUTTON"
2315 !
2316 ! LET THE DATA TRASMIT TO THE COMPUTER THROUGHR RS-232
2320 !
2321 OUTPUT 709 ;"CLS2"
2322 !
2323 ! ABOVE STATEMENT LET THE WAVEFORM INFORMATION BE TRANSFERED
2324 ! FROM CRT TO COMPUTER THROUGH RS-232 INTERFACE
2325 !
2340 ENTER 10 : I†
2360 ENTER 10 : D†
2380 ENTER 10 : N†
2390 !
2400 H0=VAL (NF[16,20])
2420 V1=(VAL (NF[21,25])-5)*10^(VAL (NF[26,30])-12)
2440 H1=(VAL (NF[31,35])-5)*10^(VAL (NF[36,40])-12)
2441 !
2443 OUTPUT 709 ;"OFN5"
2445 OUTPUT 709 ;"OFN2"
2446 ! LET THE CRT IN LIVE MODE
2447 OUTPUT 709 ;"CLS4"
2450 J=1
2480 K=5
2500 PRINT "N=",N
2520 FOR I=0 TO END†
2525 IF I<START OR I>ENDT THEN 2780
2530 !
2531 ! NORMALIZE THE VOLTAGE VALUE AND TIME FOR THE INTEREST INTERVAL
2532 !
2540 D(I)=VAL (D†[J,K])*V1
2560 T(I)=(I-H0)*H1
2580 D(I)=D(I)^2
2600 IF N=1 THEN GOTO 2640
2620 S(I)=((N-1)*S(I)+D(I))/N
2621 !
2640 IF N=1 THEN S(I)=D(I)
2660 IF I=START THEN 2760 ELSE 2680
2680 IF I=START+20 THEN 2760 ELSE 2700
2700 IF I=START+30 THEN 2760 ELSE 2720
2720 IF I=START+50 THEN 2760 ELSE 2740
2740 IF I=ENDT THEN 2760 ELSE 2780
2760 DISP T(I); "SEC    ";D(I); "VOLT   ";S(I)
2770 PRINT T(I); "SEC    ";D(I); "VOLT   ";S(I)
2771 !
2780 J=J+5
2800 K=K+5

```

```

2820 NEXT I
2840 N=N+1
2950 !
2951 ! LET THE DATA BEING STORE AFTER EVERY 10 SET OF CALCULATION
2952 !
2960 IF N MOD 10=1 THEN 2965 ELSE 2240
2965 IF N=11 THEN 2970 ELSE 2980
2970   CREATE VDATA$,200,8
2971   CREATE VCOUNT$,1,8
2972   CREATE VTIME$,200,8
2980 GOSUB WRITE_DISK
2990 IF N=51 THEN 3000 ELSE 2240
3000 END
3305 !
3306 !
3307 !
3308 ! FOLLOWING SUBROUTINE IS USED TO WRITE THE DATA TO THE DISK
3309 !
3310 !
3500 WRITE_DISK:
3510   PURGE VDATA$
3520 CREATE VDATA$,200,8
3540 ASSIGN# 1 TO VDATA$
3550 PURGE VCOUNT$
3560 CREATE VCOUNT$,1,8
3580 ASSIGN# 2 TO VCOUNT$
3590 PURGE VTIME$
3600 CREATE VTIME$,200,8
3620 ASSIGN# 3 TO VTIME$
3640 FRINT# 2 : N
3660 FOR I=START TO ENDT
3680 FRINT# 3 : T(I)
3700 FRINT# 1 : S(I)
3720 NEXT I
3740 ASSIGN# 1 TO *
3760 ASSIGN# 2 TO *
3780 ASSIGN# 3 TO *
3800 RETURN
3900 !
3910 !
3920 ! FOLLOWING SURROUTINE IS USED TO READ THE DATA FROM PREVIOUS
3930 ! WRITTEN DISK
3940 !
3950 !
4000 READ_DATA:
4020 ASSIGN# 2 TO VCOUNT$
4040 ASSIGN# 1 TO VDATA$
4060 READ# 2 : N
4061 PRINT N
4080 FOR I=START TO ENDT
4100 READ# 1 : S(I)
4120 IF I=START THEN 4220 ELSE 4140
4140 IF I=START+20 THEN 4220 ELSE 4160
4160 IF I=START+40 THEN 4220 ELSE 4180
4180 IF I=START+50 THEN 4220 ELSE 4200
4200 IF I=ENDT THEN 4220 ELSE 4240
4220 PRINT S(I)
4240 NEXT I
4260 ASSIGN# 1 TO *
4280 ASSIGN# 2 TO *
4380 RETURN

```

```

800      ! ! ! ! ! ! ! ! ! ! ! ! ! ! ! ! ! ! ! ! ! ! ! ! ! ! ! ! ! ! ! ! ! ! !
801      !
802      !
803      ! ! ! ! ! ! ! ! ! ! ! ! ! ! ! ! ! ! ! ! ! ! ! ! ! ! ! ! ! ! ! ! !
804      ! ! ! ! ! ! ! ! ! ! ! ! ! ! ! ! ! ! ! ! ! ! ! ! ! ! ! ! ! ! ! ! !
805      ! ! ! ! ! ! ! ! ! ! ! ! ! ! ! ! ! ! ! ! ! ! ! ! ! ! ! ! ! ! ! ! !
806      ! ! ! ! ! ! ! ! ! ! ! ! ! ! ! ! ! ! ! ! ! ! ! ! ! ! ! ! ! ! ! ! !
807      ! ! ! ! ! ! ! ! ! ! ! ! ! ! ! ! ! ! ! ! ! ! ! ! ! ! ! ! ! ! ! ! !
808      ! ! ! ! ! ! ! ! ! ! ! ! ! ! ! ! ! ! ! ! ! ! ! ! ! ! ! ! ! ! ! ! !
809      ! ! ! ! ! ! ! ! ! ! ! ! ! ! ! ! ! ! ! ! ! ! ! ! ! ! ! ! ! ! ! ! !
810      ! ! ! ! ! ! ! ! ! ! ! ! ! ! ! ! ! ! ! ! ! ! ! ! ! ! ! ! ! ! ! ! !
811      ! ! ! ! ! ! ! ! ! ! ! ! ! ! ! ! ! ! ! ! ! ! ! ! ! ! ! ! ! ! ! ! !
812      !
813      !
814      ! ! ! ! ! ! ! ! ! ! ! ! ! ! ! ! ! ! ! ! ! ! ! ! ! ! ! ! ! ! ! ! !
815      !
816      !
880      DIM VDATA$[20],VTIME$[20],VNUMBER$[20],VTIME_MAX$[20],VMAXIMUMS$[20]
900      DISP "WHAT IS THE NAME FOR VOLTAGE DATA FILE ?"
910      INPUT VDATA$
920      DISP "WHAT IS THE NAME FOR TIME DATA FILE ?"
930      INPUT VTIME$
940      DISP "WHAT IS THE NAME FOR FILE TO STORE THE NUMBER$ NO. ?"
950      INPUT VNUMBER$
960      DISP "WHAT IS THE NAME FOR FILE TO STORE THE TIME_MAX$ DATA ?"
970      INPUT VTIME_MAX$
980      DISP "WHAT IS THE NAME FOR FILE TO STORE THE MAXIMUMS$ ?"
990      INPUT VMAXIMUMS$
991      DISP "WHAT IS THE STARTING TIME OF YOUR DATA COLLECTING ?"
992      INPUT START
993      DISP "WHAT IS THE ENDING TIME OF THE DATA COLLECTING ?"
994      INPUT ENDT
996      !
1000      ASSIGN# 1 TO VDATA$
1020      ASSIGN# 3 TO VTIME$
1040      CREATE VNUMBER$,1,8
1060      ASSIGN# 4 TO VNUMBER$
1080      CREATE VTIME_MAX$,100,B
1100      ASSIGN# 5 TO VTIME_MAX$
1120      CREATE VMAXIMUMS$,100,B
1140      ASSIGN# 6 TO VMAXIMUMS$
1141      !
1144      INTEGER PRINTER
1146      DISP "WHAT IS THE PRINTER DEVICE ADDRESS NO. ?"
1148      ! INPUT THE PRINTER NO. SCREEN IS 1
1150      INPUT PRINTER
1152      PRINTER IS PRINTER
1154      !
1160      DIM S(1501),T(1501),TIM(100),MAXS(100)
1165      PRINT USING 1170 ; "TIME (SEC.)","VOLT"
1170      IMAGE 25X,11A,12X,4A
1180      INTEGER I,J
1200      FOR I=START TO ENDT
1220      READ# 3 : T(I)
1240      READ# 1 : S(I)
1260      NEXT I
1280      LET J=0
1290      !
1291      ! IF THE FIRST DATA BEING READ IS GREAT THAN THE SECOND ONE,

```

```

1292 ! THE FIRST ONE IS TREATED AS A LOCAL MAXIMUM.
1293 !
1300 IF S(START)>= S(START+1) THEN 1320 ELSE 1500
1320   TIM(J)=T(START)
1340   MAXS(J)=SQR (S(START))
1360 PRINT# 5 : TIM(J)
1380 PRINT# 6 : MAXS(J)
1400 PRINT USING 1410 : "J=";J,TIM(J),MAXS(J)
1410 IMAGE 12X,3A,DDD,7X,D.DDDDDD,11X,D.DDDDDDDD
1420 ! PRINT TIM(J)
1440 ! PRINT MAXS(J)
1460   J=J+1
1480 !
1500 FOR I=START+1 TO ENDT-1
1520   IF S(I)>= S(I-1) AND S(I)>= S(I+1) THEN 1540 ELSE 1720
1540     TIM(J)=T(I)
1560     MAXS(J)=SQR (S(I))
1580 !
1600 PRINT USING 1610 : "J=";J,TIM(J),MAXS(J)
1610 IMAGE 12X,3A,DDD,7X,D.DDDDDD,11X,D.DDDDDDDD
1620 ! PRINT TIM(J)
1640 ! PRINT MAXS(J)
1660 PRINT# 5 : TIM(J)
1680 PRINT# 6 : MAXS(J)
1700 J=J+1
1720 NEXT I
1730 J=J-1
1740 PRINT# 4 : J
1760 ASSIGN# 4 TO *
1800 ASSIGN# 5 TO *
1820 ASSIGN# 6 TO *
1840 ASSIGN# 1 TO *
1880 ASSIGN# 3 TO *
1900 END

```

```

900
901
903
904 PROGRAM : PLOT3
905
906
907 ! ! THIS PROGRAM IS DESIGNED TO PLOT THE ENVELOP
908 ! ! OF WAVEFORM BY READING DATA FROM DATA DISK.
909 ! ! AFTER READING, VOLTAGE DATA IS CONVERTED TO LOG
910 ! ! VALUE, THEN BE PLOTTED. AFTER PLOTTING, A LEAST-
911 ! ! SQUARE METHOD IS USED TO FIND THE BEST FIT STRAIGHT
912 ! ! LINE FOR THE LOG-ENSEMBLE. PLOT THE LINE, PRINT
913 ! ! OUT THE SLOPE OF THE LINE AND THE CORRELATION
914 ! ! COEFFICIENT.
915 !
916 !
917 !
918 !
919 !
1000 CLEAR
1020 GCLEAR
1022 INTEGER PLOTTER
1024 DISP "WHAT IS YOUR PLOTTER DEVICE ADDRESS NO. ?"
1025 ! INPUT THE PLOTTER NO. SCREEN IS 1
1026 INPUT PLOTTER
1028 PLOTTER IS PLOTTER
1040 FRAME
1041 !
1042 ! THIS PLOT SIZE IS TO FIT THE REQUIREMENT FOR THE NFS THESIS
1043 !
1060 LOCATE 30,125,30,85
1080 CSIZE 3
1100 MOVE 50,20
1120 LABEL "TIME (MICRO-SEC)"
1140 PEN UP
1160 MOVE 18,40
1180 DEG
1200 LDIR 90
1220 LABEL "LN((VOLTAGE^2)^1/2)"
1240 PEN UP
1241 !
1242 ! DEFAULT SET-UP IS TO FIX THE PLOTTING COORDINATION AS
1243 ! X-AXIS IS FROM 500 TO 670 (MICRO-SEC), Y-AXIS IS FROM
1244 ! -5 TO 2
1245 !
1250 DISP "DO YOU WANT TO USE DEFAULT SET-UP ? YES=0"
1251 INPUT BULL
1252 IF BULL=0 THEN 1253 ELSE 1260
1253 SCALE 500,670,-5,2
1255 LAXES 10,.5,500,-5,2,2
1256 XMIN=500
1257 GOTO 1710
1259 !
1260 DISP "ENTER THE XMIN OF SCALE"
1280 INPUT XMIN
1300 DISP "ENTER XMAX OF SCALE"
1320 INPUT XMAX
1340 DISP "ENTER THE YMIN OF SCALE"
1360 INPUT YMIN

```

```

1380 DISP "ENTER THE YMAX OF SCALE "
1400 INPUT YMAX
1420 SCALE XMIN,XMAX,YMIN,YMAX
1440 FXD 0,2
1460 DISP "ENTER THE X-TICKING SPACE"
1480 INPUT XT
1500 DISP "ENTER THE Y-TICKING SPACE"
1520 INPUT YT
1540 DISP "ENTER THE X INTERSECTION"
1560 INPUT XI
1580 DISP "ENTER THE Y INTER SECTION"
1600 INPUT YI
1620 DISP "ENTER THE X-MAJOR COUNT"
1640 INPUT XMC
1660 DISP "ENTER THE Y-MAJOR COUNT"
1661 !
1680 INPUT YMC
1700 LAXES XT,YT,XI,YI,XMC,YMC
1710 GRAPH
1720 PEN 1
1721 !
1740 DIM TIM(100),MAXS(100)
1741 DIM TIMEMAX$(20),MAXIMUM$(20)
1742 DISP "WHAT IS YOUR FILE NAME FOR TIMEMAX$ ?"
1744 INPUT TIMEMAX$
1746 DISP "WHAT IS YOUR FILE NAME FOR MAXIMUM$ ?"
1748 INPUT MAXIMUM$
1749 PRINT "THE DATA FILES ARE",TIMEMAX$,"AND",MAXIMUM$
1750 DISP "WHAT IS THE HIGHEST ORDER OF ARRAY NUMBER?"
1751 ! THIS GIVES A CHOICE TO CHOOSE THE END POINT OF PLOT
1752 INPUT JK
1753 !
1760 ASSIGN# 5 TO TIMEMAX$
1780 ASSIGN# 6 TO MAXIMUM$
1781 DISP "PRESS 0 IF THE FIRST LOCAL MAXIMUM IS BEING SAVED ?"
1782 INPUT OK
1790 FOR I=0 TO JK
1800 READ# 5 : TIM(I)
1802 !
1803 ! CONVERT THE TIME UNIT FROM SEC TO MICRO_SEC
1804 !
1810 TIM(I)=TIM(I)*1000000
1820 READ# 6 : MAXS(I)
1821 MAXS(I)=LOG (MAXS(I))
1822 ! CONVERT THE VOLTAGE TO NATURE LOG VALUE
1823 NEXT I
1825 K=JK+1
1826 IF OK=0 THEN GOTO 1835
1828 FOR I=1 TO JK
1831 TIM(I-1)=TIM(I)
1832 MAXS(I-1)=MAXS(I)
1833 NEXT I
1834 K=JK
1835 ! DISP "WHICH CHARACTER YOU PREFER TO USING IN PLOTTING THE DATA?"
1837 ! INPUT C$
1839 MOVE TIM(0),MAXS(0)
1840 FOR I=0 TO K-1
1920 DRAW TIM(I),MAXS(I)
1930 ! LABEL C$
1940 NEXT I

```

```

1960 FEN UP
1961 !
1962 GOSUB LEASTSQR
1980 ASSIGN# 5 TO *
2000 ASSIGN# 6 TO *
2020 END
2900 !
2910 !
2920 !      FOLLOWING SUBROUTINE IS DESIGNED TO APPLY THE LEAST
2922 !      SQUARE METHOD IN THE ABOVE DATA AND THE PLOT THE
2924 !      BEST FIT STRAIGHT LINE, PRINT OUT THE SLOPE AND
2926 !      THE CORRELATION COEFFICIENT ON THE PLOT.
2928 !      FORMULA USED PLEASE
2930 !
3000 LEASTSQR:
3040 REAL Y,XY,X1,X2,TAVE,YAVE,VARX,VARY,COVXY
3060 LET Y=0
3080 !      Y IS THE SUMMATION OF Y(I) VALUE
3100 LET XY=0
3120 !      XY IS THE SUMMATION OF X(I)*Y(I)
3140 LET X1=0
3160 !      X1 IS THE SUMMATION OF X(I)
3180 LET X2=0
3200 !      X2 IS THE SUMMATION OF X(I)^2
3220 FOR I=0 TO K-1
3240 Y=Y+MAXS(I)
3260 XY=XY+TIM(I)*MAXS(I)
3280 X1=X1+TIM(I)
3300 X2=X2+TIM(I)^2
3320 NEXT I
3340 B=(X2*Y-X1*XY)/(K*X2-X1^2)
3350 !
3351 !
3352 !      A IS THE SLOPE OF THE FITTED STRAIGHT LIGHT
3360 A=(K*XY-X1*Y)/(K*X2-X1^2)
3370 !
3371 !
3372 !      B IS THE INTERCEPT TO Y AXIS
3380 PRINT "THE SLOPE A=";A
3400 PRINT "THE Y-INTERCEPT B=";B
3420 YAVE=(MAXS(0)+MAXS(K-1))/2
3421 !
3422 !      YAVE IS THE AVERAGE VALUE FOR THE LOG VOLTAGE
3423 !
3440 TAVE=(TIM(0)+TIM(K-1))/2
3441 !
3442 !      TAVE IS THE AVERAGE VALUE FOR THE TIME VARIABLE
3443 !
3460 COVXY=0
3461 !
3480 !      COVXY IS THE COVARIANCE OF TIME AND VOLTAGE (LN)
3481 !
3500 VARX=0
3520 !      VARX IS THE VARIANCE OF TIME VARIABLE
3521 !
3540 VARY=0
3560 !      VARY IS THE VARIANCE OF VOLTAGE(LN) VARIABLE
3561 !
3562 DIM YL(100)
3580 FOR I=0 TO K-1

```

```

3600 !
3620 COVXY=COVXY+(TIM(I)-TAVE)*(MAXS(I)-YAVE)
3640 !
3660 VARX=VARX+(TIM(I)-TAVE)^2
3680 !
3700 VARY=VARY+(MAXS(I)-YAVE)^2
3720 !
3740 YL(I)=A*TIM(I)+B
3760 !      YL IS THE VALUE FITTED ON THE STRAIGHT LINE
3780 !
3780 NEXT I
3800 PEN 2
3820 MOVE TIM(0),YL(0)
3840 FOR I=0 TO K-1
3860 DRAW TIM(I),YL(I)
3880 NEXT I
3900 CORCOE=COVXY/SQR (VARX*VARY)
3910 !
3920 !      CORCOE IS THE CORRELATION COEFFICIENT
3940 !
3960 PRINT "CORRELATION COEFFICIENT IS ";CORCOE
3980 PEN 1
3990 DEG
3991 LDIR 0
3994 !
3996 !      FOLLOWING PRINT OUT THE SLOPE AND COORELATION COEFFICIENT
3998 !      ON THE PLOT
3999 !
4000 MOVE XMIN+80,1
4002 !
4004 !      LABLE ALWAYS STARTS FROM THE XMIN+80 IN X COORDINATES
4006 !
4020 LABEL USING 4021 ; "SLOPE =",A
4021 IMAGE 7A,DDD.DDDD
4040 MOVE XMIN+80,2
4060 LABEL USING 4061 ; "CORRELATION COEFF=",CORCOE
4061 IMAGE 19A,DDD.DDDD
4062 PEN UP
4080 RETURN

```

```

800 ! ! ! ! ! ! ! ! ! ! ! ! ! ! ! ! ! ! ! ! ! ! ! ! ! ! ! ! !
810 ! !
820 ! !
830 ! ! PROGRAM : AVERAGE ! !
840 ! !
850 ! ! THIS PROGRAM IS DESIGNED TO AVERAGE ! !
860 ! ! THE DATA SETS TO GET A AVERAGED ! !
870 ! ! WAVEFORM DATA. ! !
880 ! !
890 ! ! ! ! ! ! ! ! ! ! ! ! ! ! ! ! ! ! ! ! ! !
1000 DIM VDAT$[25],VDATA$[25],VDAT1$[25]
1020 DIM V1(1500),V2(1500),V3(1500)
1040 DISP "WHAT IS THE ORIGINAL DATA FILE ? DAT#"
1060 INPUT VDAT$
1080 DISP "WHAT IS THE NEW DATA FILE ? DATA#"
1100 INPUT VDATA$
1120 DISP "WHAT IS THE AVERAGED DATA FILE ? DAT1#"
1140 INPUT VDAT1$
1160 ASSIGN# 1 TO VDAT$
1180 ASSIGN# 2 TO VDATA$
1200 CREATE VDAT1$,8,110
1220 ASSIGN# 3 TO VDAT1$
1230 !
1231 ! N IS THE NUMBER HOW MANY DATA SET BEING AVERGED
1232 !
1240 DISP "WHAT IS YOUR AVERAGE No. N ?"
1260 INPUT N
1261 !
1262 ! AVERAGE ONLY APPLY TO THE SAME ARRAY NO.
1263 !
1270 FOR I=522 TO 621
1271 READ# 1 : V1(I)
1272 NEXT I
1274 FOR I=522 TO 621
1275 READ# 2 : V2(I)
1276 NEXT I
1280 FOR I=522 TO 621
1300 !
1301 ! RUNNING AVERAGE IS ADOPTED
1302 !
1340 V3(I)=((N-1)*V1(I)+V2(I))/N
1360 PRINT# 3 : V3(I)
1371 !
1372 ! PRINT OUT FOLLOWING VALUE AS A CHECKING PURPOSE
1373 !
1380 IF I=522 THEN 1500 ELSE 1400
1400 IF I=553 THEN 1500 ELSE 1420
1420 IF I=600 THEN 1500 ELSE 1440
1440 IF I=621 THEN 1500 ELSE 1520
1500 PRINT V1(I),V2(I),V3(I)
1520 NEXT I
1540 END

```

## APPENDIX C

### DECAY ENVELOPE GRAPHS FOR AGGREGATE

This appendix includes the graphs of the decay envelopes for reflection from aggregate water interface within the glass tank. Figure C.1 to C.9 show the original decay envelopes obtained from different transducer positions. The decay envelopes are also described as following data sets:

- data set 42
- data set 43
- data set 44
- data set 45
- data set 46
- data set 47
- data set 48
- data set 49
- data set 50

Figures C.10 to C.18 are the decay envelopes resulted from the running average method. They are also described as following data sets:

- data set DAT2
- data set DAT3
- data set DAT4
- data set DAT5
- data set DAT6
- data set DAT7
- data set DAT8
- data set DAT9
- data set DAT10

$\text{LN}((\langle \text{VOLTAGE}^2 \rangle)^{1/2})$

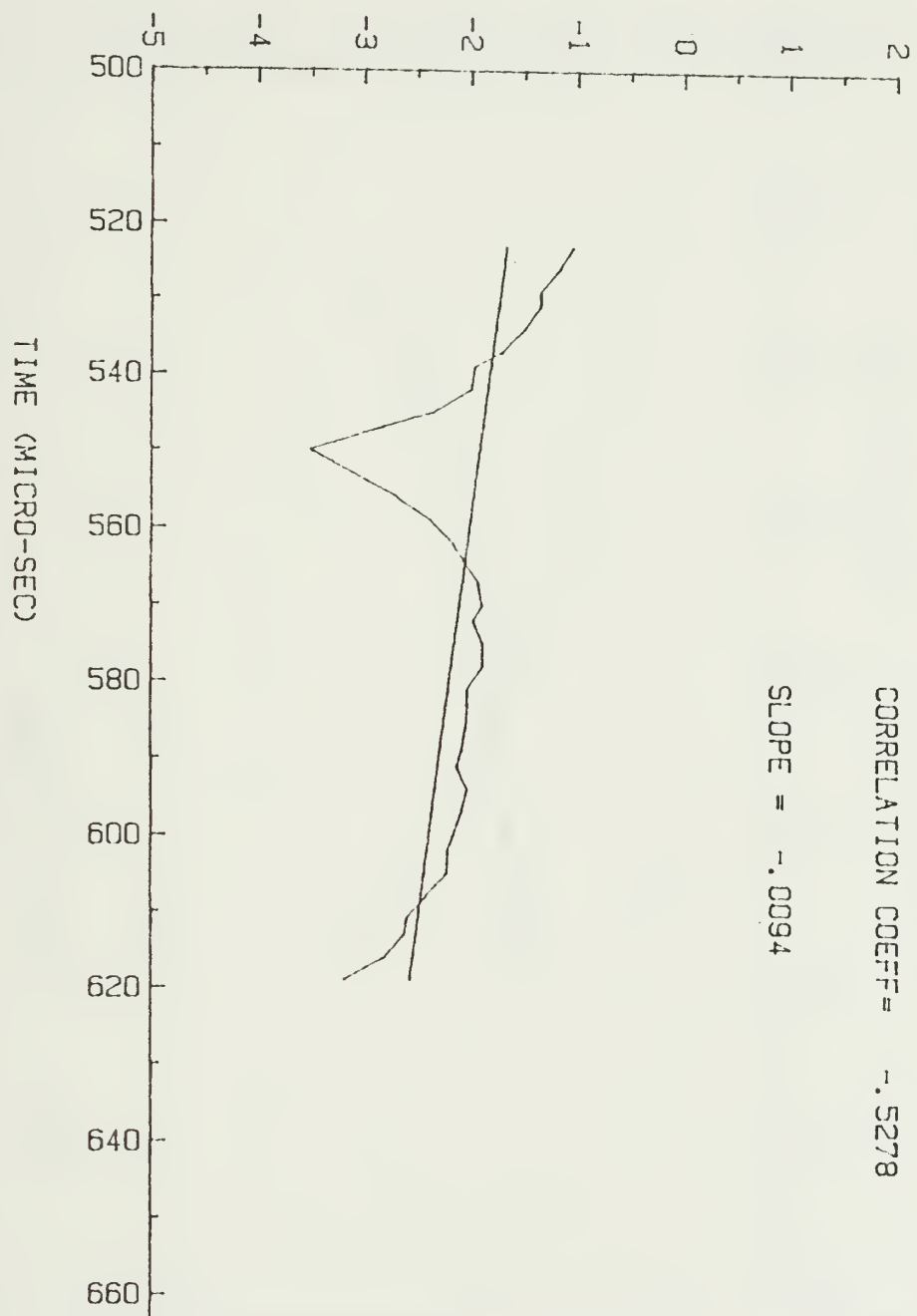


Figure C.1 Decay envelope for reflection from aggregate/water interface, transducer was 30 cm above surface (data set 42).

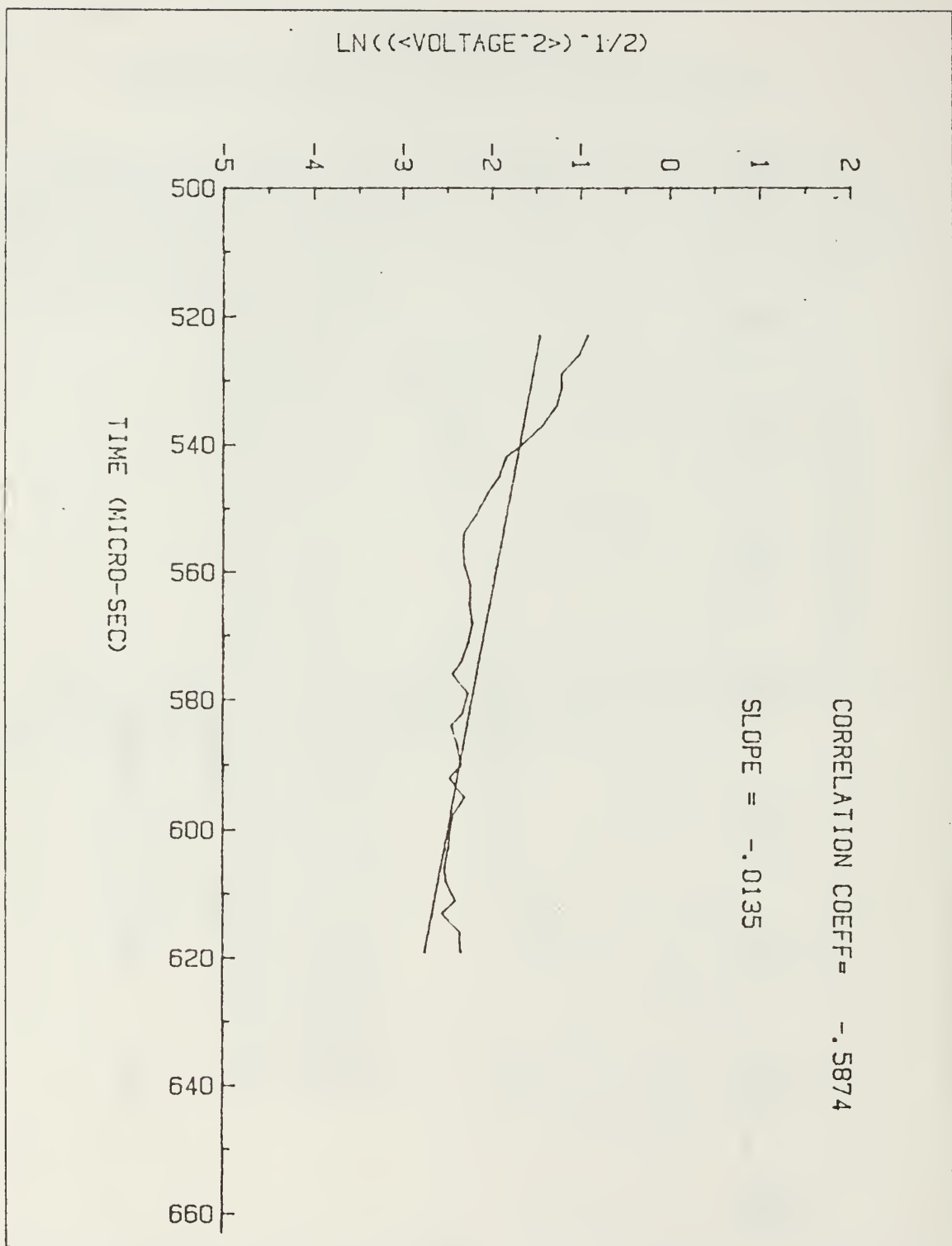


Figure C.2 Decay envelope for reflection from aggregate/water interface, transducer was 30 cm above surface (data set 43).

LN(( $\langle VOLTAGE^2 \rangle$ ) $^{1/2}$ )

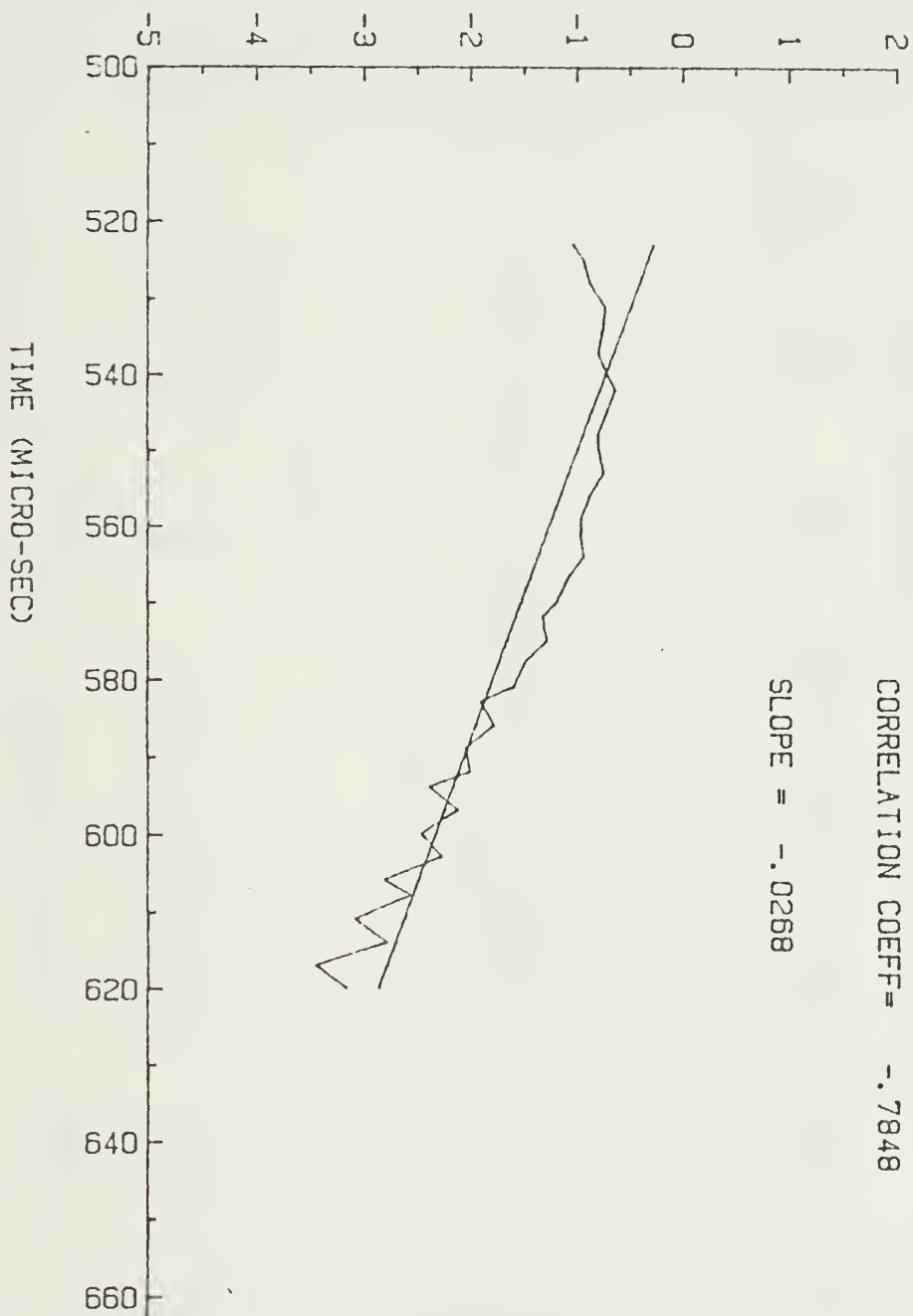


Figure C.3 Decay envelope for reflection from aggregate/water interface, transducer was 30 cm above surface (data set 44).

$\text{LN}((\langle \text{VOLTAGE}^2 \rangle)^{1/2})$

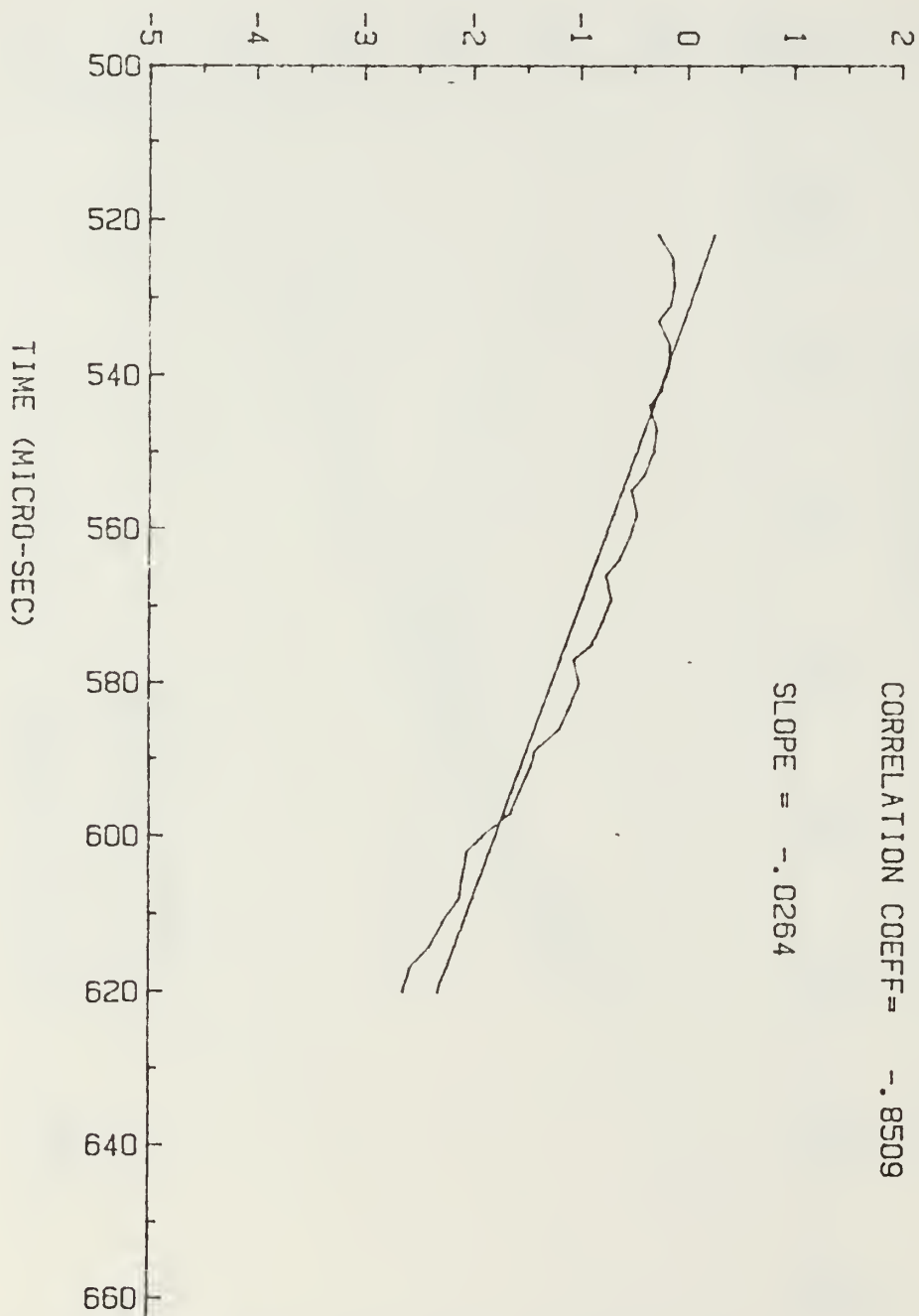


Figure C.4 Decay envelope for reflection from aggregate/water interface, transducer was 30 cm above surface (data set 45).

$\text{LN}((\langle \text{VOLTAGE}^2 \rangle)^{1/2})$

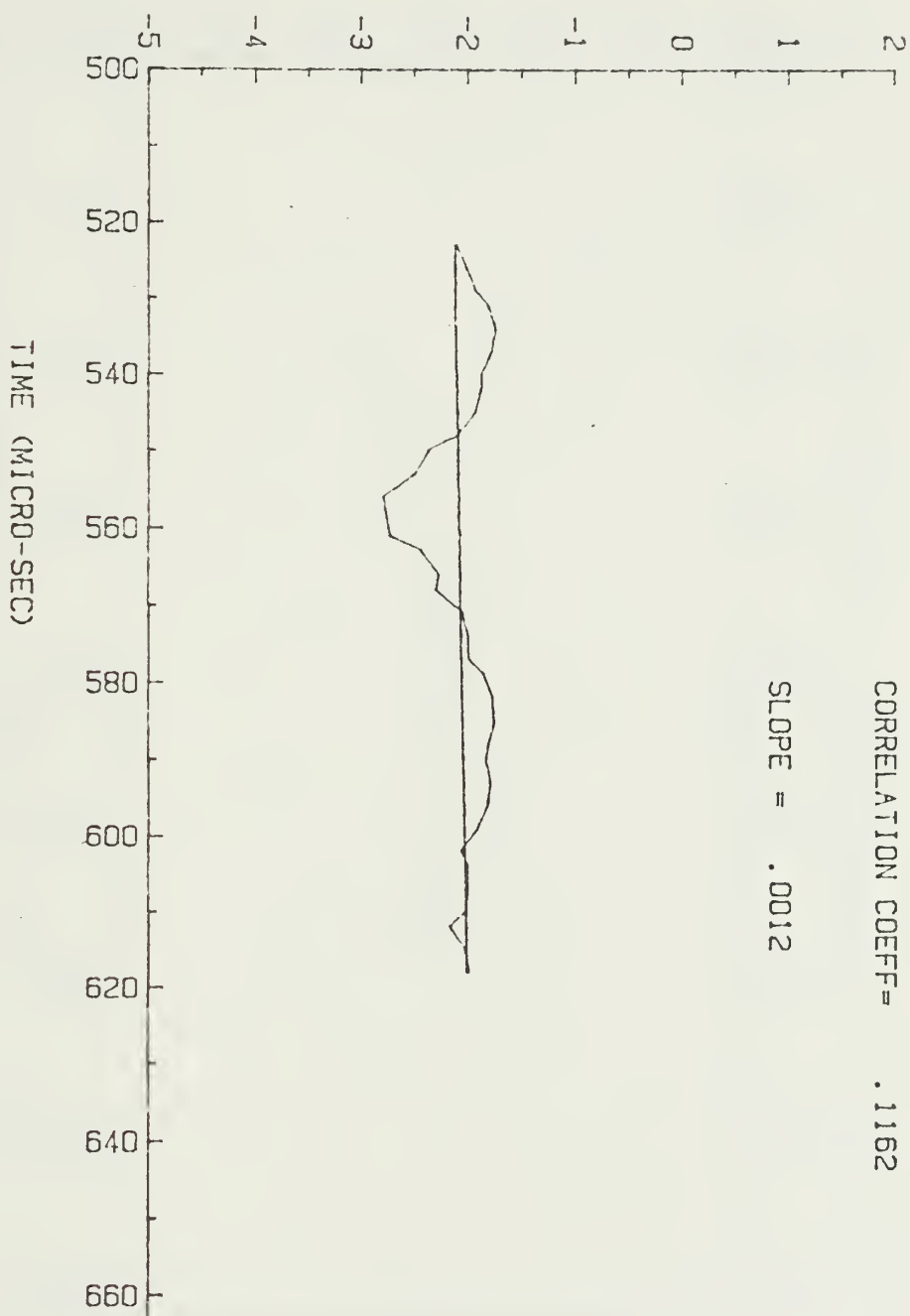


Figure C.5 Decay envelope for reflection from aggregate/water interface, transducer was 30 cm above surface (data set 46).

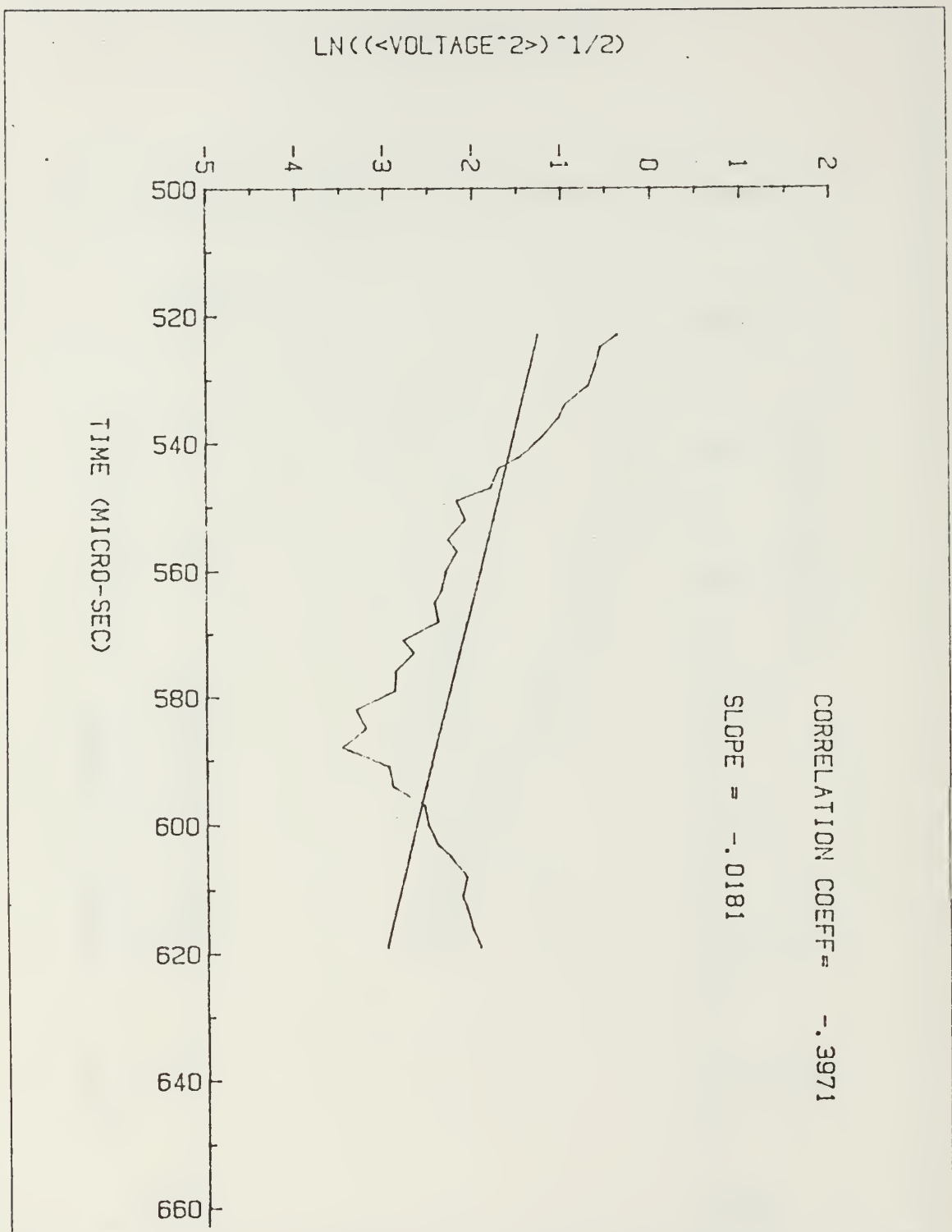


Figure C.6 Decay envelope for reflection from aggregate/water interface, transducer was 30 cm above surface (data set 47).

$\text{LN}((\langle \text{VOLTAGE}^2 \rangle)^{1/2})$

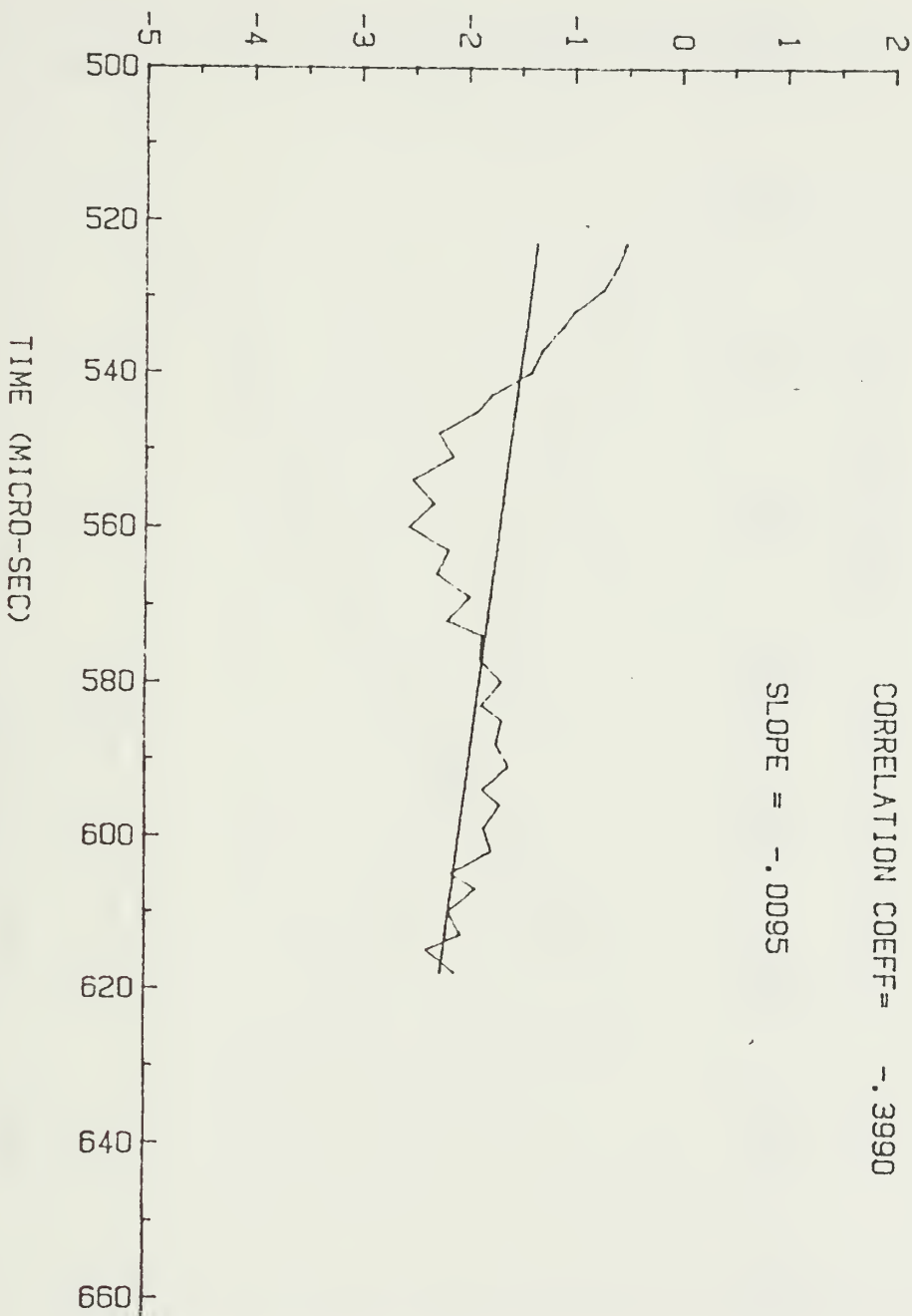


Figure C.7 Decay envelope for reflection from aggregate/water interface, transducer was 30 cm above surface (data set 48).

LN(( $<\text{VOLTAGE}^2>$ )  $^{1/2}$ )

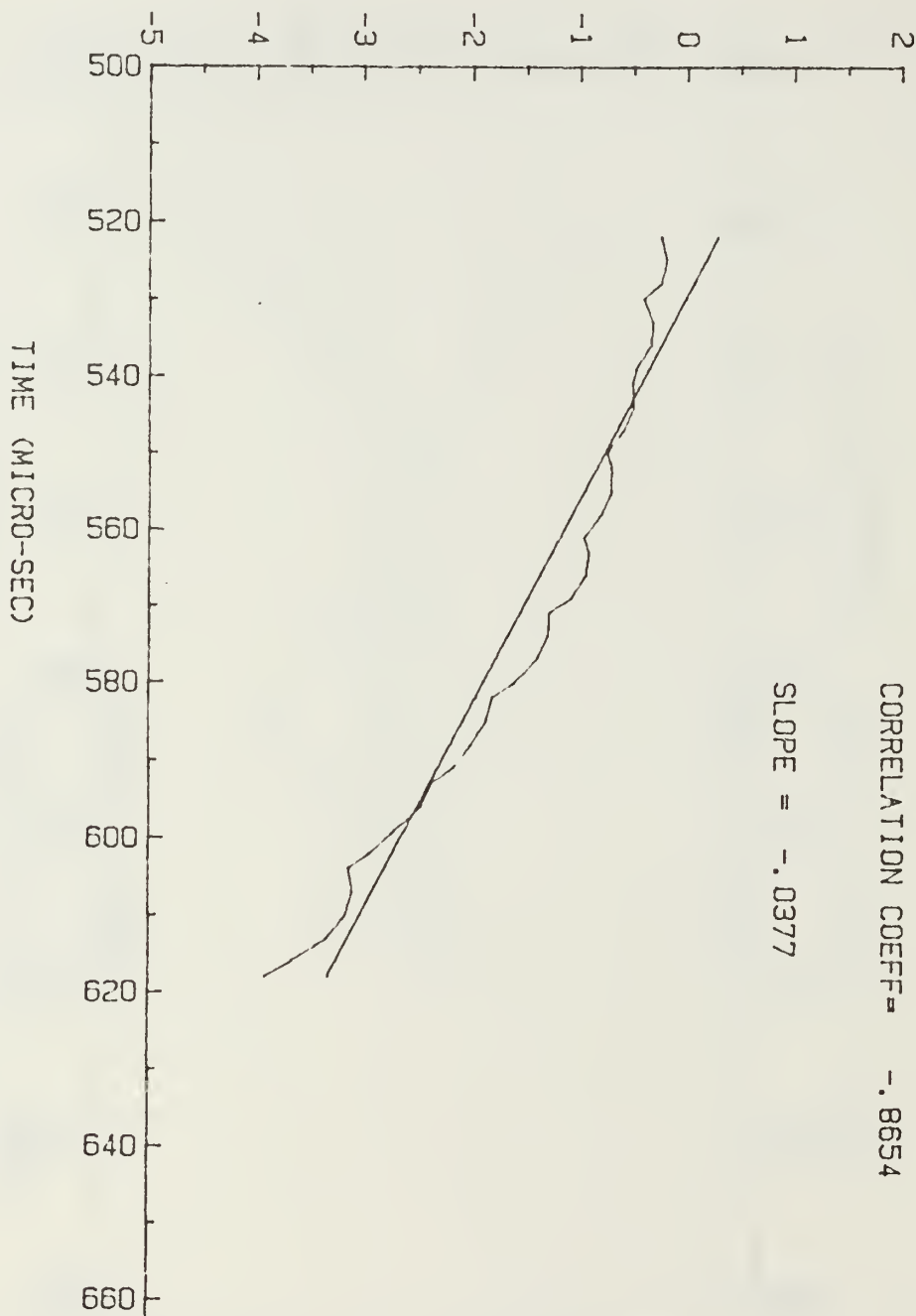


Figure C.8 Decay envelope for reflection from aggregate/water interface, transducer was 30 cm above surface (data set 49).

LN(( $\langle VOLTAGE^2 \rangle$ ) $^{1/2}$ )

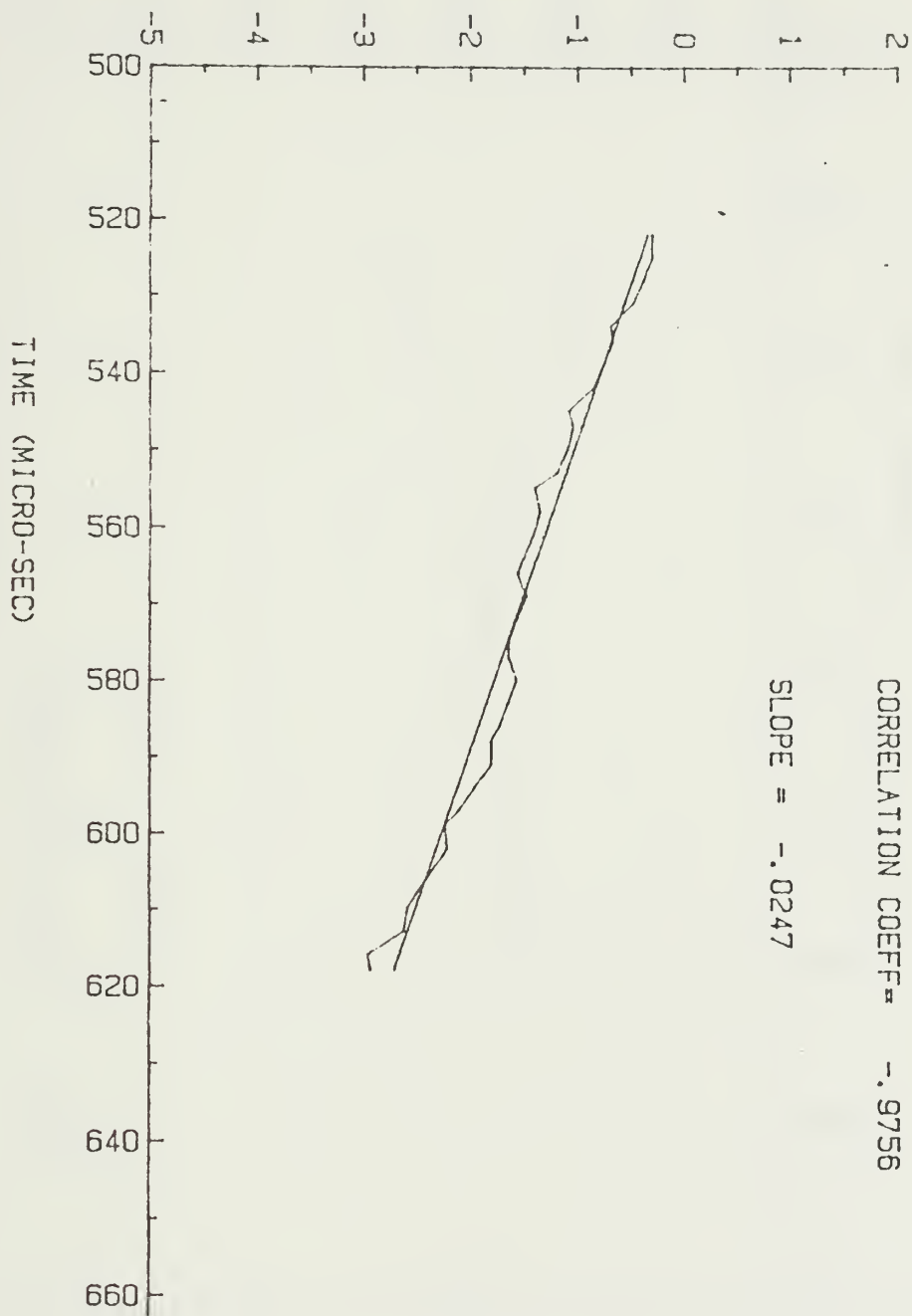


Figure C.9 Decay envelope for reflection from aggregate/water interface, transducer was 30 cm above surface (data set 50).

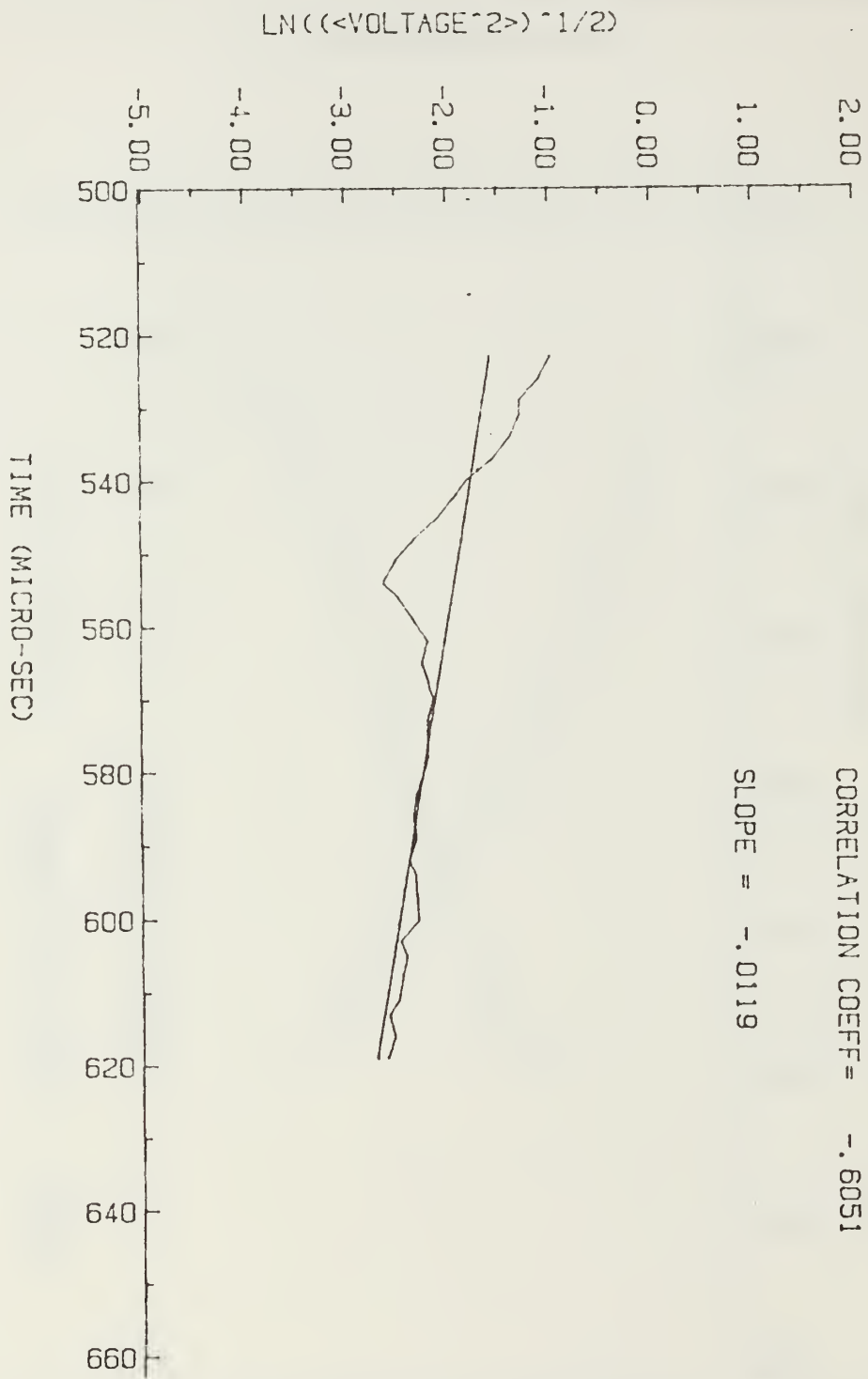


Figure C.10 Decay envelope resulted from the average of data set 42 and 43 for the aggregate/water surface (data set DAT2).

LN(( $\langle VOLTAGE^2 \rangle$ ) $^{1/2}$ )

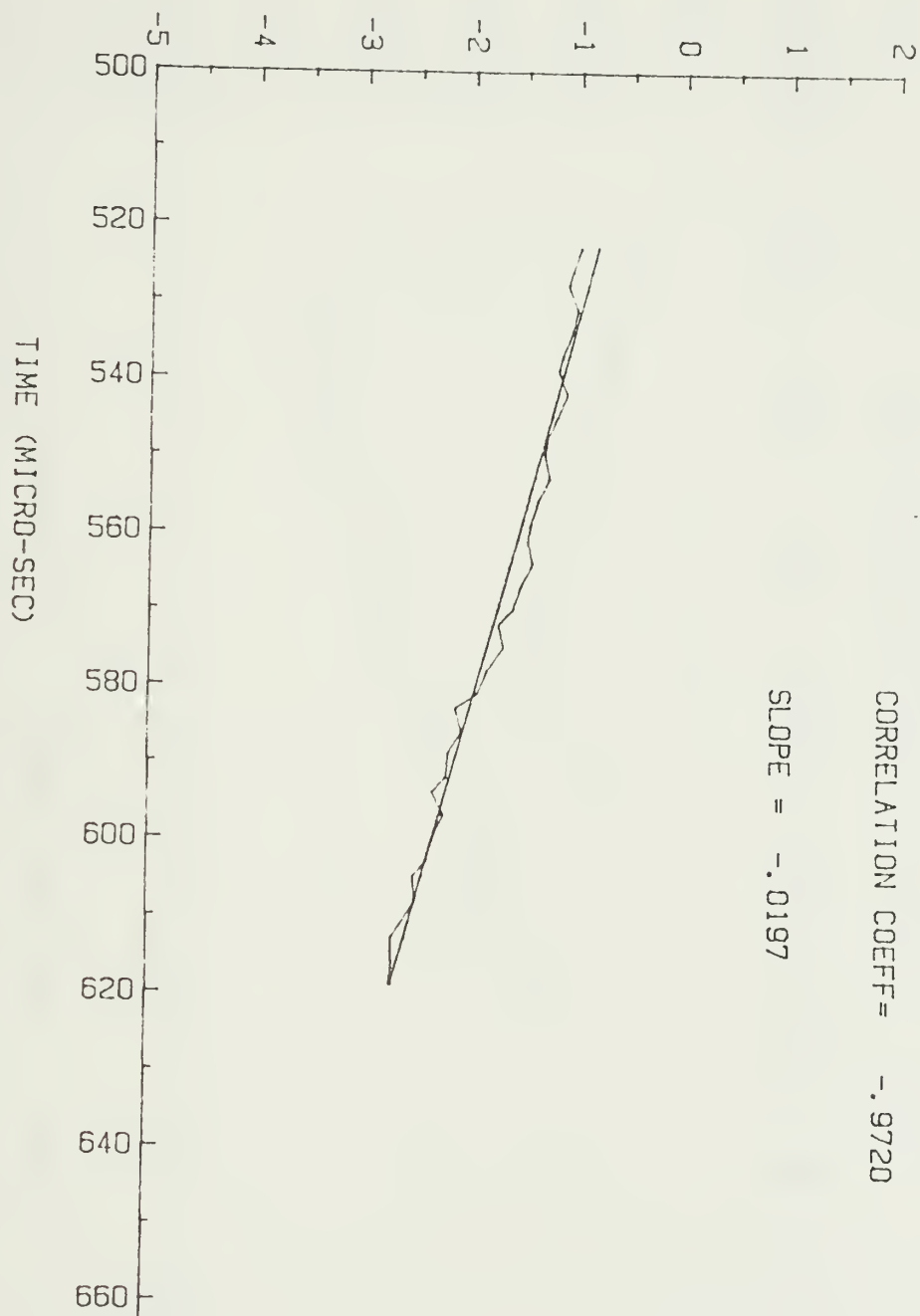


Figure C.11 Decay envelope resulted from the average from data set 42 to 44 for the aggregate/water surface (data set DAT3).

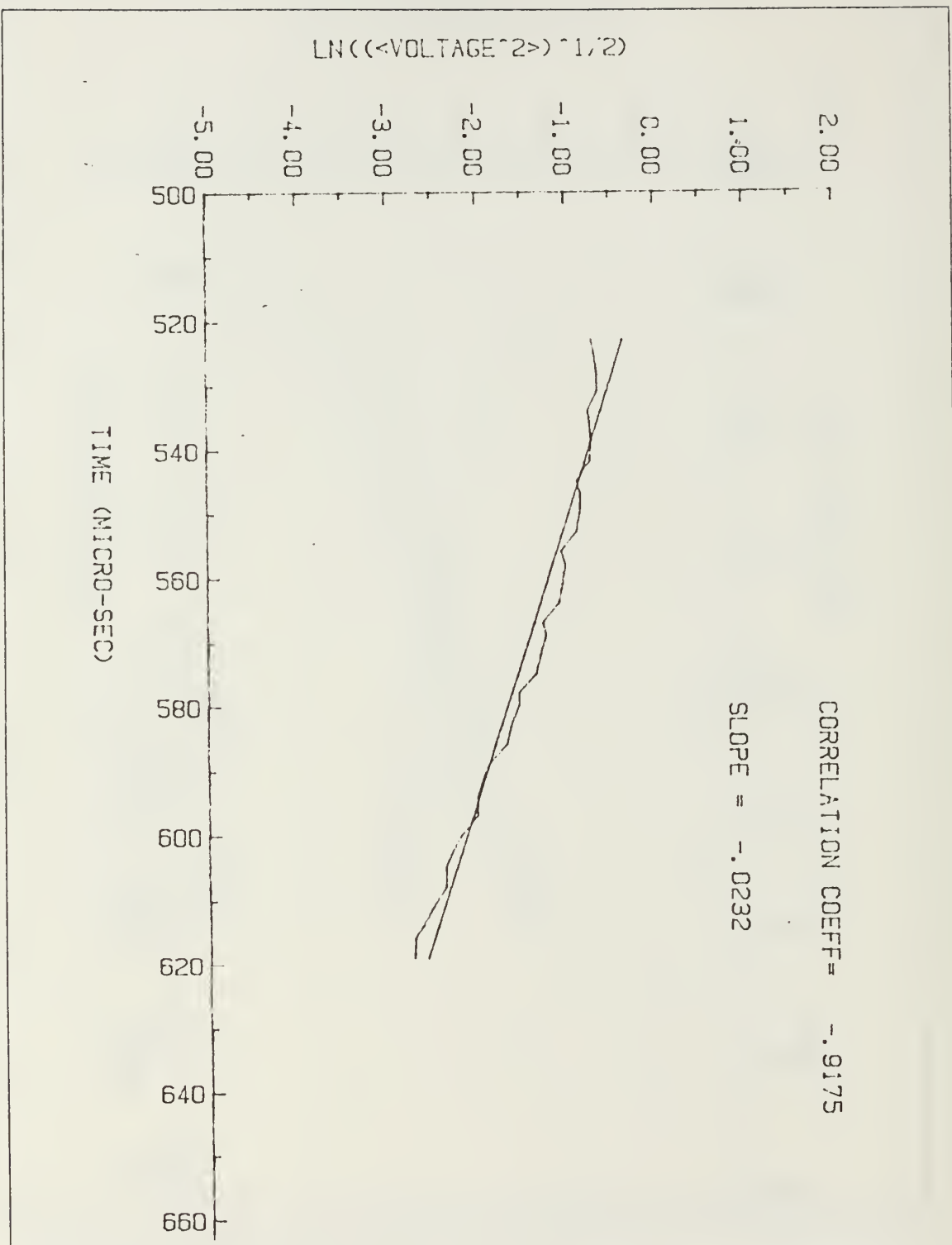


Figure C.12 Decay envelope resulted from the average from data set 42 to 45 for the aggregate/water surface (data set DAT4).

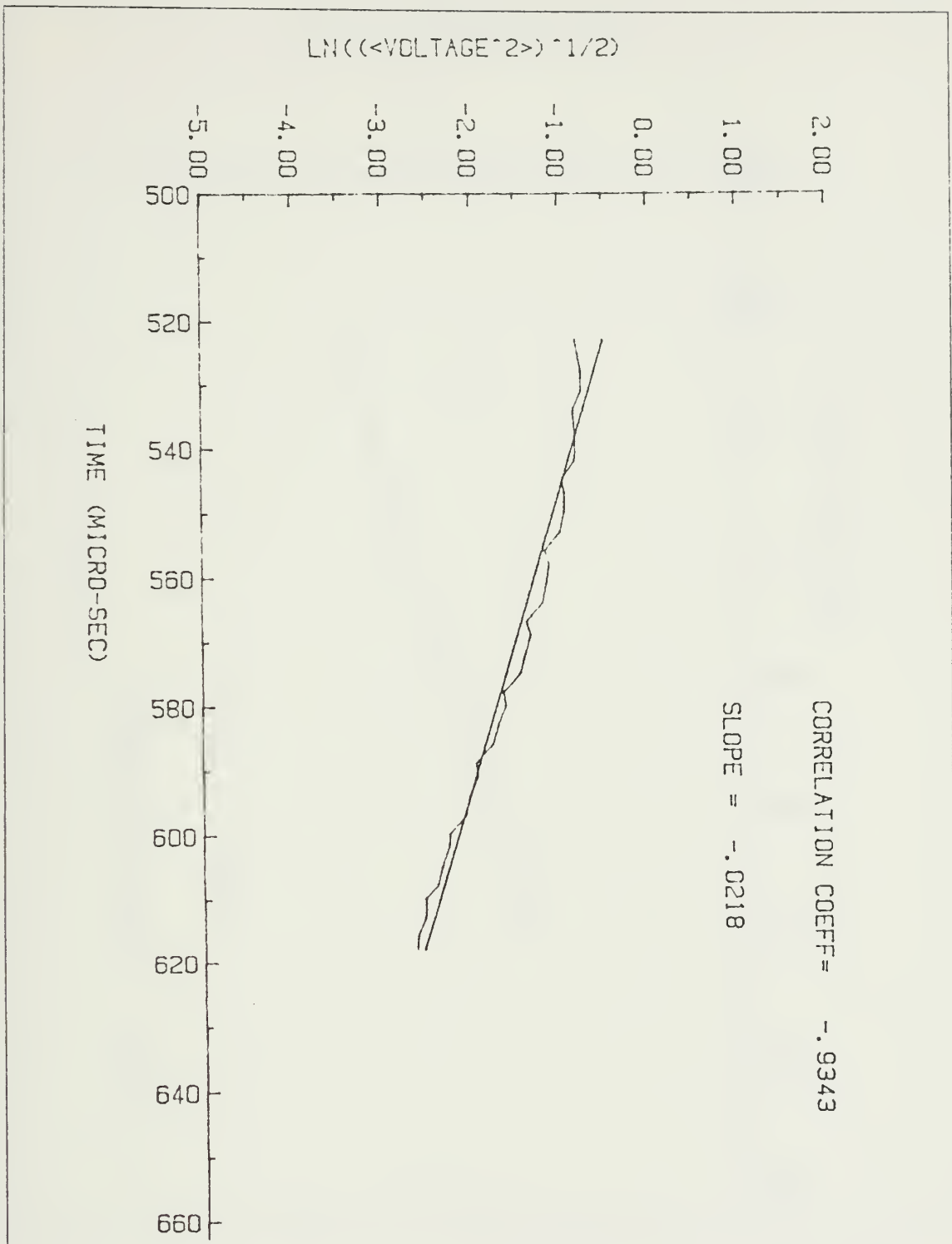


Figure C.13 Decay envelope resulted from the average from data set 42 to 46 for the aggregate/water surface (data set DAT5).

LN(( $\langle VOLTAGE^2 \rangle$ )  $^{1/2}$ )

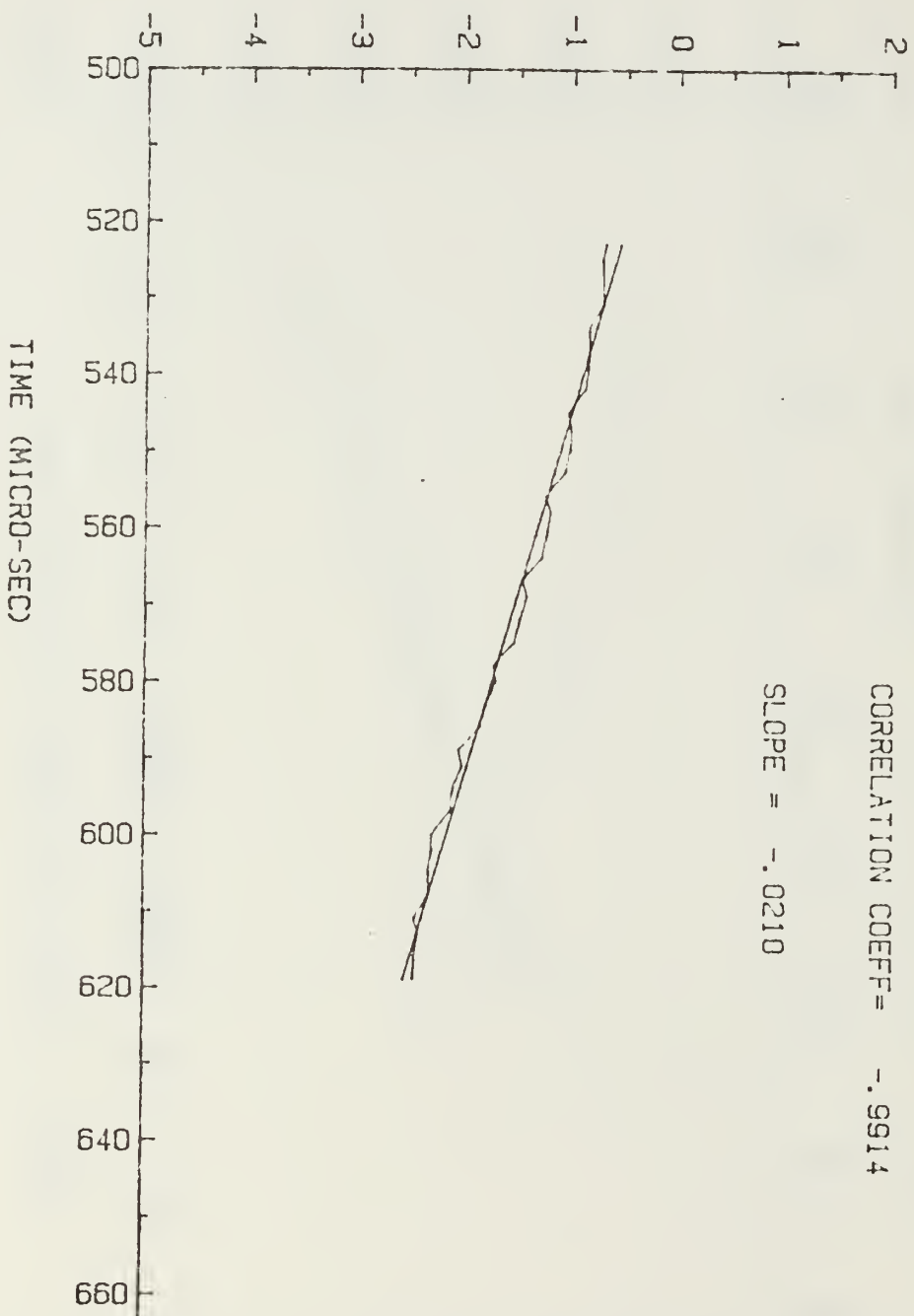


Figure C.14 Decay envelope resulted from the average from data set 42 to 47 for the aggregate/water surface (data set DAT6).

LN(( $<VOLTAGE^2>$ ) $^{1/2}$ )

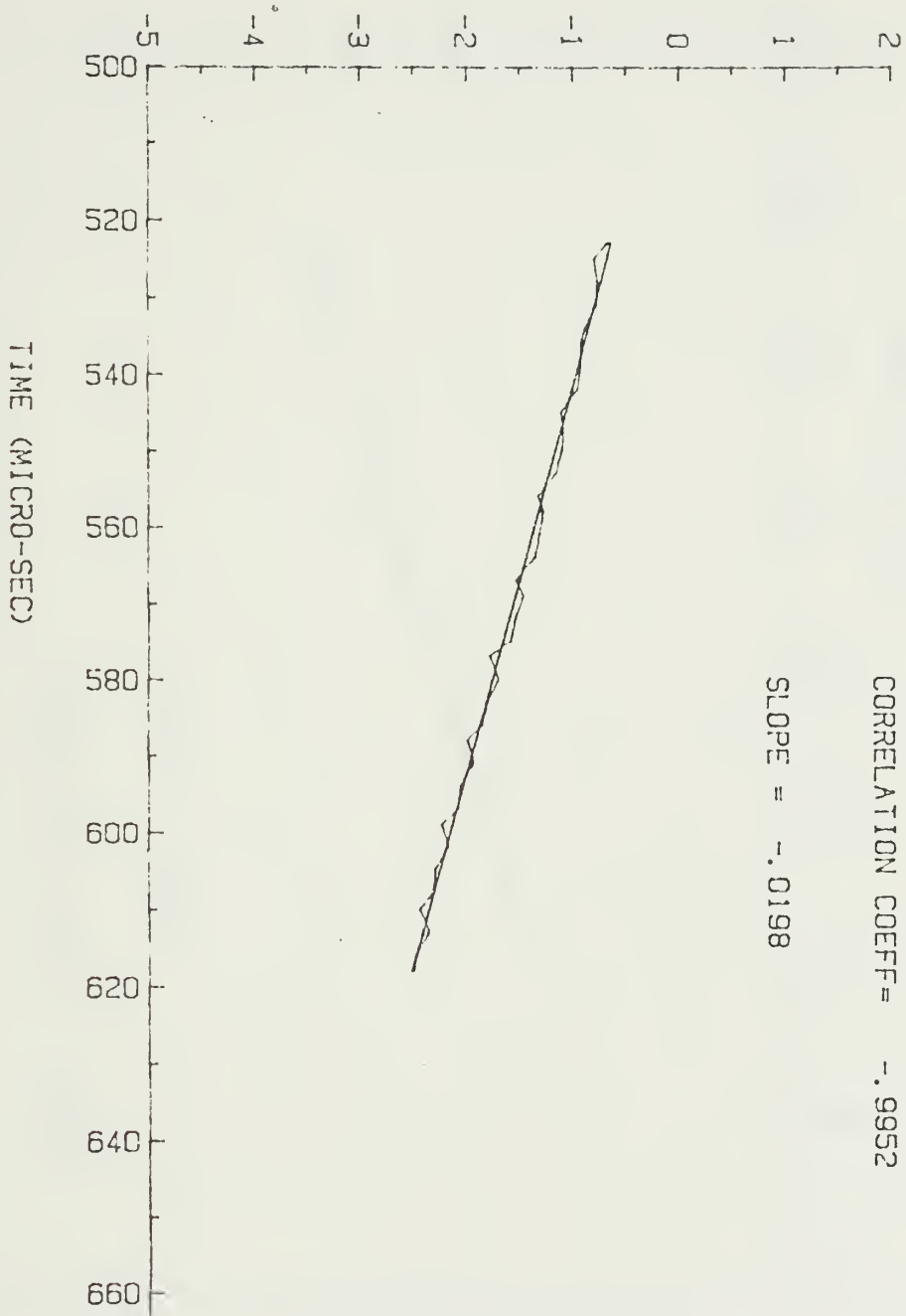


Figure C.15 Decay envelope resulted from the average from data set 42 to 48 for the aggregate/water surface (data set DAT7).

LN(( $\langle VOLTAGE^2 \rangle$ ) $^{1/2}$ )

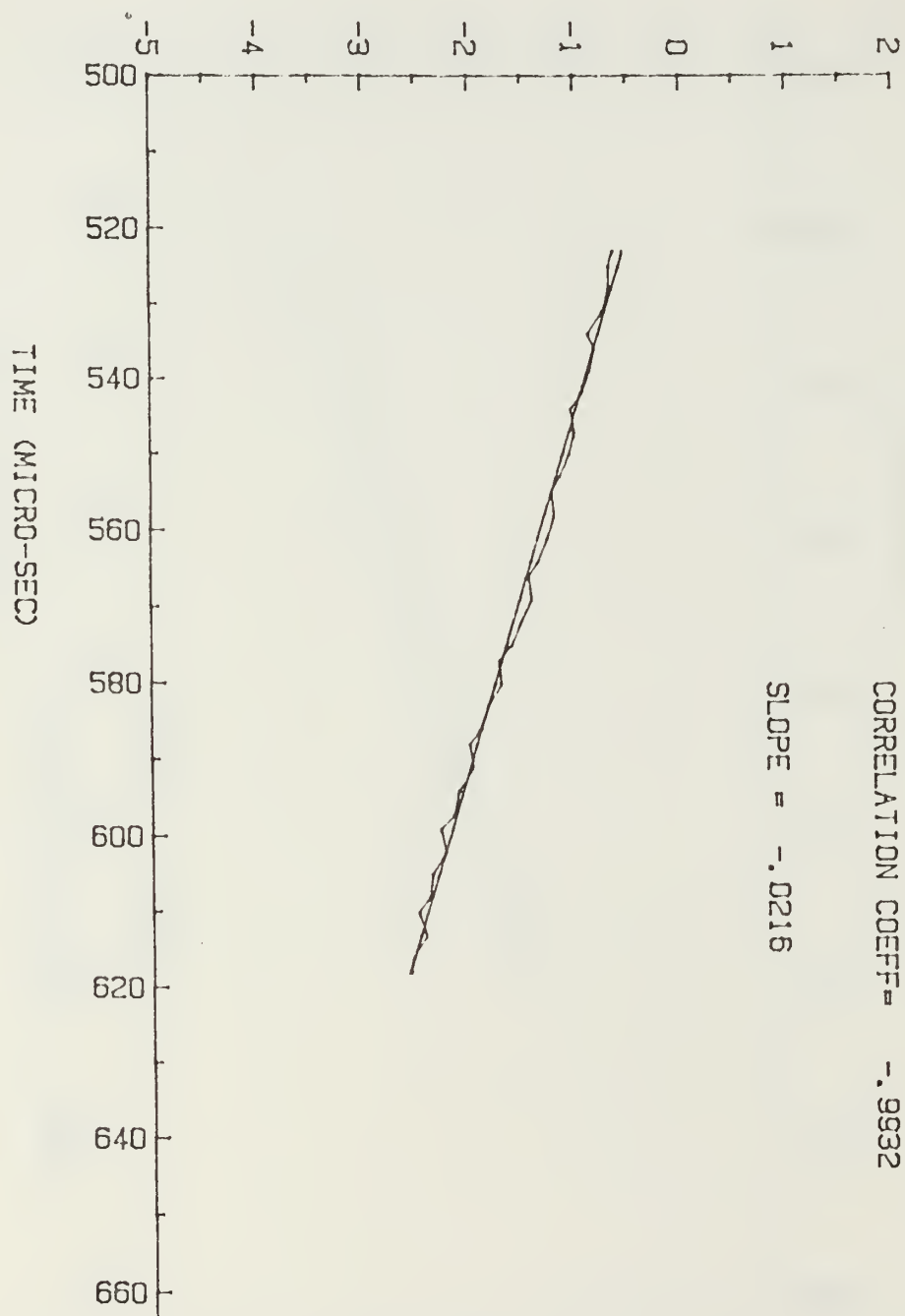


Figure C.16 Decay envelope resulted from the average from data set 42 to 49 for the aggregate/water surface (data set DAT8).

LN(( $\langle VOLTAGE^2 \rangle$ ) $^{1/2}$ )

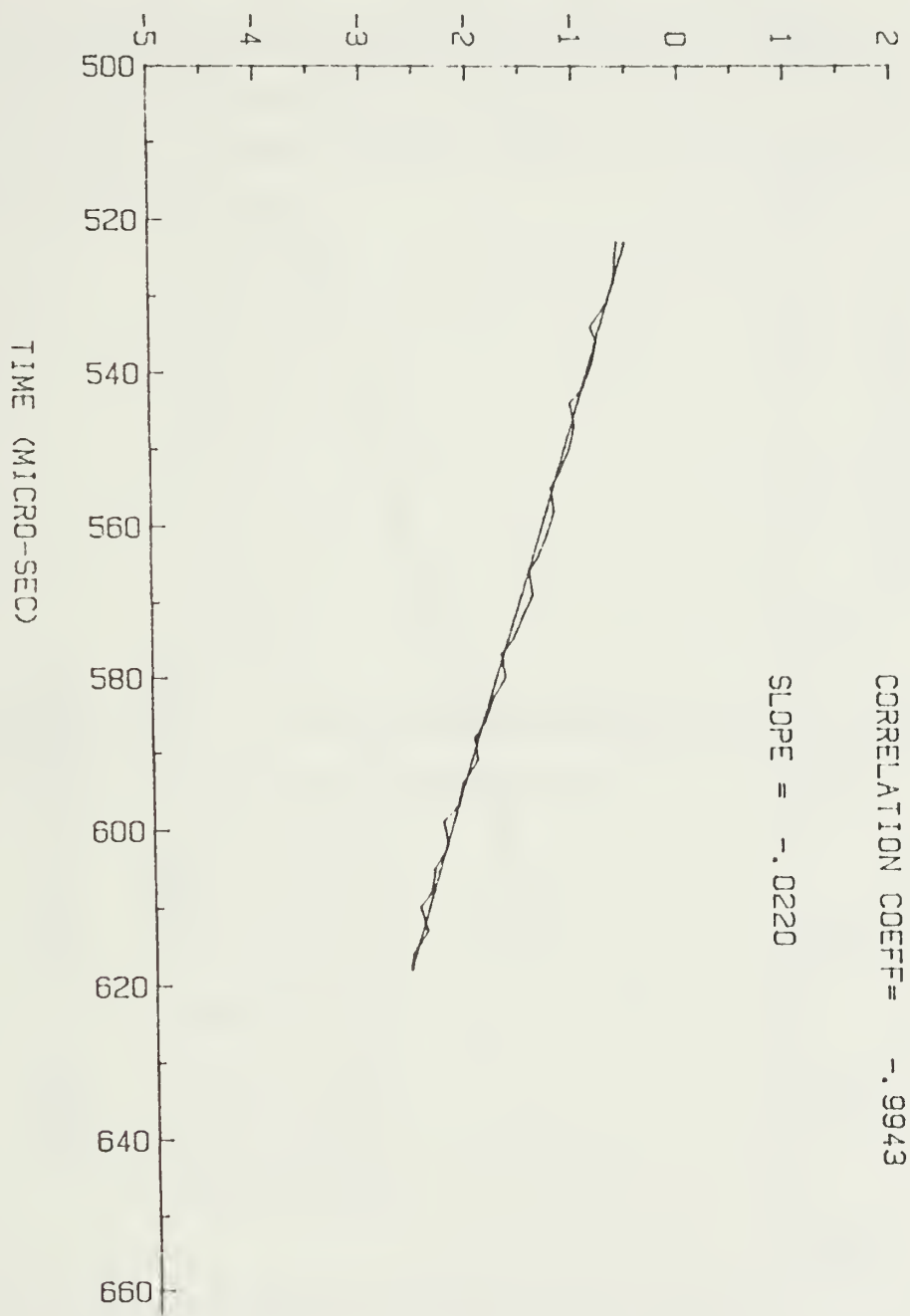


Figure C.17 Decay envelope resulted from the average from data set 42 to 50 for the aggregate/water surface (data set DA19).

LN(( $\langle VOLTAGE^2 \rangle$ )  $^{1/2}$ )

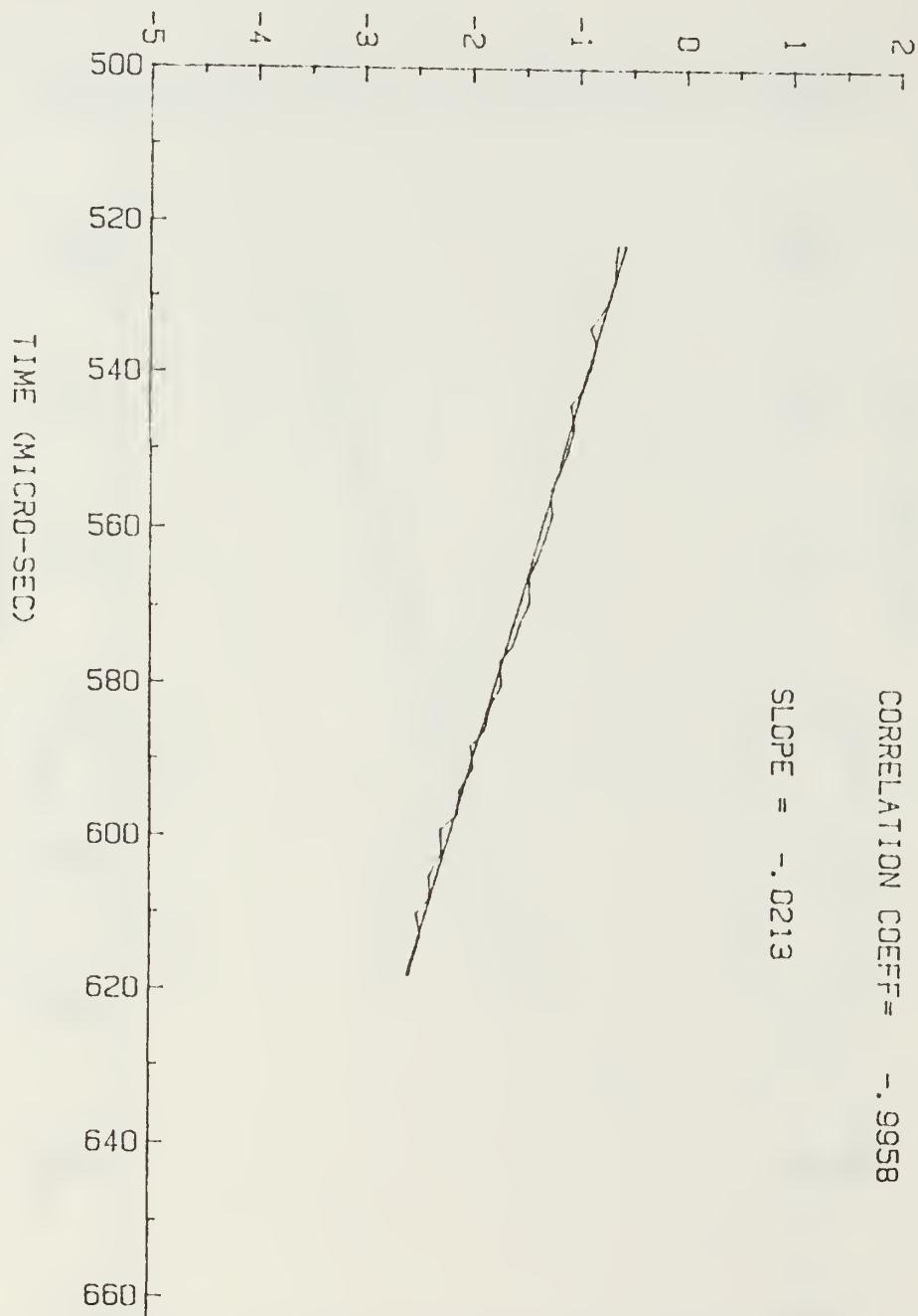


Figure C.18 Decay envelope resulted from the average from data set 42 to 51 for the aggregate/water surface (data set DAT10).

## APPENDIX D

### DECAY ENVELOPE GRAPHS FOR FINE SAND

This appendix includes the graphs of the decay envelopes for reflection from fine-sand/water interface within the glass tank. Figure D.1 to D.10 show the original decay envelopes obtained from different transducer positions. The decay envelopes are also described as following data sets:

- data set 55
- data set 56
- data set 57
- data set 58
- data set 59
- data set 60
- data set 61
- data set 62
- data set 63
- data set 64

Figures D.11 to D.19 are the decay envelopes resulted from the running average method. They are also described as following data sets:

- data set DAT12
- data set DAT13
- data set DAT14
- data set DAT15
- data set DAT16
- data set DAT17
- data set DAT18
- data set DAT19
- data set DAT20

$\text{LN}((\langle \text{VOLTAGE}^2 \rangle)^{1/2})$

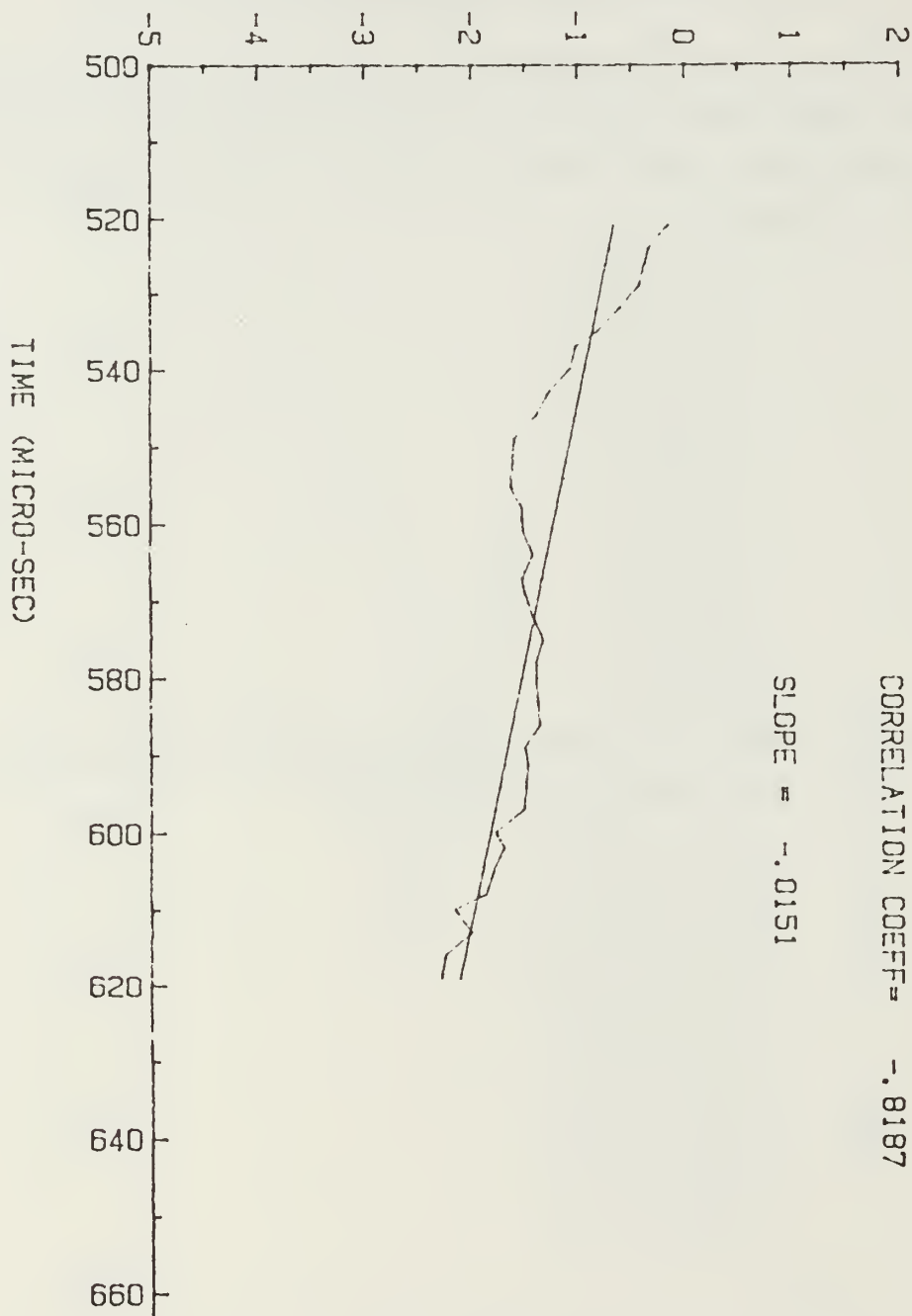


Figure D.1 Decay envelope for reflection from fine-sand/water interface, transducer was 30 cm above surface (data set 55).

$\text{LN}(\langle \text{VOLTAGE}^2 \rangle)^{1/2}$

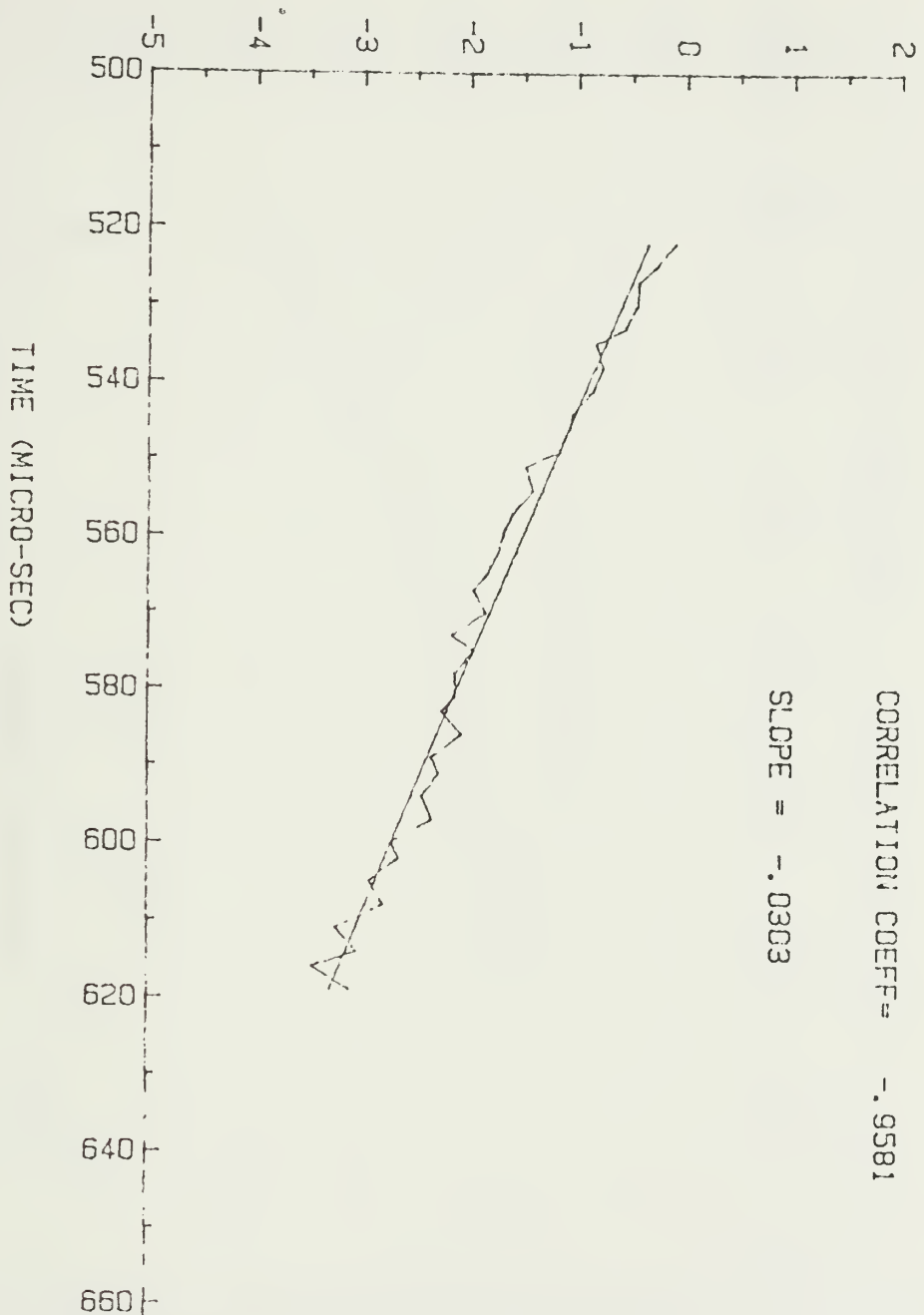


Figure D.2 Decay envelope for reflection from fine-sand/water interface, transducer was 30 cm above surface (data set 56).

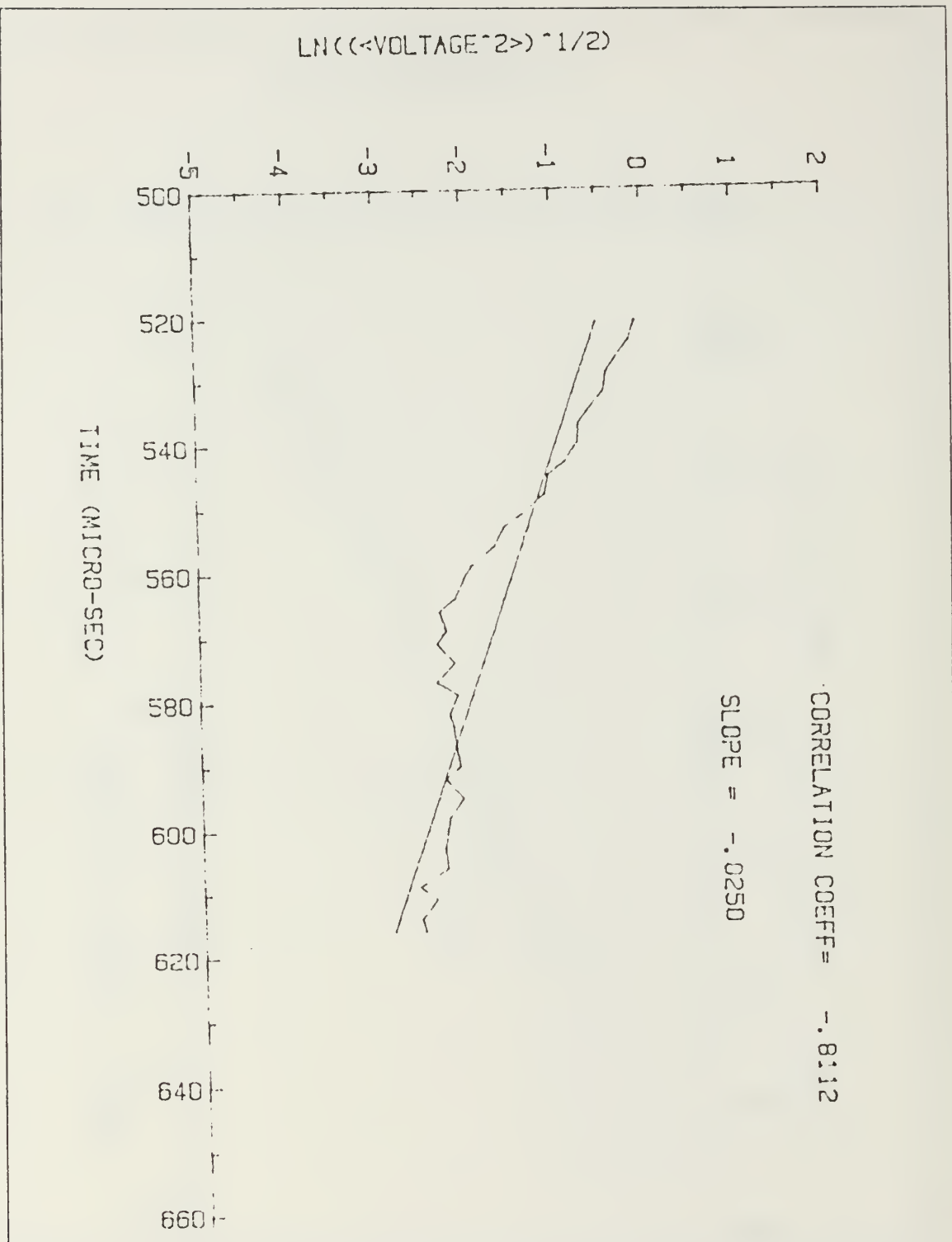


Figure D.3 Decay envelope for reflection from fine-sand/water interface, transducer was 30 cm above surface (data set 57).

LN(( $\langle VOLTAGE^2 \rangle$ ) $^{1/2}$ )

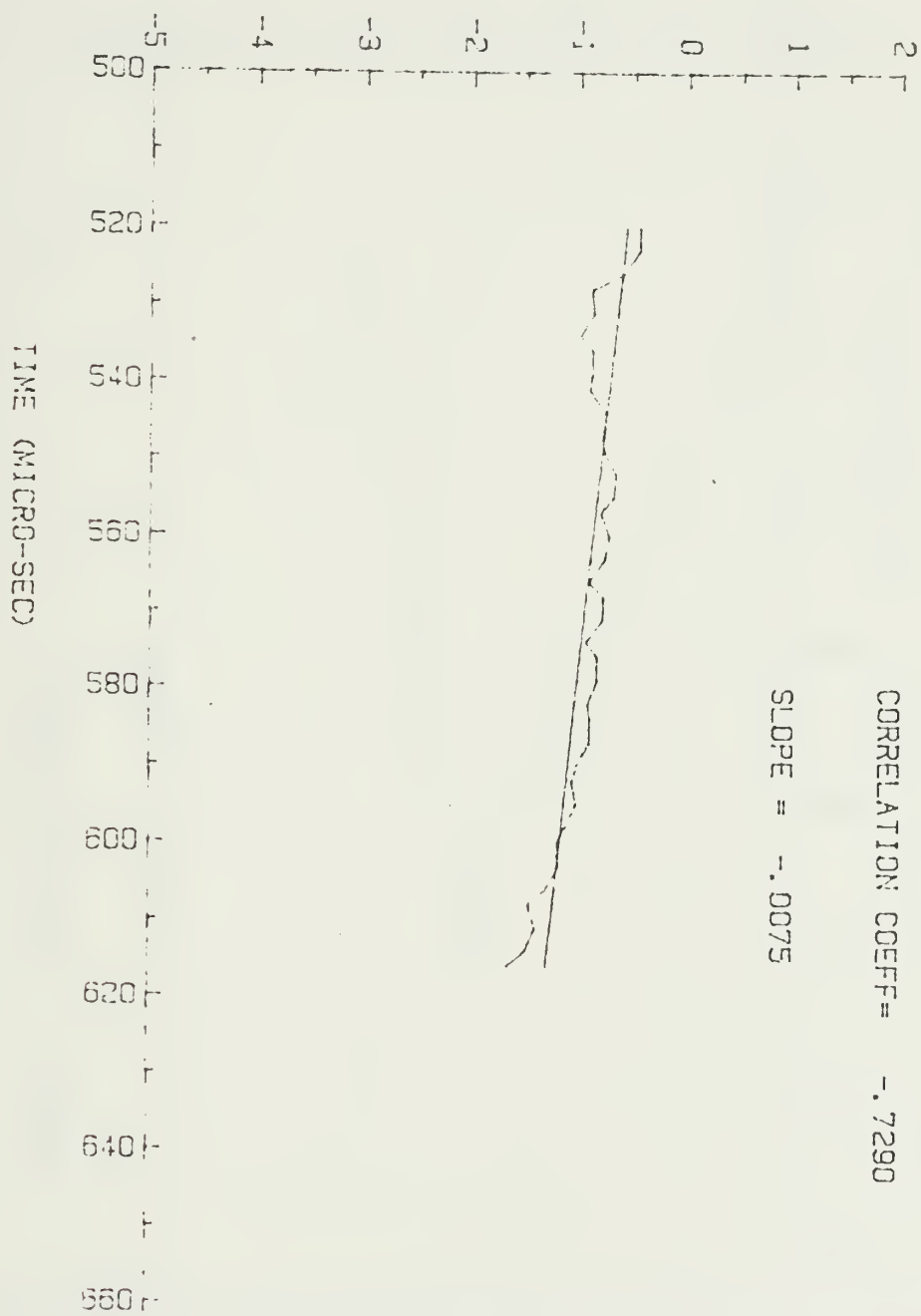


Figure D.4 Decay envelope for reflection from fine-sand/water interface, transducer was 30 cm above surface (data set 58).

LN(( $\langle VOLTAGE^2 \rangle$ ) $^{1/2}$ )

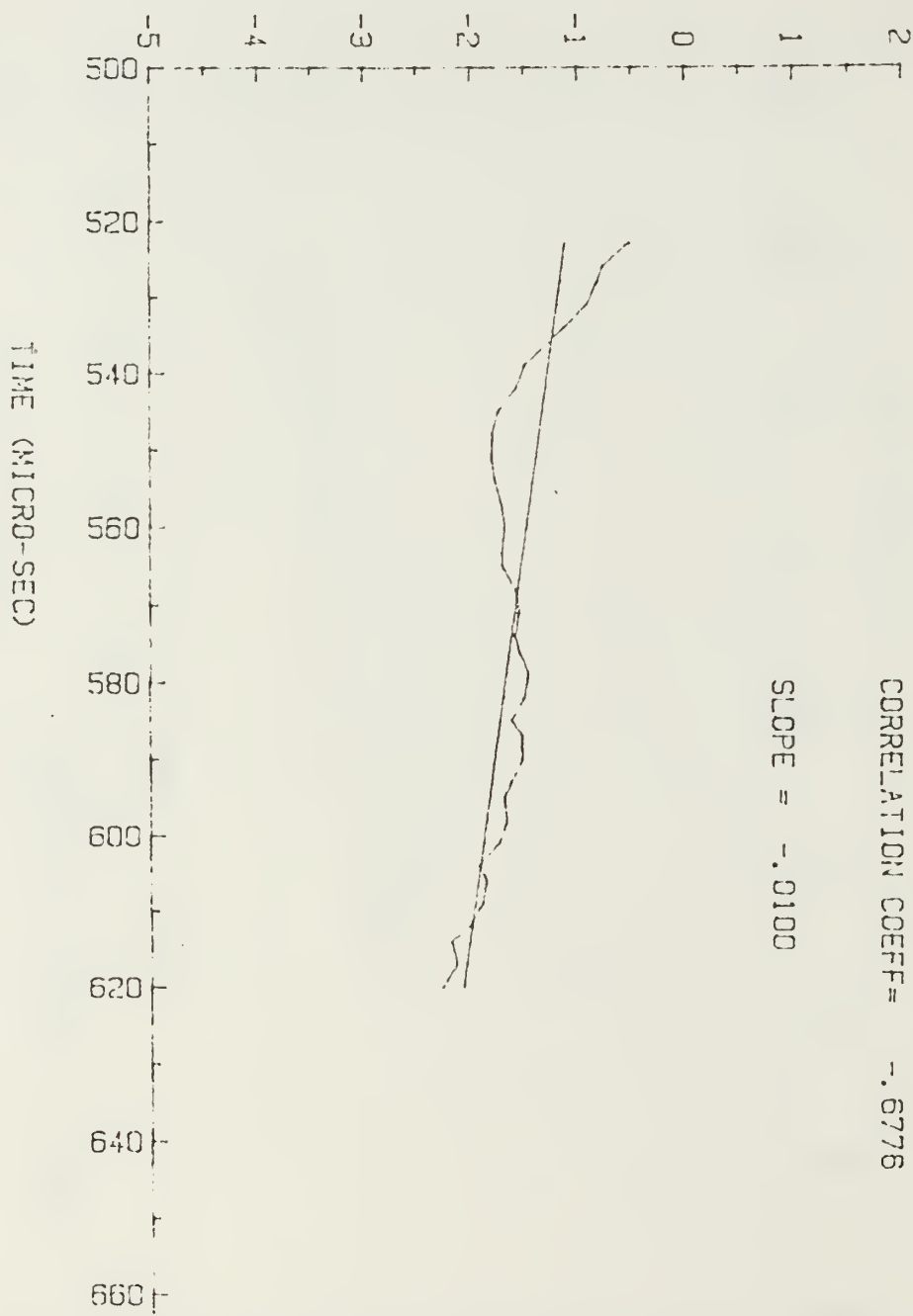


Figure D.5 Decay envelope for reflection from fine-sand/water interface, transducer was 30 cm above surface (data set 59).

LN(( $\langle VOLTAGE^2 \rangle$ ) $^{1/2}$ )



Figure D.6 Decay envelope for reflection from fine-sand/water interface, transducer was 30 cm above surface (data set 60).

$\text{LN}((\langle \text{VOLTAGE}^2 \rangle)^{1/2})$

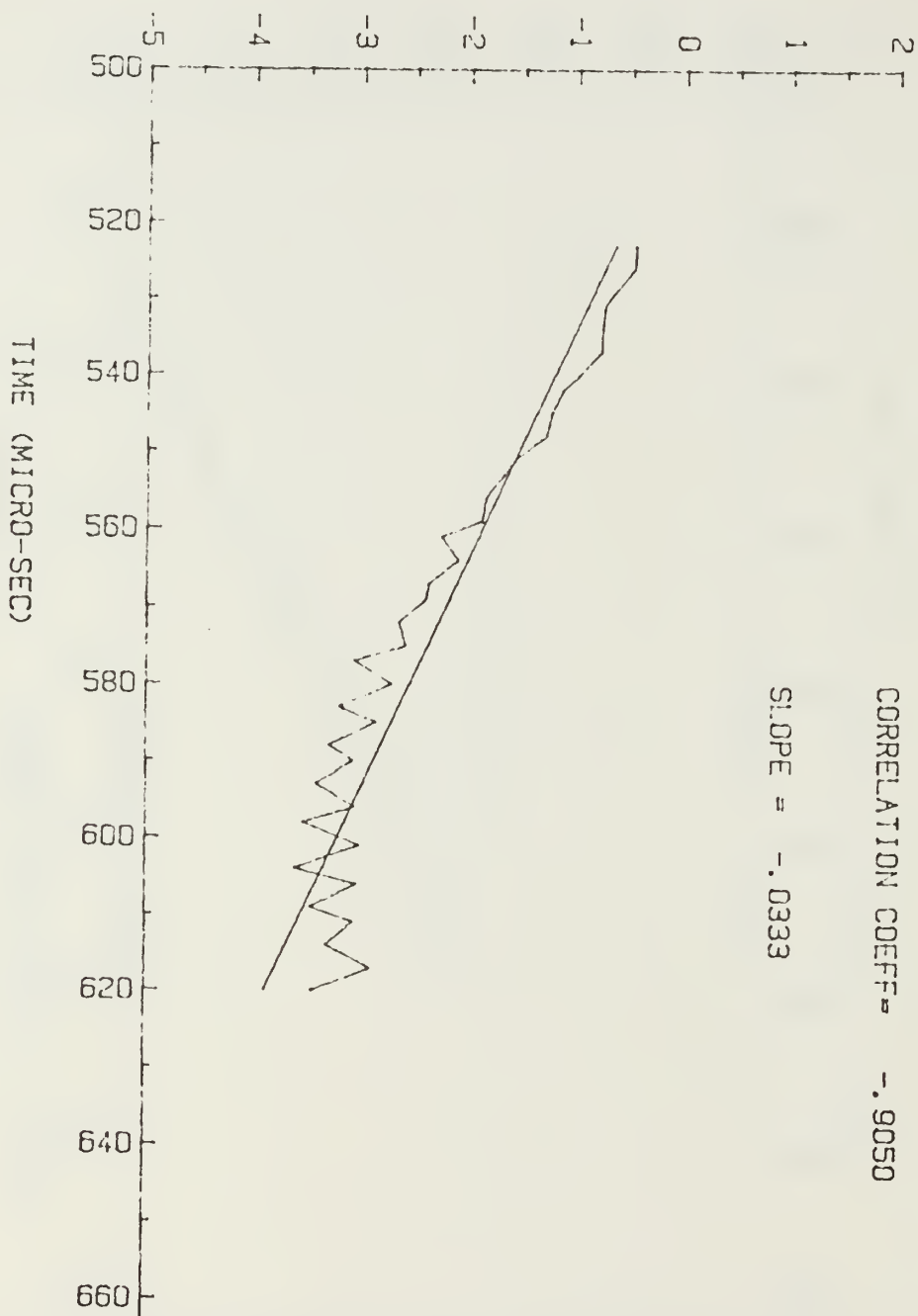


Figure D.7 Decay envelope for reflection from fine-sand/water interface, transducer was 30 cm above surface (data set 61).

$\text{LN}((\langle \text{VOLTAGE}^2 \rangle)^{1/2})$

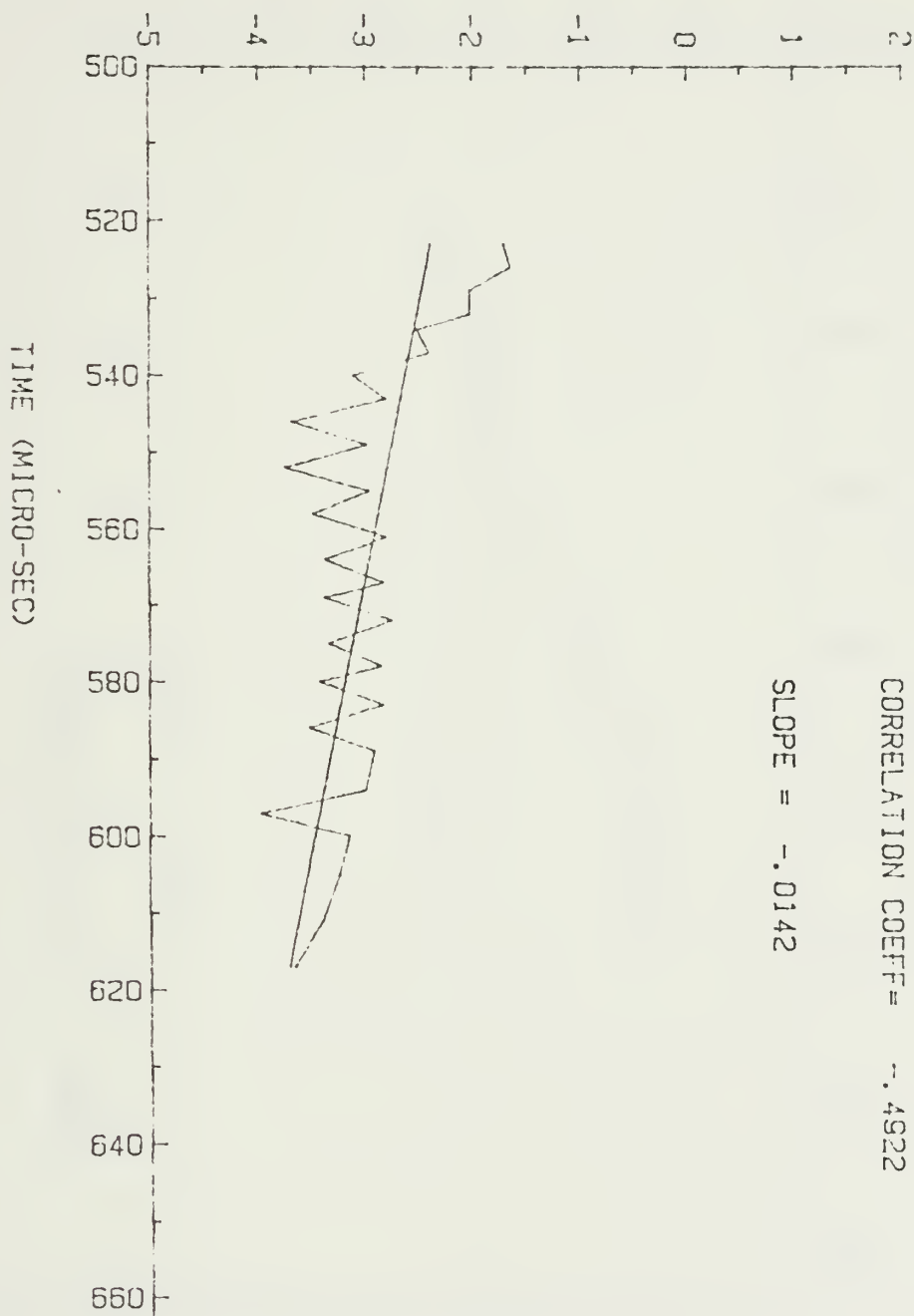


Figure D.8 Decay envelope for reflection from fine-sand/water interface, transducer was 30 cm above surface (data set 62).

$\text{LN}((\text{VOLTAGE}^2)^{1/2})$

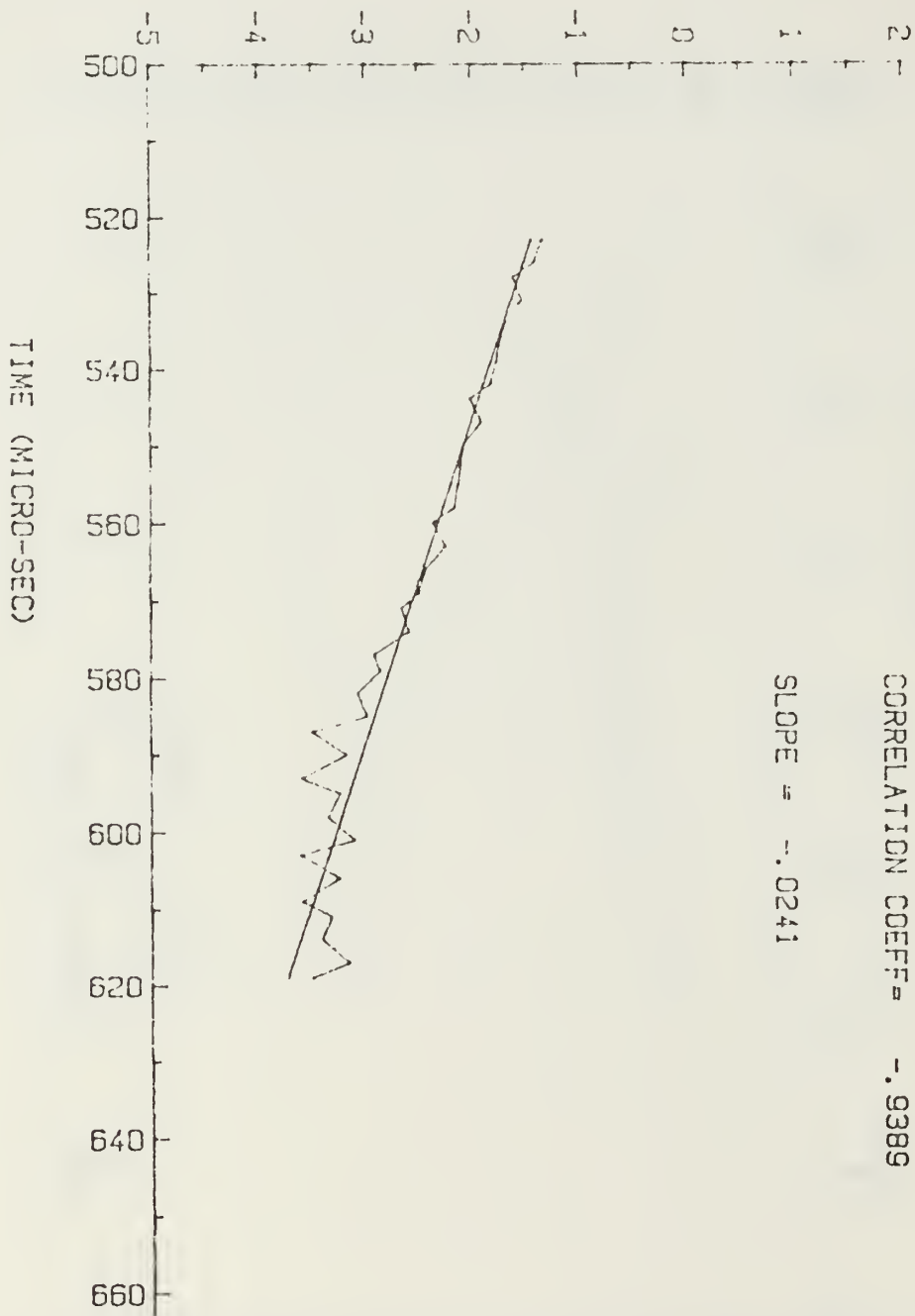


Figure D.9 Decay envelope for reflection from fine-sand/water interface, transducer was 30 cm above surface (data set 63).

LN(( $\langle VOLTAGE^2 \rangle$ ) $^{1/2}$ )

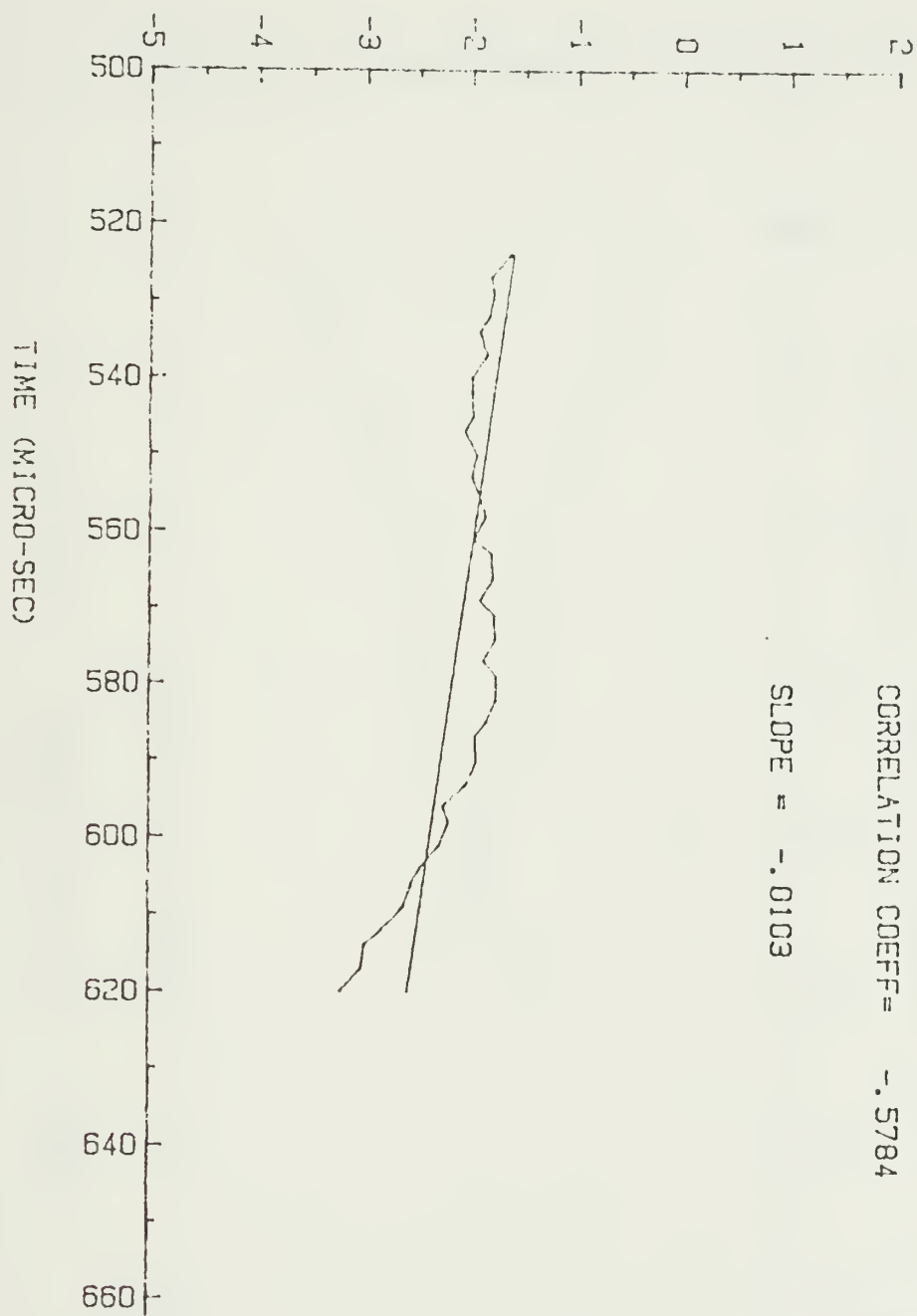


Figure D.10 Decay envelope for reflection from fine-sand/water interface, transducer was 30 cm above surface (data set 64).

$\text{LN}((\langle \text{VOLTAGE}^2 \rangle)^{1/2})$

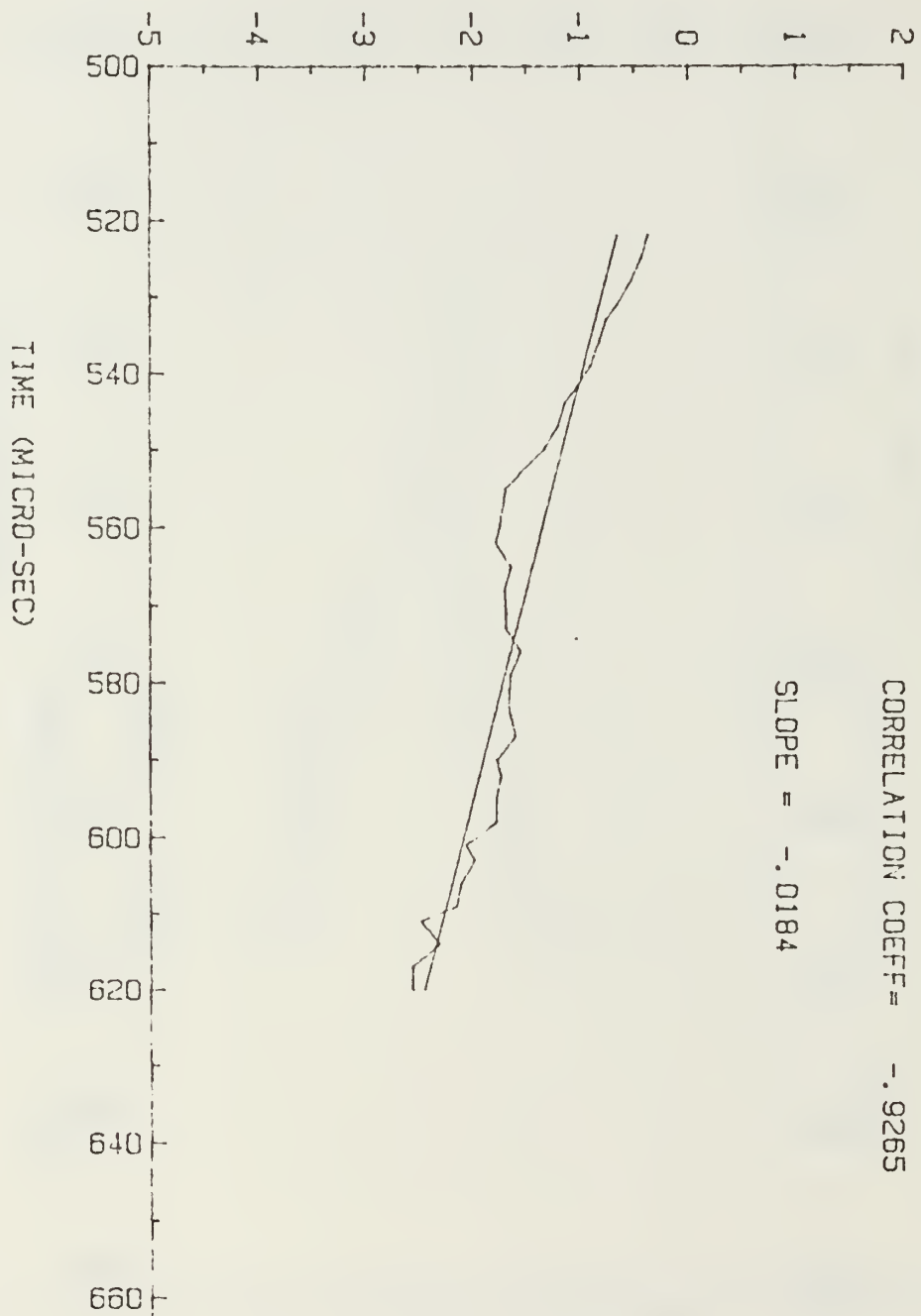


Figure D.11 Decay envelope resulted from the average of data set 55 and 56 for the fine-sand/water surface (data set DAT12).

LN(( $\langle VOLTAGE^2 \rangle$ ) $^{1/2}$ )

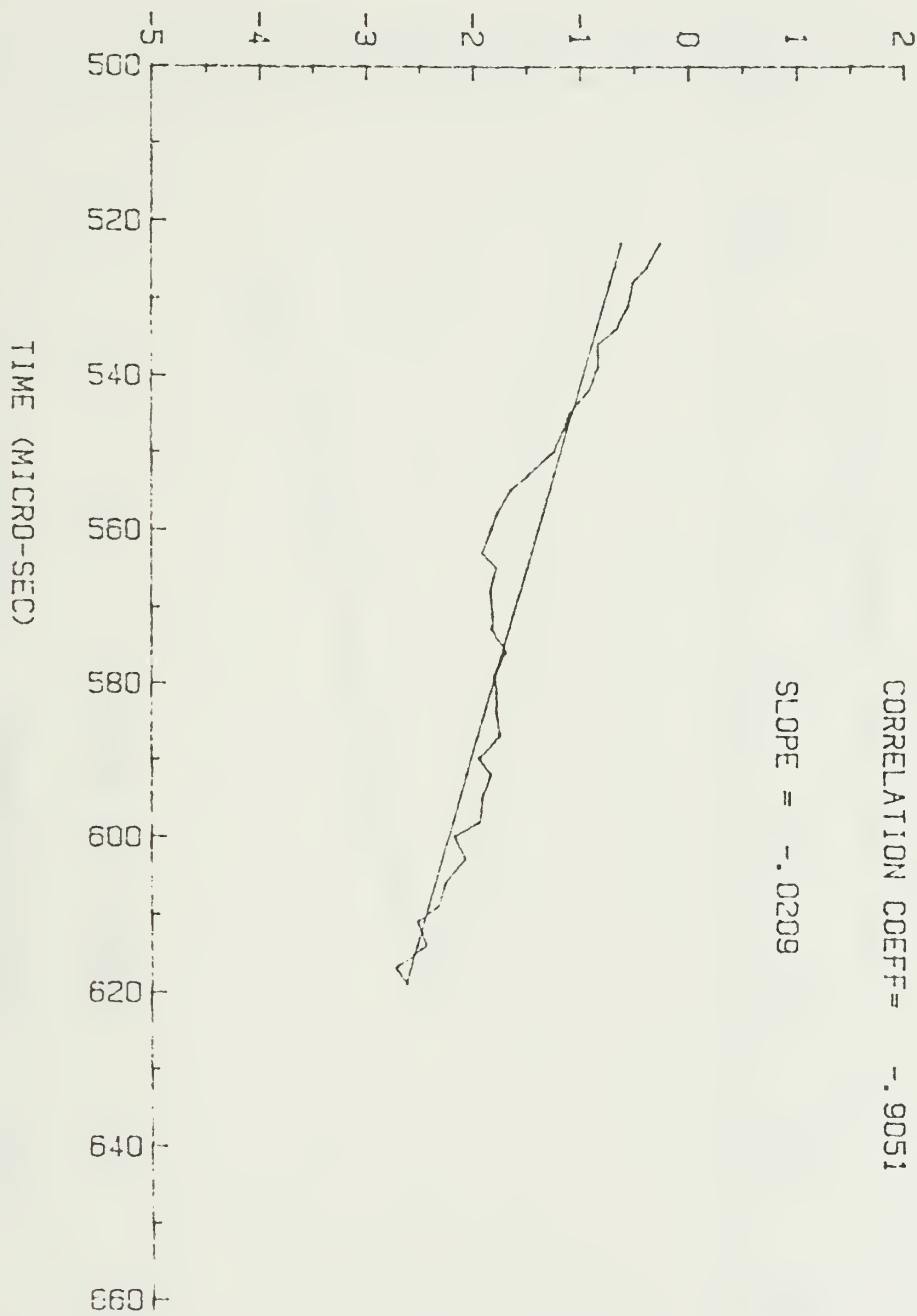


Figure D.12 Decay envelope resulted from the average from data set 55 to 57 for the fine-sand/water surface (data set DAT13).

LN(( $\langle VOLTAGE^2 \rangle$ ) $^{1/2}$ )

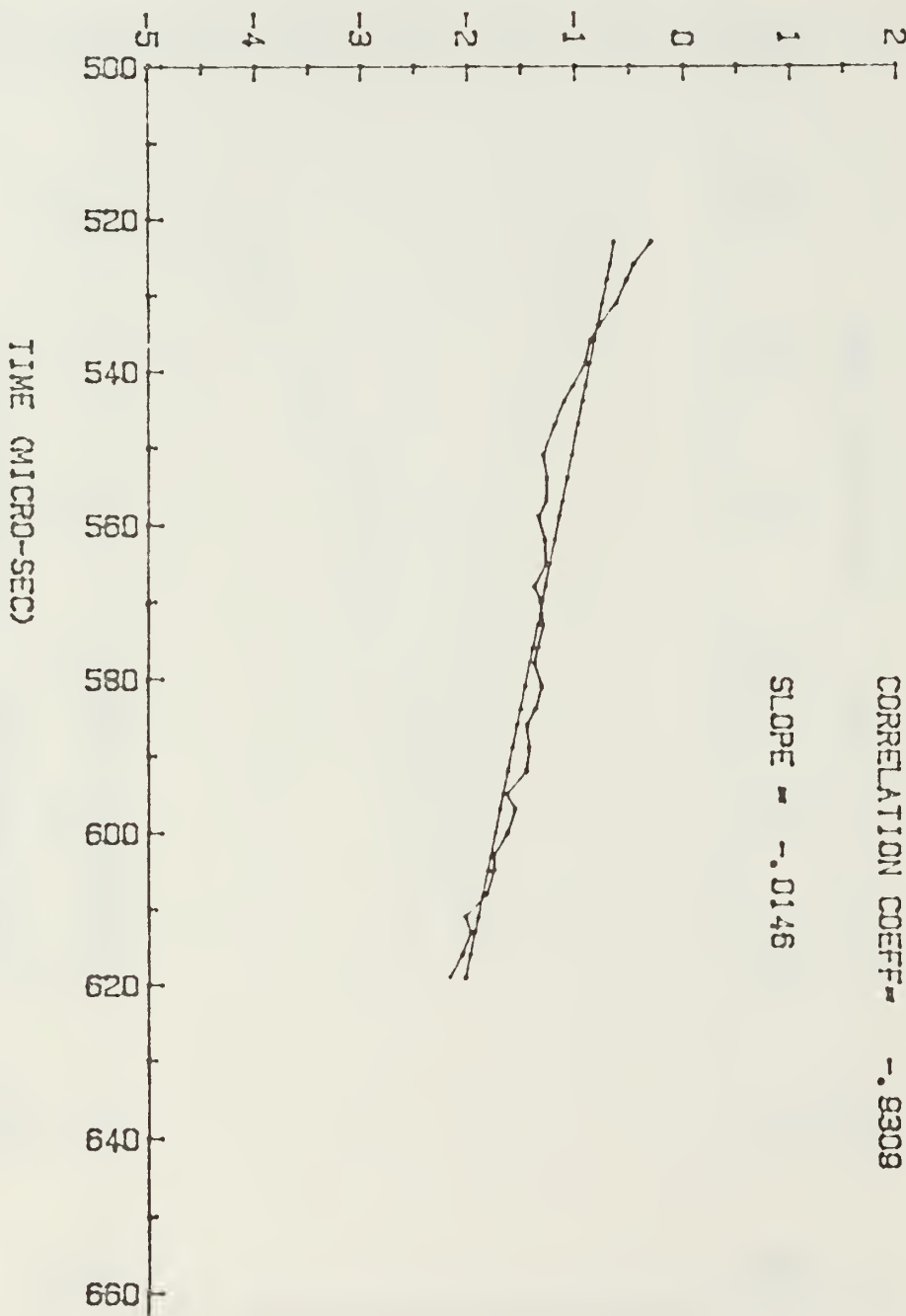


Figure D.13 Decay envelope resulted from the average from data set 55 to 58 for the fine-sand/water surface (data set DAT14).

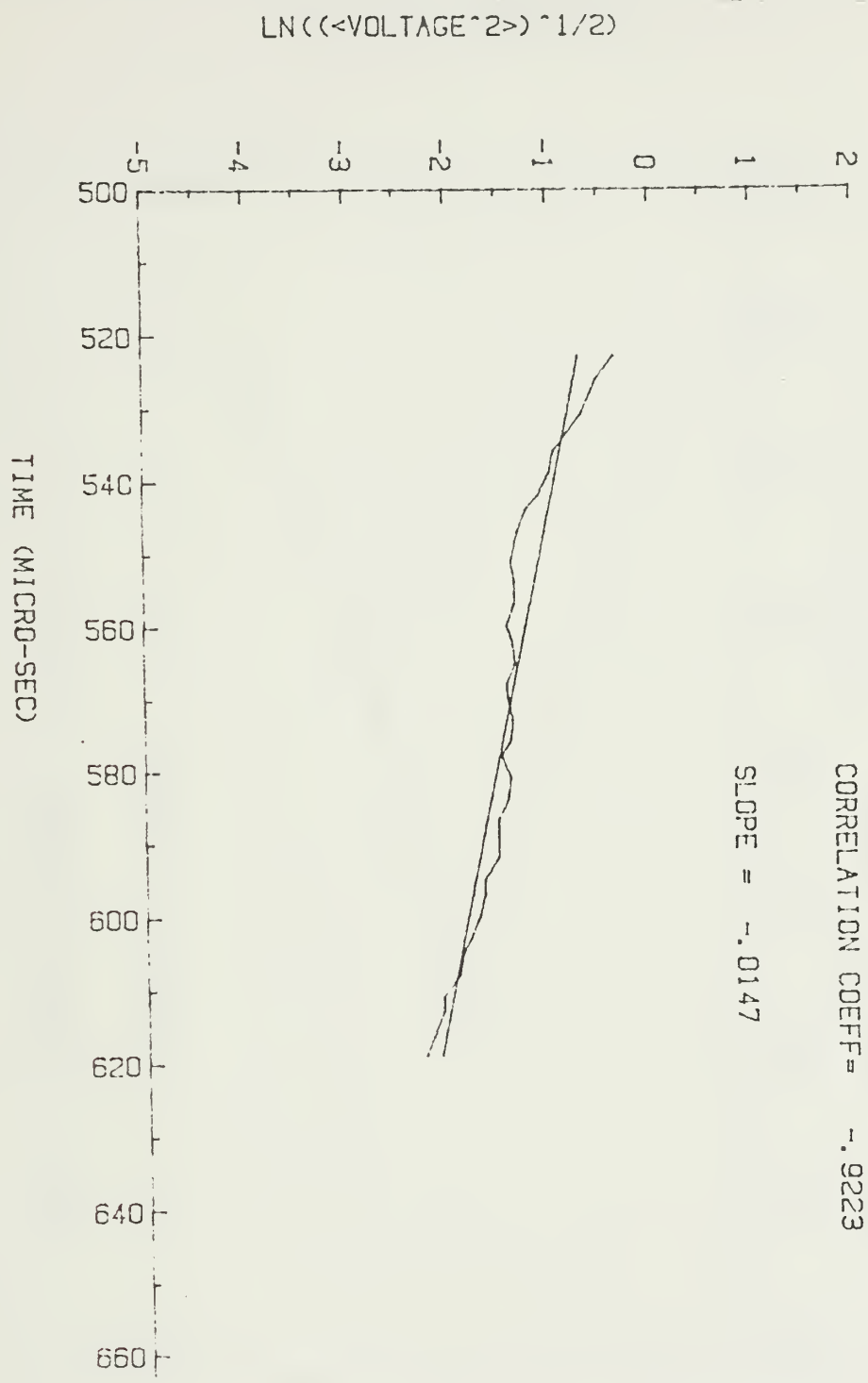


Figure D.14 Decay envelope resulted from the average from data set 55 to 59 for the fine-sand/water surface (data set DAT15).

$\text{LN}(\langle \text{VOLTAGE}^2 \rangle)^{1/2}$

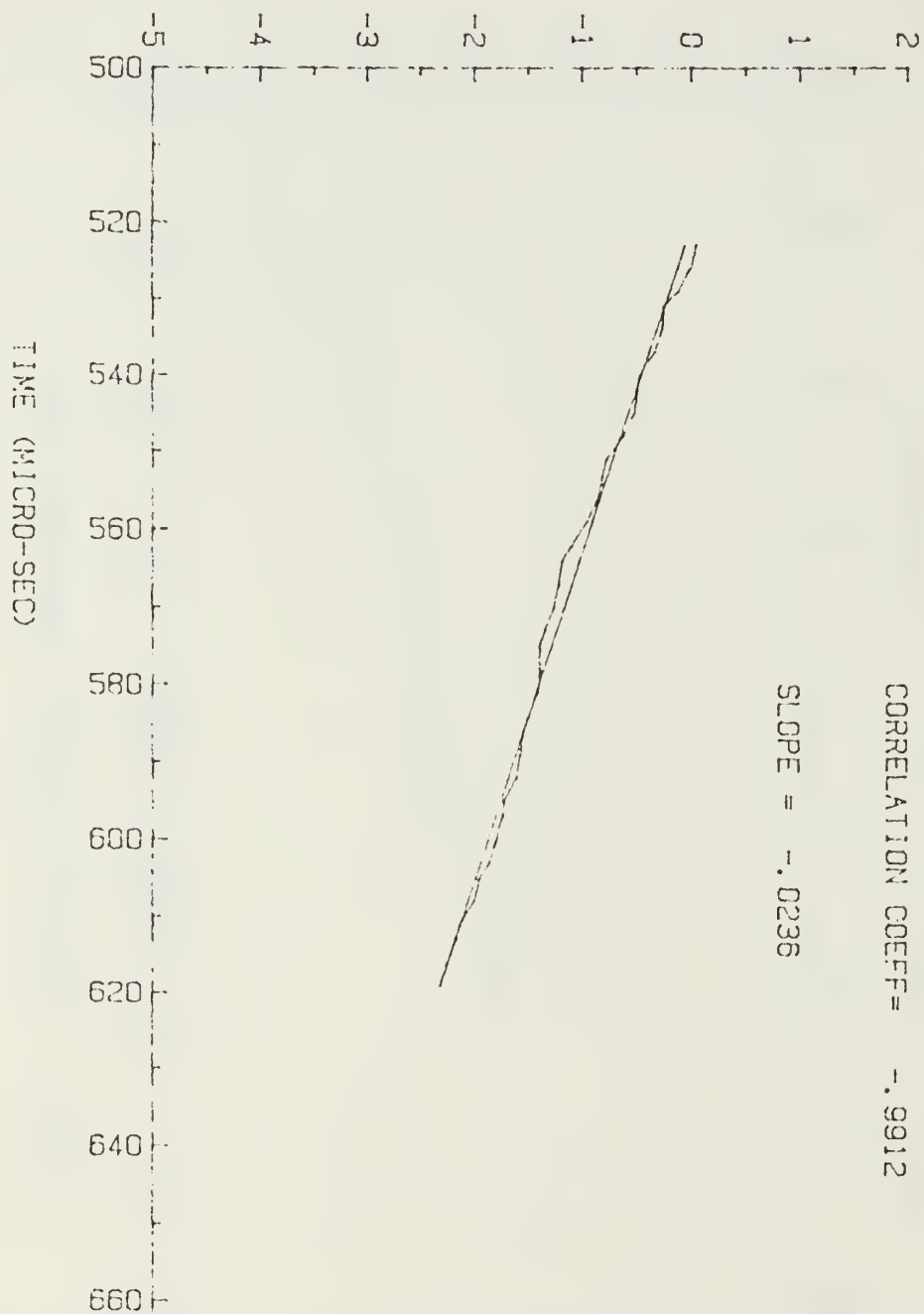


Figure D.15 Decay envelope resulted from the average from data set 55 to 60 for the fine-sand/water surface (data set DAT16).

LN(( $\langle VOLTAGE^2 \rangle$ ) $^{1/2}$ )

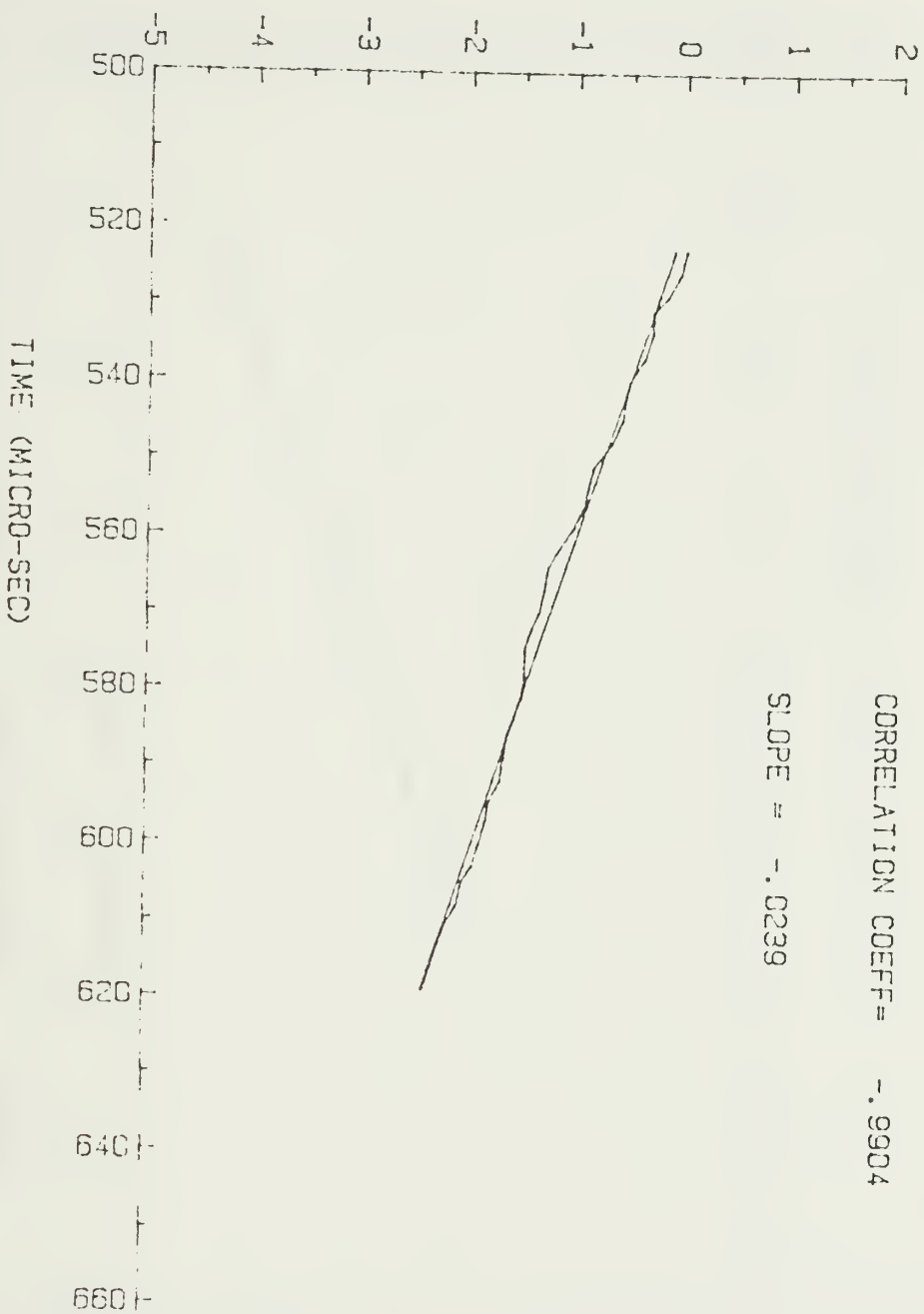


Figure D.16 Decay envelope resulted from the average from data set 55 to 61 for the fine-sand/water surface (data set DAT17).

LN(( $\langle VOLTAGE^2 \rangle$ ) $^{1/2}$ )

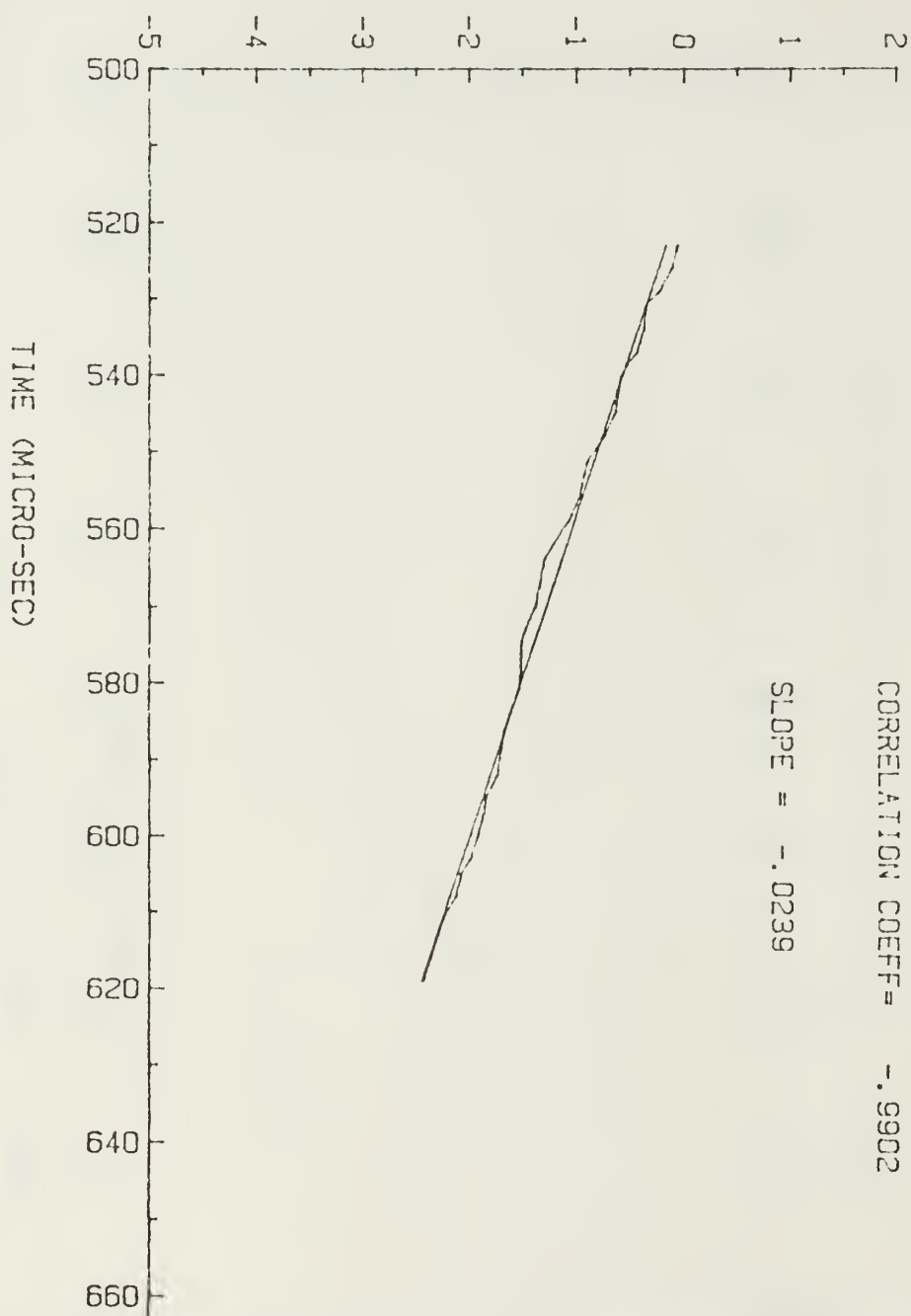


Figure D.17 Decay envelope resulted from the average from data set 55 to 62 for the fine-sand/water surface (data set DAT18).

LN(( $\langle VOLTAGE^2 \rangle$ ) $^{1/2}$ )

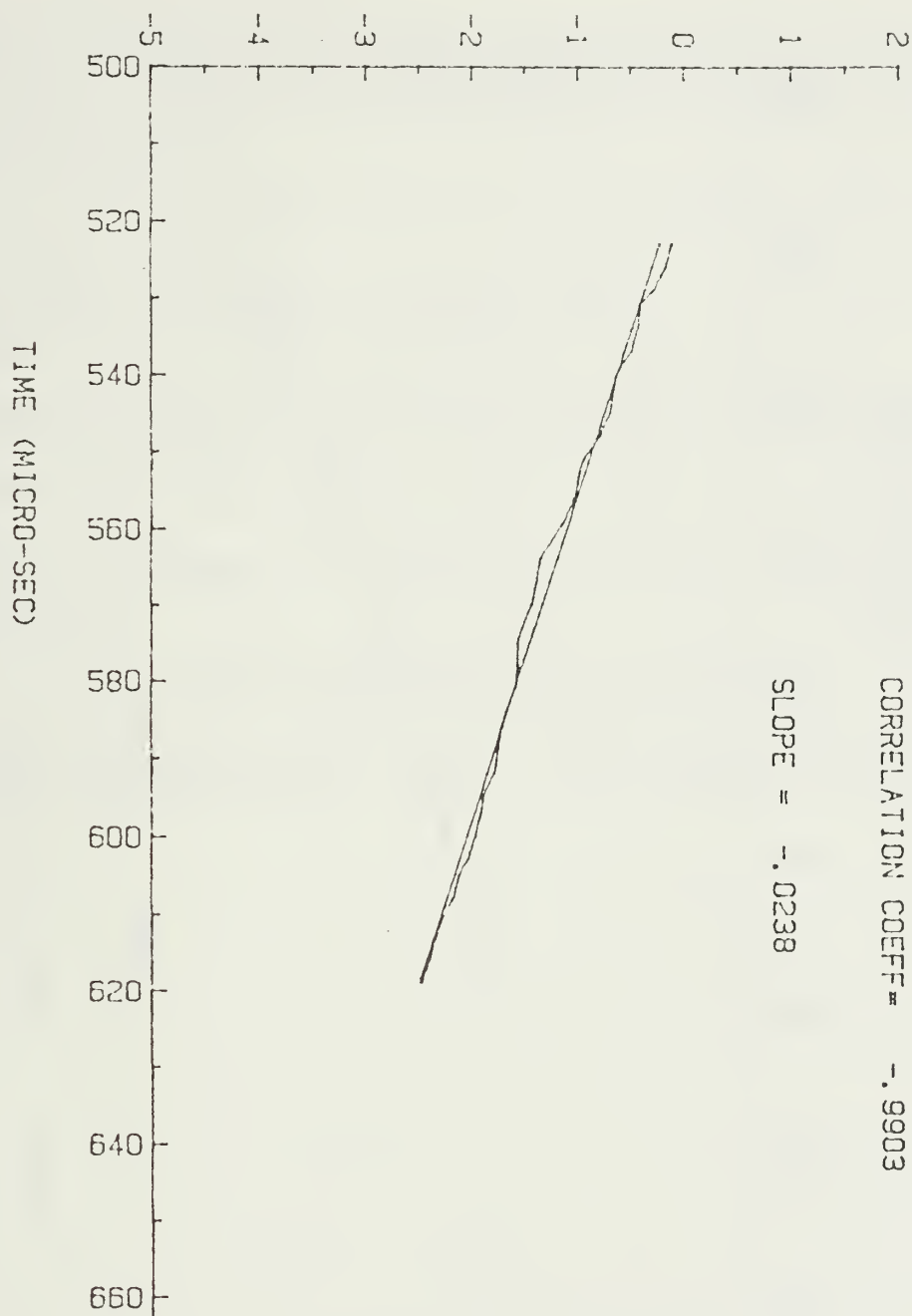


Figure D.18 Decay envelope resulted from the average from data set 55 to 63 for the fine-sand/water surface (data set DAT19).

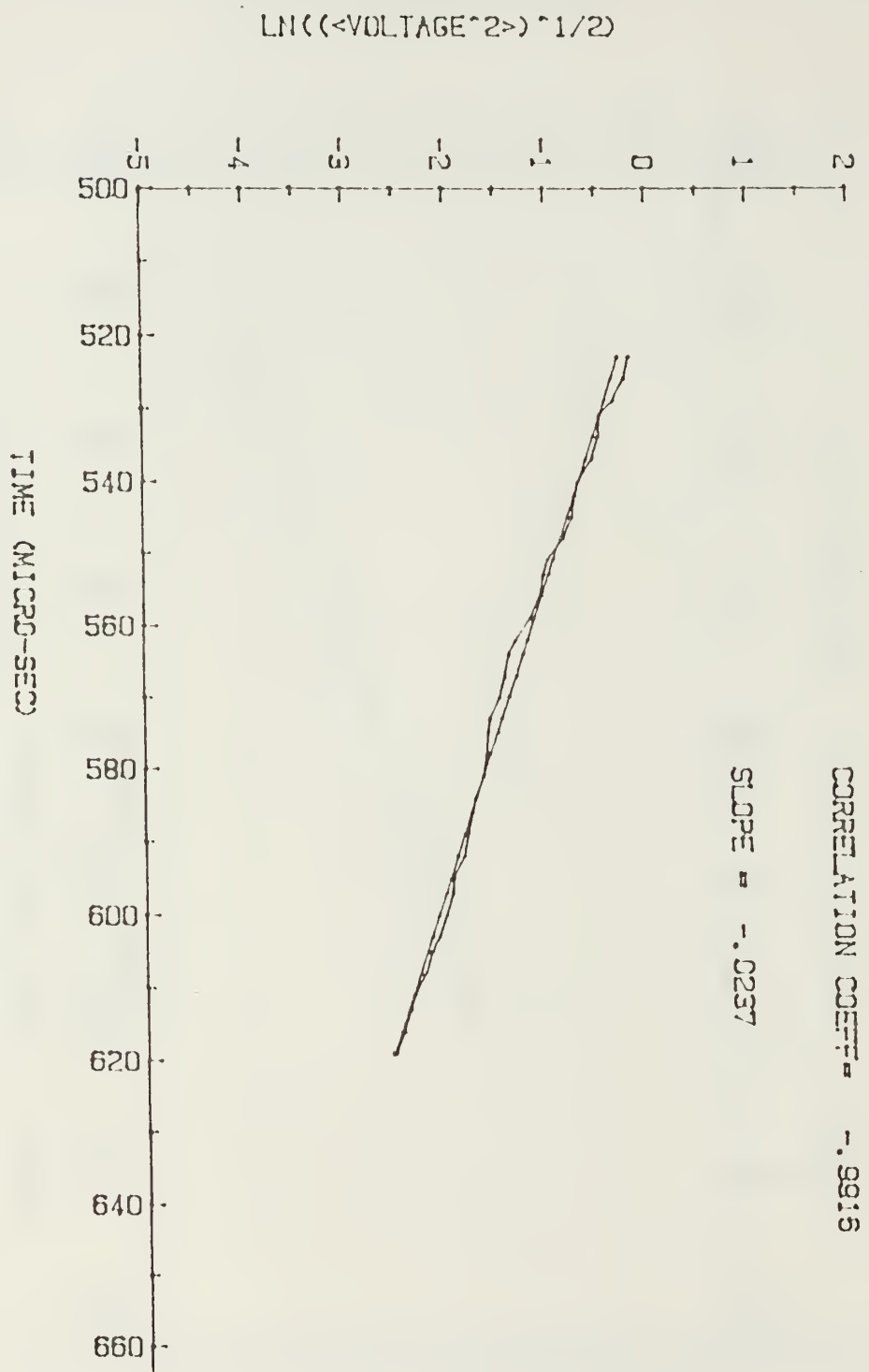


Figure D.19 Decay envelope resulted from the average from data set 55 to 64 for the aggregate/water surface (data set DA120).

## BIBLIOGRAPHY

Berkson, J. M., *Measurements of Coherence of Sound Reflected From Ocean Sediments.* *The Journal of Acoustic Society of America*, Volume 68, No. 5, November 1980.

Dunsiger, A. D., MacIsaac, R. R., *Broadband Seismic Data Used for Seafloor Sediment Classification.* *OCEAN'78.* MTS-IEEE, 1978.

Eyring, C. F., *Reverberation in the Sea.* *The Journal of Acoustic Society of America*, Volume 20, No. 4, July 1948.

Hamilton, E. L., *Geoacoustic Modeling of the Sea Floor.* *The Journal of Acoustic Society of America*, Volume 68, No. 5, November 1980.

Hampton, L., *Physics of Sound in Marine Sediments,* Plenum Press, 1974.

Mackenzie, K. V., *Bottom Reverberation for 530- and 1030-cps Sound in Deep Water.* *The Journal of Acoustic Society of America*, Volume 33, No. 11, November 1961.

Merklinger, H. M., *Bottom Reverberation Measured With Explosive Charges Fired Deep in the Ocean.* *The Journal of Acoustic Society of America*, Volume 44, No. 2, January 1968.

Milligan, S. D., LeBlance, L. R., Middleton, F. H., *Statistical Grouping of Acoustic Reflection Profiles.* *The Journal of Acoustic Society of America*, Volume 64, No. 3, September 1978.

Urick, R. J., *Low-Frequency Sound Attenuation in the Deep Ocean.* *The Journal of Acoustic Society of America*, Volume 35, No. 9, September 1963.

Young, R. A., Merrill, J. T., Clarke, T. L., Proni, J. R., *Acoustic Profiling of Suspended Sediments in the Marine Bottom Boundary Layer.* *Geophysical Research Letters*, Volume 9, No. 3, March 1983.

## INITIAL DISTRIBUTION LIST

	No. Copies
1. Defense Technical Information Center Cameron Station Alexandria, VA 22304-6145	2
2. Library, Code 0142 Naval Postgraduate School Monterey, CA 93943-5002	2
3. Chairman, Department of Oceanography Code 68 Naval Postgraduate School Monterey, CA 93943	1
4. Cherry, James R. Code 68CH Naval Postgraduate School Monterey, CA 93943	1
5. Professor J. V. Sanders, Code 61Sd Department of Physics Naval Postgraduate School Monterey, CA 93943	1
6. Professor A. B. Coppens, Code 61Cz Department of Physics Naval Postgraduate School Monterey, CA 93943	1
7. Professor S. P. Tucker, Code 68Tx Department of Oceanography Naval Postgraduate School Monterey, CA 93943	1
8. Director, Charting and Geodetic Sciences N CG, Room 1006, WSC-I National Oceanic and Atmospheric Administration Rockville, MD 20552	1
9. Director Yao, Neng Chun Chinese Naval Hydrographic and Oceanographic Office Tsoying, Kaohsiung Taiwan 813 Republic of China	1
10. Kuo, Feng-Yu Chinese Naval Hydrographic & Oceanographic Office Tsoying, Kaohsiung Taiwan 813 Republic of China	1
11. Facada, Joao SMC #1947 Naval Postgraduate School Monterey, CA 93943	1
12. LI, Yu-Ming SMC #1191 Naval Postgraduate School Monterey, CA 93943	1

13.	John R. Proni National Oceanic and Atmospheric Administration Atlantic Oceanographic and Meteorological Laboratory 4301 Ricenbacker Causeway Miami, FL 33149	1
14.	Ma, Wei-Ming SMC #2229 Naval Postgraduate School Monterey, CA 93943	1
15.	Yu, Ta-Te SMC #1343 Naval Postgraduate School Monterey, CA 93943	1
16.	Chief, Hydrographic Surveys Branch N CG24, Room 404, WSC-1 National Oceanic and Atmospheric Administration Rockville, MD 20852	1
17.	Ao, Cha-Lin SMC #2073 Naval Postgraduate School Monterey, CA 93943	1
18.	Wang, Chung-Wu Chinese Naval Hydrographic & Oceanographic Office Tsoying, Kaohsiung Taiwan 813 Republic of China	1
19.	Chang, Chin-Wen Chinese Naval Hydrographic and Oceanographic Office Tsoying, Kaohsiung Taiwan 813 Republic of China	10







DUDLEY KNOX LIBRARY  
NAVAL POSTGRADUATE SCHOOL  
MONTEREY CALIFORNIA 93943-5002

Thesis

C3713  
c.1

Chang  
Remote sensing of  
ocean sediment volume  
reverberation.

thesC3713  
Remote sensing of ocean sediment volume



3 2768 000 70553 7  
DUDLEY KNOX LIBRARY